DEVELOPMENT OF METHODS TO QUANTIFY BITUMEN-AGGREGATE ADHESION AND LOSS OF ADHESION DUE TO WATER

A Dissertation

by

AMIT BHASIN

Submitted to the Office of Graduate Studies of
Texas A&M University
in partial fulfillment of the requirements for the degree of

DOCTOR OF PHILOSOPHY

May 2006

Major Subject: Civil Engineering

DEVELOPMENT OF METHODS TO QUANTIFY BITUMEN-AGGREGATE ADHESION AND LOSS OF ADHESION DUE TO WATER

A Dissertation

by

AMIT BHASIN

Submitted to the Office of Graduate Studies of
Texas A&M University
in partial fulfillment of the requirements for the degree of

DOCTOR OF PHILOSOPHY

Approved by:

Chair of Committee,	Dallas N. Little
Committee Members,	Robert L. Lytton
	Eyad Masad
	Hung J. Sue
	Bruce E. Herbert
Head of Department,	David V. Rosowsky

May 2006

Major Subject: Civil Engineering

ABSTRACT

Development of Methods to Quantify Bitumen-Aggregate Adhesion and Loss of Adhesion Due to Water. (May 2006)
Amit Bhasin, B.Tech., Institute of Technology, India;
M.Eng., Texas A&M University
Chair of Advisory Committee: Dr. Dallas N. Little

Moisture induced damage of hot mix asphalt pavements has a significant economic impact in terms of excessive maintenance and rehabilitation costs. The moisture sensitivity of an asphalt mix depends on the combined effects of material properties, mixture design parameters, loading conditions and environmental factors. Traditional methods to assess moisture sensitivity of asphalt mixes rely on mechanical tests that evaluate the mix as a whole. These methods do not measure material properties and their role in moisture sensitivity of the mix independently. This information is very important to select materials resistant to moisture induced damage, or to modify locally available materials to improve their resistance to moisture damage for economic reasons. The objective of this research is to develop experimental and analytical tools to characterize important material properties that influence the moisture sensitivity of asphalt mixes.

Quality of adhesion between the aggregate and bitumen binder in wet and dry conditions plays an important role on the moisture sensitivity of the asphalt mix. A part of this research work was to develop the Wilhelmy plate method and the Universal Sorption Device to measure the surface free energy components of the bitumen and aggregate with adequate precision and accuracy, respectively. Surface energy of these materials was used to identify parameters based on thermodynamics that can quantify their interfacial adhesion and propensity to debond in the presence of water. The thermodynamic parameters were shown to correlate well with the moisture sensitivity of asphalt mixes determined from laboratory tests. Specific surface areas of the aggregates were also used to account for the influence of mechanical interlocking at the micro scale. In some mixes, chemical bonding also contributes to the adhesion between bitumen and

aggregate. The use of a micro calorimeter was introduced in this research as a versatile and fast tool to quantify the combined effects of physical and chemical adhesion between these materials.

DEDICATION

To all those who pursue knowledge for the betterment of society.

ACKNOWLEDGEMENTS

I would like to express my sincere gratitude to Dr. Dallas N. Little, my committee chair for providing me with the opportunity and invaluable support to conduct this research. What I have learned working under his guidance far exceeds the research that is documented in this dissertation. I wish to acknowledge the National Cooperative Highway Research Program (NCHRP) which has provided the necessary financial support for a major part of this research, and the Texas Transportation Institute (TTI) where this research was conducted. Thanks to my graduate committee members, Dr. Robert Lytton, Dr. H. J. Sue, Dr. Eyad Masad, and Dr. Bruce Herbert for their support and valuable insights. I would also like to thank Mr. Joe Button and Mr. Arif Chowdhary for their support and encouragement.

I appreciate the support of my colleagues, Dr. Arno Hefer, Mr. Corey Zollinger, Mr. Jonathan Howson, and Ms. Kamilla Vasconcellos, who were directly involved in various stages of this research, Mr. Syam Nair, and Ms. Veronica Castelo Branco, with whom I have shared several intriguing academic conversations, and Ms. Barbara Hein who has extended the necessary administrative support for executing this research project.

I acknowledge the support and encouragement of my parents, Mr. Satish and Mrs. Neera, who provided me with the necessary moral and vital financial support from time to time. Finally, I wish to acknowledge the support and encouragement of my wife, Reema, who inspired me to pursue this path and stood by me through all its rough and smooth patches.

TABLE OF CONTENTS

Page

CHAPTER Page

LIST OF FIGURES

FIGURE Page

FIGURE Page

LIST OF TABLES

TABLE Page

TABLE Page

CHAPTER I

INTRODUCTION

Overview

Approximately 2.4 million miles of pavements in the United States have a Hot mix asphalt (HMA) surface [1]. Hot mix asphalt (HMA) or asphalt concrete is composed of mineral aggregates that are bound together using bitumen. Bitumen is a by-product from the distillation of naturally occurring crude oil. Mineral aggregates are obtained by quarrying and processing natural rocks. Since physical and chemical properties of these materials are source dependent, mechanical properties of the composite asphalt concrete varies significantly depending on the proportioning (mix design) and source of the constituent materials.

Moisture induced damage or moisture damage is a form of distress in asphalt concrete pavements. Moisture sensitivity of an asphalt mix can be defined as the degradation of its mechanical properties (such as stiffness and fatigue cracking life) in the presence of water. The economic impact of moisture damage due to premature pavement failure and excessive maintenance costs has prompted research in this area since the early 1900's. Methods to identify materials and asphalt concrete mixes that are prone to moisture damage are an important part of the mixture design process.

Factors such as physical and chemical properties of the constituent materials, loading conditions, and environmental conditions influence the rate of moisture induced damage or moisture sensitivity of an asphalt concrete mix. Two important attributes related to material properties that determine the moisture sensitivity of a mix are:

- Adhesion between the bitumen and the aggregate in dry condition, and
- Degradation of adhesion between the bitumen and the aggregate in presence of water.

This dissertation follows the style of *Transportation Research Record.*

In this dissertation, the term “debonding” will be used to describe the loss of adhesion between bitumen and aggregate in the presence of water.

Several mechanisms responsible for adhesion and debonding between the bitumen and aggregate are identified in the literature. Most of these mechanisms are based on physio-chemical interactions between the bitumen and the aggregate, and can be classified into the following three broad categories: 1) mechanical adhesion, 2) physical adhesion, and 3) chemical bonding.

Mechanical adhesion is due to the surface texture of aggregates that causes mechanical interlocking of the bitumen binder with the aggregate. In this context, physical adhesion and debonding between the binder and aggregate is defined as the adhesion or debonding between these materials that is due to their surface free energies. Chemical reactions between the bitumen and the minerals on aggregate surface are also responsible for their adhesion and debonding. For example, reaction of weak acids from the bitumen with the aggregate results in formation of salts at their interface. The durability of this interface in the presence of water depends on the water solubility of these salts. Extensive laboratory testing using various sophisticated experimental and analytical techniques described in the literature support the development and understanding of these mechanisms. Despite the advanced understanding of fundamental mechanisms that cause moisture damage, little has been done to directly quantify physical or chemical properties that control these mechanisms.

Currently, many highway agencies use the ratio of one or more mechanical property (modulus, tensile strength) of an asphalt mix after it is moisture conditioned to the unconditioned mix as a measure of the moisture sensitivity of the mix. Although this methodology evaluates the moisture sensitivity of asphalt mixes based on their mechanical properties, it does not measure physical or chemical properties related to the mechanisms of adhesion and debonding. Also, according to the literature, the ability of this methodology to accurately predict field performance of asphalt concrete mixes is questionable.

This research is motivated by the understanding that, development of accurate and efficient methods to measure material properties related to adhesion and debonding in asphalt mixes will serve to bridge the gap between the current state of knowledge and

current state of practice to identify moisture sensitive mixes. This will in turn improve the efficiency the materials design process in identifying moisture sensitive asphalt mixes.

Objective and Scope of Study

The important causes of moisture damage in asphalt mixes related to material properties are, poor adhesion between the bitumen and the aggregate, and degradation of the adhesion in the presence of water (debonding). According to the literature, mechanical interlocking, physical adhesion, and chemical bonding are the three main types of mechanisms responsible for adhesion between the bitumen and the aggregate. Also, the durability of physical adhesion and chemical bonds in the presence of water determines the propensity of these materials to debond. The surface free energies of bitumen and aggregate can be used to quantify physical adhesion and debonding between these materials, which is correlated to the moisture sensitivity of the asphalt mix. The main objectives of this research are to:

- Identify, develop and validate test and analytical methods to accurately and efficiently determine the moisture sensitivity of asphalt mixes based on the surface free energy of bitumen and aggregates, and
- Introduce a methodology to quantify the combined affects of physical and chemical interactions responsible for adhesion between bitumen and aggregate using a micro calorimeter.

Fulfillment of the objectives of this research will enable users to quantify physical adhesion and debonding between various types of bitumen and aggregates using surface energies of these materials. This can be used to assess the contribution of material properties to the moisture sensitivity of asphalt mixes. Results from this study can also be used to quantify the cumulative effects of physical and chemical interactions on bitumen-aggregate adhesion.

Outline of the Dissertation

Chapter II of this dissertation presents a literature review of the mechanisms of adhesion and debonding between bitumen and aggregates. This chapter also presents the state of the art of practice in quantifying moisture sensitivity of asphalt mixes. There are two broad methodologies used to determine the moisture sensitivity of asphalt mixes. The first methodology is to conduct mechanical tests on the whole asphalt mix. For example, ratio of one or more mechanical property of the mix measured in dry condition and after moisture conditioning (accelerated moisture damage) is used to quantify its moisture sensitivity. This methodology is widely accepted by several agencies for identifying and eliminating moisture sensitive asphalt mixtures during the materials design process. Despite its ease of interpretation, this methodology can be at best described as empirical and is critiqued to be of poor reliability in the literature. The second methodology is to measure and use material properties of both the bitumen and aggregate to estimate moisture sensitivity of the mix based on the fundamental mechanisms responsible for adhesion and debonding. An example of this methodology is to estimate moisture sensitivity of asphalt mixes based on the adhesive bond strength between bitumen and aggregate, and their tendency to debond in the presence of water. Both these parameters can be computed by measuring surface free energies of the bitumen and aggregate. Chapter II presents a discussion on these methodologies, the need for adopting the latter methodology in the materials design process, and its relevance with this research.

In earlier studies the Wilhelmy plate method and the Universal Sorption Device were introduced as methods to determine the surface free energies of bitumen and aggregates, respectively. Part of the effort in this research was to modify these methods for use with bitumen and aggregates. Chapters III and IV describe the improvements in experimental and analytical procedures related to the use of these methods. The chapter also includes results and discussions on surface free energy components measured for a suite of bitumen and aggregate types.

The primary purpose of measuring surface energies of bitumen and aggregates is to estimate moisture sensitivity of asphalt mixes. Chapter V presents a description of the

bond energy parameters based on surface energies of these materials that can be used to estimate moisture sensitivity of asphalt mixes. The chapter also presents data that demonstrates the correlation between the proposed bond energy parameters and moisture sensitivity of asphalt mixes based on laboratory and field performance of asphalt mixes.

Adhesion and debonding between bitumen and aggregates is a result of the combined effects of physical adhesion due to surface free energy of these materials, chemical interactions at the interface, and mechanical interlocking. It is likely that physical adhesion due to the surface free energy of the constituent materials contributes predominantly to overall adhesion in most bitumen-aggregate systems. However, according to the literature, chemical interactions at the bitumen-aggregate interface in dry condition and in the presence of water can also be significant when chemically active aggregates such as limestone are used. Chemical bonding is also a significant contributor to adhesion when active fillers such as hydrated lime or liquid anti-strip agents are added to the bitumen. The second part of this research introduces the application of micro calorimeter as a fast and rapid tool to quantify physical and chemical interactions at the bitumen-aggregate interface. Chapter VI presents the theoretical background for the use of this technique and results that support the proposed applications of this technique. Chapter VII presents a comprehensive summary of the results from this research and recommendations for future work.

CHAPTER II

LITERATURE REVIEW

Moisture Sensitivity of Asphalt Mixes

Moisture induced damage in asphalt concrete pavements is a major cause for high maintenance costs of state and federal highways. Research to investigate the causes of moisture damage in asphalt concrete pavements and methods to prevent or reduce the impact of moisture damage has been continuing since the early 1950's. One or both of the following objectives have motivated most of this research:

- To understand the mechanisms that are responsible for moisture damage.
- To develop test methods that identify moisture sensitive asphalt mixes that are susceptible to failure before the completion of their intended service life.

An important material related property that influences moisture sensitivity of asphalt mixes is the quality of adhesion between bitumen and aggregate in dry condition and in the presence of water. In earlier studies, Rice [2], identified chemical reaction, mechanical bonding, and physical adhesion based on surface free energy as some of the mechanisms responsible for adhesion and debonding between bitumen and aggregate. Ishai and Craus [3] reiterate the significance of chemical, mechanical and physical interactions for adhesion and debonding. They demonstrate the role of physical and chemical interactions between the bitumen and aggregate to resist moisture damage using active fillers such as hydrated lime. Scott [4] demonstrates the importance of adhesion between polar functional groups from bitumen with the aggregate surface and influence of pH of the system in determining the moisture sensitivity of an asphalt mix. In a state of the art paper, Taylor and Khosla [5] critiqued the several mechanisms that are responsible for moisture damage of asphalt mixes. These mechanisms also fall in one or more of the three broad mechanisms of mechanical, physical or chemical interactions between bitumen and aggregate. The influence of these three broad mechanisms on the adhesion and debonding between bitumen and aggregate is reiterated in more recent literature [6,7,8].

Pocius [9] describes the contribution of surface roughness to improve adhesion in terms of mechanical interlocking between the bitumen and aggregate. Surface roughness in context of mechanical interlocking is significant at both a macroscopic and microscopic scale. Tarrar and Wagh [10] reiterate the importance of surface texture in mechanical bonding between the bitumen and aggregate. An effective way to quantify macroscopic roughness of aggregates is by measuring its surface texture using aggregate image analysis methods [11]. Surface texture of aggregates at a microscopic level can significantly differ from their surface texture at the macroscopic level. Specific surface areas of aggregates may be used as a measure of the surface texture of aggregates at the microscopic level. This research demonstrates that aggregates have a very broad range of specific surface areas (0.1 to 10 m^2/gm) for the same size fraction.

The chemical bonding model suggests that adhesion between the aggregate and bitumen is due to the formation of weak chemical bonds between various polar functional groups from the bitumen with the active functional groups on the surface of the aggregate. Petersen et al. [12] report the existence of eight different types of functional groups in bitumen typically used for asphalt mixes. Examples of weak acid type functional groups are carboxylic acids and anhydrides, and examples of weak base type functional groups are sulfoxides and pyridines. Jamieson et al. [13] reports that, surface functional groups on aggregate surfaces associated with high affinity for bitumen include elements such as aluminum, iron, magnesium and calcium. Elements associated with low bonding affinity include sodium and potassium. Little et al. [8] reports the formation of calcium or sodium salts when carboxylic acid from the bitumen chemically interacts with the available calcium or sodium on the aggregate surface. While sodium salts are readily soluble in water and accelerate moisture damage, calcium salts are relatively less soluble and therefore are more resistant to water induced damage. The utility of active fillers such as hydrated lime and liquid anti-strip additives to retard moisture induced damage is also explained based on similar chemical interactions. Details of specific interactions between various types of aggregates and bitumen functional groups are available in the literature.

Majidzadra and Brovold [14] explain that adhesion between bitumen and aggregate is a key factor that determines the moisture sensitivity of an asphalt mix. They

also report that a water-aggregate interface reduces free energy of the aggregate surface more than the water-bitumen interface. Therefore, displacement of bitumen from the bitumen-aggregate interface by water is a thermodynamically favorable phenomenon. Theories from thermodynamics related to surface free energy of materials can be used to determine the work of adhesion between two materials if their surface free energy components are known. In a three component system, this theory can be applied to determine the propensity of one liquid to displace another, from a solid surface based on their surface free energy components. Cheng [15] and Kim et al. [16] demonstrate the correlation between these thermodynamic parameters and the moisture sensitivity of asphalt mixes. They were able to compute these thermodynamic parameters by measuring the surface free energy components of the constituent bitumen and aggregates.

Mixture Response and Empirical Tests to Assess Moisture Sensitivity

Identifying moisture sensitive asphalt mixes is an important part of the materials selection and mix design process. Improper selection of materials and failure to accurately estimate the moisture sensitivity of a mix can result in premature failure of the asphalt pavement and excessive repair or reconstruction costs.

A common method to quantify moisture sensitivity of an asphalt mix is to determine the ratio of a mechanical property of the mix (eg. stiffness, tensile strength) before and after moisture conditioning [17,18,19]. The term moisture conditioning in this context refers to any of the several available techniques that are used to cause accelerated moisture damage in an asphalt mix specimen. The Lottman Test [17] and modified Lottman Test [20] are typical examples of this type of tests. In the Lottman test, several replicate samples of an asphalt mix are divided into three groups. The tensile strength of the first group of specimen, referred to as the control group, is measured using an indirect tension test. The second group of specimen is vacuum saturated with water for 30 minutes and the third group is vacuum saturated for the same duration followed by freezing at -18°C for 15 hours and at 60°C water bath for 24 hours. These two groups are referred to as the moisture conditioned groups and represent short term and long term resistance of the mix to moisture damage. The tensile strength of the moisture

conditioned mixes is also determined using the indirect tension test. The moisture sensitivity of the asphalt mix is reported as the ratio of the tensile strength of the moisture conditioned mix to the tensile strength of the unconditioned mix. Most other tests in this category are a variation of this basic algorithm of testing.

Several qualitative or subjective tests are also used to identify moisture sensitivity of asphalt mixes. Examples of such tests are the boiling water test [21] and the static immersion test [22]. In these tests, loose aggregates coated with bitumen are placed in boiling water for a specified period of time, after which they are removed and visually examined for the approximate percentage area of the bitumen coating that is retained on the aggregate surface.

Although empirical, most of these tests have the advantage that they quantify moisture sensitivity of the asphalt mix by taking into account the cumulative effect of material properties, mixture design parameters, and environmental conditions. However, despite these advantages and popularity, this methodology suffers from drawbacks such as,

- poor correlation with field performance,
- requirement of extensive test time,
- lack of measurement of material properties related to the mechanisms that cause moisture induced damage, and
- inability to explain causes for good or poor performance of an asphalt mix.

These shortcomings are well identified in the literature [23, 24]. It is evident from the literature review that the understanding of fundamental mechanisms responsible for moisture induced damage in asphalt mixes has greatly improved over the last five decades. However, the current state of practice to identify moisture sensitive asphalt mixes relies on mechanical tests that do not measure material properties related to these fundamental mechanisms.

Principles of Physical Adhesion Related to Surface Free Energy

Molecules in the bulk of a material are surrounded from all sides by other molecules, and as a result have a higher magnitude of bond energy compared to the

molecules on the surface. Therefore, work must be done in order to extract the molecules from the bulk and create a new area of surface molecules with excess energy. A formal definition of surface free energy is the work required to create unit area of a new surface of the material in vacuum, commonly denoted by the Greek letter γ. The term "free energy" is used in this context since the definition is based on work done, which is different from the total excess energy. The most common units of surface free energy are ergs/cm^2 or mJ/m^2. The terms surface tension, surface energy and surface free energy are often used interchangeably, although surface free energy is technically the correct term for use with principles of thermodynamics.

Several theories explain the molecular origin of surface free energy of solids. The Good-van Oss-Chaudhury (GVOC) theory is widely applied to explain the surface free energy components of various materials and determine these components by measuring work of adhesion of the material with other liquids or vapors [25, 26]. According to this theory, the total surface free energy of any material is divided into three components based on the type of molecular forces on the surface. These components are: 1) the non-polar component, also referred to as the Lifshitz-van der Waals (LW) or the dispersive component, 2) the Lewis acid component, and 3) the Lewis base component. The total surface free energy is obtained by combining these components as follows:

$$\gamma = \gamma^{LW} + \gamma^{+-} = \gamma^{LW} + 2\sqrt{\gamma^{+}\gamma^{-}} \qquad \textbf{(2.1)}$$

where, γ is the total surface free energy of the material, γ^{LW} is the Lifhsitz-van der Waals (LW) or dispersive component, γ^{+-} is the acid-base component, γ^{+} is the Lewis acid component, and γ^{-} is the Lewis base component. According to this theory, the work of adhesion, W_{AB} between two materials 'A' and 'B' in terms of their respective surface free energy components is given by:

$$W_{AB} = 2\sqrt{\gamma_A^{LW}\gamma_B^{LW}} + 2\sqrt{\gamma_A^{+}\gamma_B^{-}} + 2\sqrt{\gamma_A^{-}\gamma_B^{+}} \qquad \textbf{(2.2)}$$

For a bitumen-aggregate system, equation (2.2) can be used to compute their interfacial

work of adhesion if the surface free energy components of both these materials are known.

In order to quantify the propensity of one material to displace another, use of interfacial energies of these materials is necessary. Interface is a surface that forms a common boundary between two different materials. Figure 2.1 shows the idealized representation of an interface between two materials 'A' and 'B'. The molecules of both these materials at the interface are subjected to unequal forces as compared to their respective bulk molecules. This creates a misbalance of forces at the interface and results in interfacial energy between the two materials, represented as γ_{AB}. Analogous to the surface free energy in vacuum, the interfacial energy between two materials can be defined as the work required to create unit area of the interface.

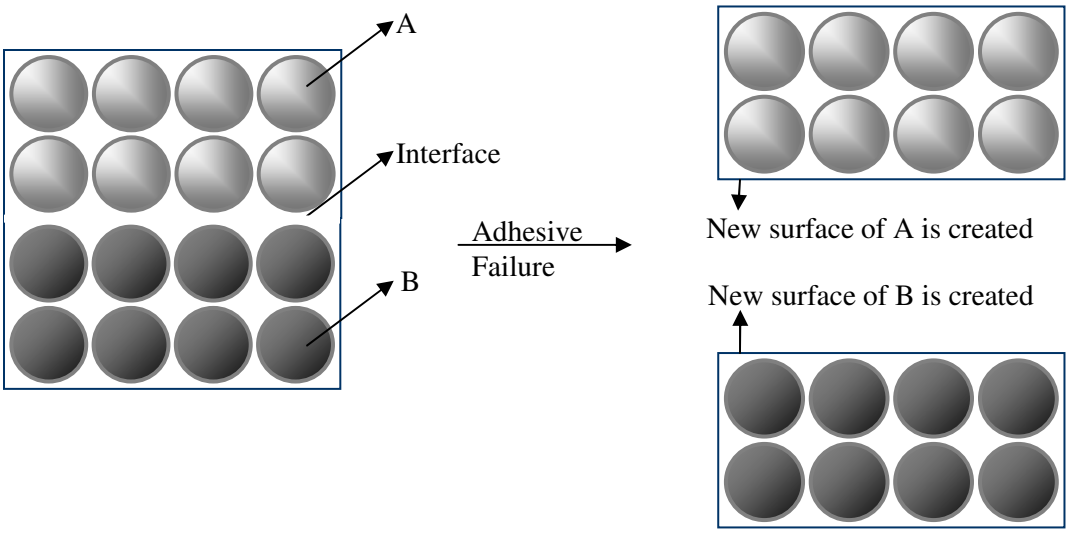

Figure 2.1. Adhesive Failure Between Two Materials 'A' and 'B'.

Consider a three phase system comprising of bitumen, aggregate, and water (Figure 2.2) represented by 'B', 'A', and 'W', respectively. The following processes occur when water displaces bitumen from the bitumen-aggregate interface. The interface of the aggregate with bitumen is lost and is associated with external work, $-\gamma_{AB}$, from the definition of interfacial free energy. Similarly, two new interfaces, between water and bitumen, and between water and aggregate are created during this process. The work

done for the formation of these two new interfaces is $\gamma_{WB} + \gamma_{WA}$. Therefore, the total work done for water to displace bitumen from the surface of the aggregate is, $\gamma_{WB} + \gamma_{WA} - \gamma_{AB}$. If the displacement process is thermodynamically favorable then it must be associated with an overall reduction in free energy of the system. In other words the total work done on the system during the displacement process must be less than zero. In this context, the energy associated with the displacement of bitumen by water from the bitumen-aggregate interface or debonding is referred to as the work of debonding and is expressed as:

$$W_{ABW}^{wet} = \gamma_{AW} + \gamma_{BW} - \gamma_{AB} \quad \textbf{(2.3)}$$

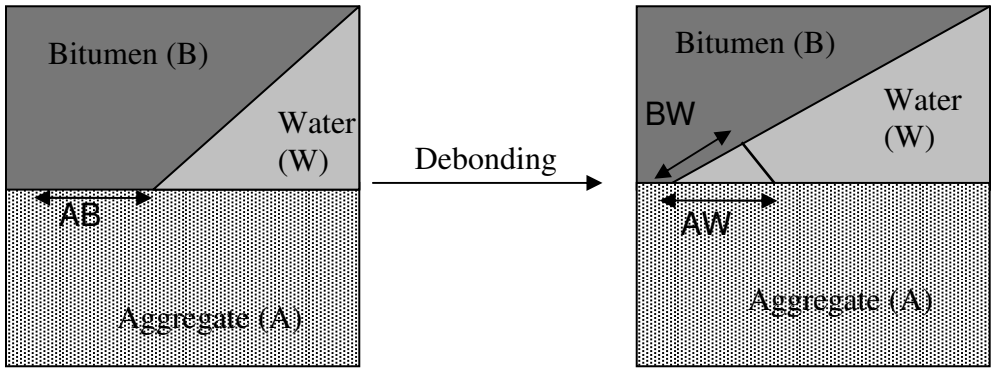

Figure 2.2. Displacement of Bitumen from Bitumen-Aggregate Interface by Water.

For practically all bitumen-aggregate systems the work of debonding, W_{ABW}^{wet}, is negative indicating that debonding in the presence of water is thermodynamically favorable. However, the magnitude of work of debonding can differ significantly depending on the material and surface properties of bitumen and aggregate. The higher the magnitude of work of debonding, the greater is the thermodynamic potential for water to cause debonding. Presence of external work, such as when external traffic loads applied to the pavement, further aggravates the debonding process.

Based on the above theory, adhesion between the bitumen and aggregate and their propensity to debond can be quantified in terms of their dry work of adhesion, W_{AB}, and work of debonding, W_{ABW}^{wet}, respectively. For an asphalt mix to be durable with low

sensitivity to moisture damage, the dry adhesive bond strength, W_{AB}, must be high and the magnitude of work of debonding, W_{ABW}^{wet}, must be low. Therefore, surface free energy components of bitumen and aggregate can be used to compute these energy parameters and estimate the moisture sensitivity of an asphalt mix based on the principles of physical adhesion. However, surface free energy components of solids such as bitumen and aggregates can only be determined indirectly by measuring their works of adhesion with different probe liquids with known surface free energy components. According to the literature there are several methods that can be used to determine the surface free energies of bitumen and aggregate. Table 2.1 presents a summary of these methods. Appendix A presents a more detailed discussion of the theories related to surface free energy, thermodynamics of various interfaces, and methods commonly used to measure surface free energies of solids.

Any error in determining the surface free energy components of bitumen and aggregates will be inherited by the calculated energy parameters and consequently effect the accuracy of prediction of moisture sensitivity of the mix based on this theory. Therefore, it is extremely important to select a test method and develop a protocol that is appropriate for these materials based on factors such as, accuracy of measurement, precision, speed and convenience of testing.

Table 2.1. Summary of Methods to Measure Surface Free Energy of Solids

Test Method	Working Principle	Results vs. Work of Adhesion	Suitable Materials	Remarks
Sessile Drop Method	Captures image of probe liquids dispensed on solid surfaces to determine contact angles.	Contact angles of the probe liquid with the solid.	Low energy surfaces such as polymers. Sample must have a physically smooth surface.	Expected surface free energy of the solid must be less than the surface free energy of probe liquids. Spreading pressure must be negligible Test is usually conducted in a static mode.
Wilhelmy Plate Method	Compares weight of a solid sample slide in air with its weight in a probe liquid after correcting for buoyancy to determine the contact angle of the liquid.	Contact angle of the probe liquid with the solid.	Low energy surfaces such as polymers. Sample must be prepared in the form of a smooth surface on a suitable substrate.	Expected surface free energy of the solid must be less than the surface free energy of probe liquids. Spreading pressure must be negligible Test is conducted in a dynamic mode. Measures both advancing and receding contact angles.
Adsorption Method	Determines the adsorption isotherm of various solids with vapors of probe liquids. The adsorption isotherm is used to calculate the surface area of the solid and spreading pressure of the vapor with the solid surface.	Equilibrium spreading pressure of vapors of the probe vapor liquids with the solid.	High energy solids. Quantity of the sample must provide sufficient surface area for adsorption that can be precisely measured by the instrument.	Preconditioning the sample is important to ensure all physically adsorbed molecules are removed from the surface. This test is inherently time consuming.

Table 2.1. (Continued)

Test Method	Working Principle	Results vs. Work of Adhesion	Suitable Materials	Remarks
Inverse gas chromatogr -aphy	Measures the retention time for vapors of various probe liquids as it interacts with the solid.	Retention time and retention volume.	High or low energy solids. Choice of capillary or larger diameter columns to hold sample can be made depending on the nature of the sample.	Since the test is conducted at an infinitely diluted condition the concentration of the probe vapors is very low and therefore it interacts with only high energy "spots" on the solid surface and therefore this test will usually yield slightly higher values compared to other methods.
Micro calorimeter	Measures enthalpy of immersion of solids in various probe liquids. The free energy of immersion is obtained from the enthalpy of immersion by making suitable approximations for the entropy term or determining the contribution from entropy by testing at different temperatures.	Free energy of immersion.	High energy solids are best suited. Preconditioning requirements are the same as for adsorption method. Sufficient specific surface area of the sample must be available to generate heat of immersion that can be measured precisely using a Micro calorimeter.	This test is much faster than the adsorption measurements but the effect of entropy must be accommodated before determining the surface free energy components from work of adhesion equations.

Material Property Tests to Assess Moisture Sensitivity

A possible solution to overcome the drawbacks associated with the mechanical tests currently used to identify moisture sensitive mixes is to include the use of material properties associated with the fundamental mechanisms of adhesion and debonding in conjunction with these tests. The three main mechanisms related to adhesion and debonding identified previously are, physical adhesion, chemical interactions at the interface, and mechanical interlocking. Accordingly, tests and analytical methods to measure material properties related to moisture sensitivity of asphalt mixes must focus on one or more of these mechanisms. This section reviews some of the work done in this area and the need for further development of test procedures.

Test Methods to Quantify Physical Adhesion

Surface energies of bitumen and aggregate can be used to estimate the moisture sensitivity of asphalt mixes based on physical adhesion. Cheng [15] used the Wilhelmy plate (WP) method and the Universal Sorption Device (USD) to measure surface energies of bitumen and aggregates respectively. Cheng demonstrates the use of surface energies of these materials to calculate the dry work of adhesion between the bitumen and aggregate, the work of debonding when water displaces bitumen from the bitumen-aggregate interface, and the correlation of these parameters with the moisture sensitivity of asphalt mixtures. However, results from this study are limited and do not rigorously examine the accuracy or suitability of the test protocol adopted for measuring surface energies of bitumen and aggregate.

Test Methods to Quantify Physical and Chemical Adhesion

According to the literature [27-30], chemical interactions at the bitumen-aggregate interface may also contribute to their adhesion and debonding in addition to physical adhesion due to their surface free energies. Evidence of such interactions is supported by several analytical experiments. Typically these experiments are very time consuming, require a substantial infrastructure, and cannot be performed on a routine basis.

Petersen [29] and Curtis et al. [27] report that interaction between polar groups from the bitumen with the aggregate surface is largely responsible for adhesion of these materials. Curtis et al. [31] reports the use of model compounds to represent the various polar functionalities in the bitumen. However, the methodologies adopted in these studies do not directly quantify the strength of interaction between the functional groups and various aggregates. Ensley et al. [32], Ensley [33], and Ensley and Scholz [34], use a micro calorimeter to measure the enthalpy of immersion of different aggregate types with liquid bitumen at high temperatures. They demonstrate the relationship between measurements from the micro calorimeter and the tenderness of asphalt mixes. Although the enthalpy of immersion is directly related to the magnitude of interfacial bonding between these materials, it does not differentiate between physical and chemical interactions that cause bonding. It is hypothesized that the micro calorimeter, combined with the work of adhesion computed using surface free energies, can be used to determine the relative contributions of physical and chemical interactions for different bitumen-aggregate systems. An important advantage of using the micro calorimeter is that it unifies the effects of both physical and chemical interactions into a single energy parameter, the enthalpy of immersion. This information can be used to judiciously select additives for bitumen and design asphalt mixes that are more resistant to moisture damage.

Problem Statement

Moisture damage in hot mix asphalt is the result of combination of several factors including material properties, environmental conditions and nature of loading. Physical adhesion, chemical interactions and mechanical interlocking are three broad mechanisms that can be used to explain the adhesion and debonding between the bitumen and aggregate in an asphalt mix based on material properties. The current practice to identify moisture sensitive asphalt mixes is by conducting mechanical tests on the whole mix. This approach is associated with several disadvantages that can be overcome if material properties relevant to the mechanisms of adhesion and debonding are also included in the materials selection and design process.

Surface free energy is a material property that can be used to quantify the dry work of adhesion and work of debonding, which can in turn be used to estimate the moisture sensitivity of asphalt mixes. Use of accurate test and analytical methods is essential to apply this theory to identify material combinations that may result in a moisture sensitive asphalt mix. The Wilhelmy plate method and the Universal Sorption Device were introduced in earlier research as possible methods to measure the surface free energies of bitumen and aggregate, respectively. However, a significant effort was still required in tailoring these methods and applying them to accurately measure the surface properties of bitumen and aggregates. A part of the effort in this research was to,

- develop methods to measure surface free energies of bitumen and aggregate with acceptable precision and accuracy,
- accurately measure specific surface areas of aggregates, and
- introduce and validate parameters based on these properties that can be used to estimate moisture sensitivity of asphalt mixes.

According to the literature chemical interactions are also an important mechanism of adhesion, especially when chemically active minerals such as limestone are used or when active fillers or liquid anti-strip agents are added to the bitumen. Therefore it is important that the physical adhesion between bitumen and aggregates due to their surface energies be considered in conjunction with the possibility of other mechanisms such as chemical interactions. The second part of this research introduces the use of a micro calorimeter to measure the total interaction energy between bitumen and aggregates using a multi-faceted approach.

CHAPTER III

WILHELMY PLATE METHOD

Problem Description

The three surface free energy components of bitumen, aggregates, and water are the inputs for computing the work of adhesion and work of debonding between bitumen and aggregate. The surface free energy components of bitumen can be determined by measuring the contact angle of the bitumen with different probe liquids of known surface free energy components. The Wilhelmy plate method is a fast and efficient technique that measures the contact angles of bitumen with various probe liquids. Cheng [15] used this technique to measure the contact angles of solids with three different probe liquids to determine its surface free energy components. Results from Cheng [15] indicate that further development of this technique is required before it can be used to accurately estimate surface free energy components of bitumen. For example, magnitude of the base component of surface free energy reported for some of the bitumen types was very high and does not reconcile well with their chemical properties. In some cases, square roots of the calculated surface free energy components of the binders were large negative numbers that do not have any physical interpretation. The methodology was also extremely sensitive to the experimentally measured contact angles and the accuracy of results required validation. The methods developed in this research address these issues and present a test and analytical procedure that can be used on a routine basis to determine the surface free energy components of bitumen.

Background and Theory

Based on the Young-Dupre' equation, Good, Van Oss, and Chaudhury, (GVOC) [25, 26] proposed the following relationship between the Gibbs free energy of adhesion, ΔG_{LS}^{a} , work of adhesion, W_{LS}, contact angle, θ, of a probe liquid, *L*, in contact with a solid, *S*, and surface free energy characteristics of both the liquid and solid:

$$-\Delta G^{a}_{L,S} = W^{a}_{L,S} = \gamma_L(1+Cos\theta) = 2\sqrt{\gamma_S^{LW}\gamma_L^{LW}} + 2\sqrt{\gamma_S^{+}\gamma_L^{-}} + 2\sqrt{\gamma_S^{-}\gamma_L^{+}} \quad \textbf{(3.1)}$$

Equation (3.1) is used to calculate surface free energy components of bitumen by measuring contact angles. In this equation, the solid represented by suffix 'S' is the bitumen under consideration and the liquid represented by suffix 'L' is any probe liquid. A probe liquid in this context is defined as a liquid for which the three surface free energy components are known from existing literature or standards and does not effect the physical properties of bitumen surface. If the square roots of the three unknown surface free energy components of the bitumen are represented as x_1, x_2, and x_3, then equation (3.1) can be rewritten as follows:

$$\gamma_L(1+Cos\theta) = \left(2\sqrt{\gamma_L^{LW}}\right)x_1 + \left(2\sqrt{\gamma_L^{-}}\right)x_2 + \left(2\sqrt{\gamma_L^{+}}\right)x_3 \quad \textbf{(3.2)}$$

The contact angle of a probe liquid with the bitumen (measured experimentally) and surface free energy components of the probe liquid (from literature or standard tables) are substituted into equation (3.2) to generate a linear equation with three unknowns x_1 through x_3. It follows that contact angles of a bitumen measured with three different probe liquids will result in a set of three linear equations that can be solved for the unknowns x_1, x_2, and x_3, which are the square roots of the surface energy components of bitumen.

In 1863, Wilhelmy first proposed indirect contact angle measurement by immersing a plate into a liquid and deriving the angle from the measured force [35]. This is a dynamic contact angle measurement technique since the plate is in motion (moving at a few microns per minute) throughout the process. From simple force equilibrium considerations, the difference between weight of a plate measured in air and partially submerged in a probe liquid, ΔF, is expressed in terms of buoyancy of the liquid, liquid surface energy, contact angle, and geometry of the plate. The contact angle between the liquid and surface of the plate is calculated as follows:

$$\cos\theta = \frac{\Delta F + V_{im}(\rho_L - \rho_{air} g)}{P_t \gamma_L} \quad \textbf{(3.3)}$$

where, P_t is the perimeter of the bitumen coated plate, γ_L is the total surface energy of the liquid, θ is the dynamic contact angle between the bitumen and the liquid, V_{im} is the volume immersed in the liquid, ρ_L is the density of the liquid, ρ_{air} is the air density, and g is the local gravitational force.

Figure 3.1 illustrates a schematic of the dynamic contact angle analyzer (DCA 315, Thermo Chan Instruments) used in this research. Two different contact angles are obtained during the test as the plate in immersed into the liquid up to a predetermined depth, and as it recedes from the liquid after being immersed. Theoretically, for a surface that does not undergo any permanent change by coming into contact with the probe liquid, these two angles must be the same. However, in most cases a hysteresis effect is seen in the force measurements due to differences in the advancing and receding contact angles. Figure 3.2 illustrates a typical hysteresis effect obtained during force measurements.

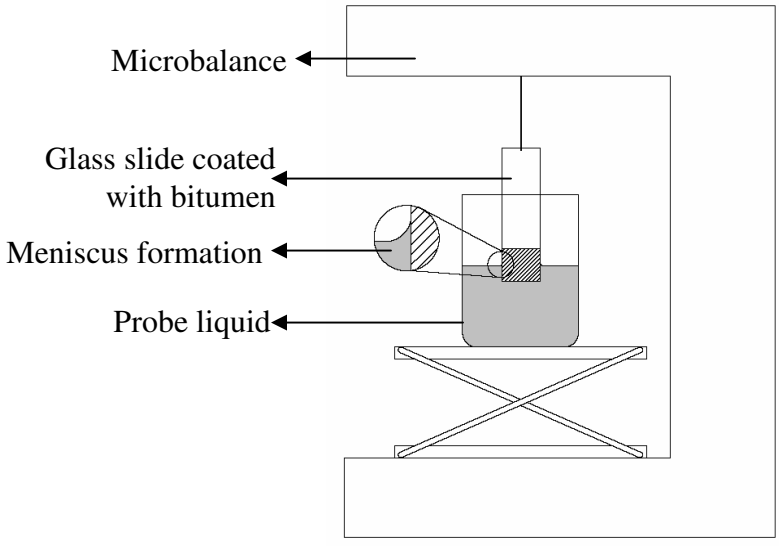

Figure 3.1. Schematic of a Wilhelmy Plate Device.

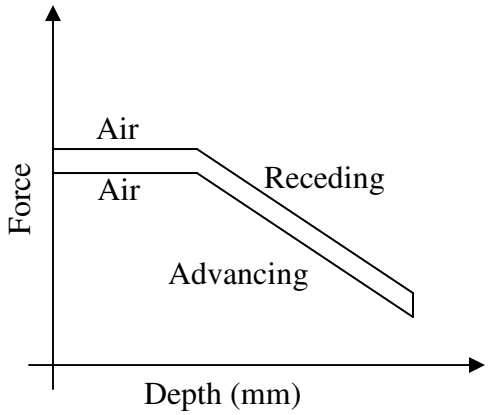

Figure 3.2. Hysterisis in Advancing and Receding Force Measurements.

Development of Test Method

Based on literature review it was determined that two important elements to use this method successfully to determine surface free energy components of bitumen are, 1) selection of appropriate probe liquids, and 2) ensuring that the measured contact angles satisfy the requirements to be used with the selected theory.

Selection of Probe Liquids

A liquid or vapor can be used as a probe if,

- its three surface energy components based on the GVOC theory are known,
- it is homogenous and pure, and
- it does not chemically interact (react or dissolve) with the solid surface that is being measured.

There are approximately sixty liquids with values of the surface energy components based on the GVOC theory that are reported in the literature. A careful screening and testing of various liquids with bitumen revealed that most of these liquids dissolve bitumen to some extent. Only five liquids, distilled water, glycerol, formamide, ethylene glycol, and methylene iodide (diiodomethane), were short listed as appropriate

probes for testing bitumen.

From equation (3.2), three different probe liquids are required to determine the three unknown surface free energy components of any bitumen. Although theoretically correct, an improper choice of liquids combined with small experimental errors can significantly affect the calculated surface free energy components [36]. For example, if two or more of the probe liquids have similar surface free energy components, then the calculated surface free energy components of bitumen will be unduly sensitive to small errors in measurement of contact angles. A mathematical measure of this sensitivity is referred to as the condition number. Since, the condition number is a function of the surface free energy components of the selected probe liquids, it can be computed even before conducting the experiments. A large condition number indicates that the calculated results are very sensitive to small experimental errors and vice versa. Appendix B presents the mathematical methods used to calculate the condition number for various combinations of probe liquids in this research.

The three probe liquids that were used in the previous research were water, formamide and glycerol [15]. The condition number for this set of liquids is 18.6 and therefore the calculated surface free energy components of bitumen based on these three probe liquids can accumulate significant errors even if the errors in the measured contact angles are small. If formamide is replaced by methyleneiodide then the condition number reduces to 4.9 which reduces the sensitivity of the computed results significantly. In order to minimize errors and ensure satisfactory results, all five liquids were used as probes. Using five liquids introduces redundancy since there are only three unknowns (surface free energy components of bitumen) and five linear equations (one equation by measuring contact angle with each probe liquid), however, using five liquids reduces the sensitivity and improves reliability of the calculated results.

Validity of Contact Angles

Equation (3.2) is based on the Young's equation for contact angles. In order to use this equation to compute the surface free energy components of the solid, it is important to ensure that the contact angles measured experimentally satisfy the requirements necessary for Young's equation to be valid. One of the important

requirements is that the probe liquid is pure, homogenous and does not chemically interact with bitumen. Certain forms of chemical interactions are easily identifiable, such as when the probe liquid dissolves the bitumen. However, in some cases complex interactions between the bitumen and probe liquid might not be apparent and other methods to screen liquids must be considered. The following paragraphs describe a method based on a detailed study by Kwok et al. [37, 38].

Kwok and Neumann use a technique called the axisymmetric drop shape analysis profile (ADSA-P) to determine contact angle of probe liquids over different polymer surfaces. This technique records the drop profile of a probe liquid in three stages:

- as the liquid is being dispensed till the drop reaches the expected size,
- as the liquid drop is retained in equilibrium over the solid surface, and
- as the liquid drop recedes by reverse action back into the plunger.

The dynamic means of recording data enabled Kwok and Neumann to identify liquids that demonstrate anomalous behavior such as excessive stick slip and change in contact angle of a stationary drop over time. They regard contact angle data from such liquids as "meaningless". They also recommend that liquids demonstrating such anomalous behavior are in violation of one or more of the assumptions required for applying Young's equation, and must not be used to calculate surface energies. In their experiment they used up to 17 liquids on various polymer surfaces. They also report that a plot of $\gamma_L Cos\theta$ versus γ_L, for a given solid with various liquids yields a smooth curve. They showed that the points corresponding to liquids undergoing complex interactions in their tests did not lie on this smooth curve. As a corollary, it can be expected that if a liquid deviates from a smooth curve plot of $\gamma_L Cos\theta$ versus γ_L, then data from that liquid must not be included for calculation of surface energies. Some other researchers argue that the plot of $\gamma_L Cos\theta$ versus γ_L might not necessarily be a smooth curve. Deviations of individual points are possible due to polar or acid-base interactions between the solid surface and the liquid. Based on the knowledge of bitumen chemistry, bitumen has polar function groups corresponding to weak acids or weak bases. Therefore, it is reasonable to expect that the acid-base components of bitumen will not be very large and the significant contribution to work of adhesion will be due to the LW component of surface free

energy. Without rejecting either point of view, the plot of $\gamma_L Cos\theta$ versus γ_L must at least approximate a smooth curve. This requirement was used to screen and validate the accuracy of measured contact angles from the five probe liquids.

Test Method

Microscope glass slides (24mm x 60mm, No.1.5) are used as substrates for preparation of bitumen surfaces. As mentioned earlier, five probe liquids were used in this research and three replicate slides of the same bitumen were tested with each probe liquid. A total of at least 15 slides for each bitumen type were prepared as follows. A tin with an approximate capacity of 50g, pre-filled with bitumen, was placed in an oven at the mixing temperature of the bitumen under consideration. The tin with bitumen was removed from the oven after about one hour, stirred, and placed on a hot plate to maintain the desired temperature during the coating process. The end of the glass slide intended for coating was passed six times on each side through the blue flame of a propane torch to remove any moisture, after which it was dipped into the molten bitumen to a depth of approximately 15 mm. Excess bitumen was allowed to drain from the plate until a very thin (0.18 to 0.35 mm) and uniform layer of at least 10 mm remained on the plate. A thin coating is required to reduce variability of the results. The plate was then turned with the uncoated side downwards and carefully placed into a slotted slide holder. If necessary, the heat-resistant slide holder, with all the coated slides was placed in the oven after coating for 15 to 30 seconds to obtain the desired smoothness. The bitumen-coated plates were placed in a desicator overnight.

A DCA 315 microbalance with WinDCA software from Thermo Cahn Instruments was used to perform the test, acquire force data, and calculate contact angles. Balance calibration was performed with a 500 mg weight according to the manufacturer's specification. The five probe liquids (HPLC grade, Sigma-Aldrich) used for these experiments are distilled water, glycerol, formamide, ethylene glycol, and methylene iodide (diiodomethane). Important method parameters include the total surface free energy of the probe liquids, local gravitational force, plate speed, and penetration depth. A speed of 20 microns per second and penetration depth of 5 mm was used in these experiments. A slow speed is required to ensure quasi-equilibrium conditions, which

approaches the assumption of equilibrium. The width and thickness were measured to an accuracy of 0.01 mm for calculation of the slide perimeter. The slide was suspended from the micro balance using a crocodile clip – hook assembly. It was ensured that the glass slide was suspended at right angles to the base of the balance. A glass beaker was filled with the probe liquid to a depth of at least 10 mm and placed on the balance stage. The stage was raised or lowered during the test at the desired rate via a stepper motor controlled by the Win DCA software. The weight of the slide measured by the microbalance was recorded continuously during the advancing (stage is raised to dip the slide) and receding (stage is lowered to retract the slide from the liquid) process. A dark beaker was used for methylene iodide since this liquid is light sensitive. Liquid surface tension data suggests that a fresh sample should be used for each set comprising of three replicate slides.

After data acquisition, manual analysis of the force-distance data was performed. Buoyancy correction based on slide dimensions and liquid density can introduce unwanted variability into the resulting contact angles. To eliminate these effects, a regression analysis of the buoyancy line and extrapolation to the force at zero depth was performed. It is important in this procedure to select a representative area of the line for regression analysis.

Calculating Surface Free Energy Components

For any given ith probe liquid L_i, equation (3.2) can be rewritten as:

$$\sqrt{\gamma_{Li}^{LW}}\,x_1 + \sqrt{\gamma_{Li}^{-}}\,x_2 + \sqrt{\gamma_{Li}^{+}}\,x_3 = \frac{1}{2}\gamma_{Li}(1+Cos\theta_i) \qquad \textbf{(3.4)}$$

In equation (3.4), x_1 through x_3 are the square roots of the unknown bitumen surface free energy components and other terms are as described earlier. For *m* liquids equation (3.4) can be written in matrix form as:

$$\begin{bmatrix} \sqrt{\gamma_{L1}^{LW}} & \sqrt{\gamma_{L1}^{+}} & \sqrt{\gamma_{L1}^{-}} \\ \sqrt{\gamma_{L2}^{LW}} & \sqrt{\gamma_{L2}^{+}} & \sqrt{\gamma_{L2}^{-}} \\ \dots & \dots & \dots \\ \sqrt{\gamma_{Lm}^{LW}} & \sqrt{\gamma_{Lm}^{+}} & \sqrt{\gamma_{Lm}^{-}} \end{bmatrix}_{mx3} \begin{bmatrix} x_1 \\ x_2 \\ x_3 \end{bmatrix}_{3x1} = \frac{1}{2} \begin{bmatrix} \gamma_{L1}^{Tot}(1+Cos\theta_1) \\ \gamma_{L2}^{Tot}(1+Cos\theta_2) \\ \dots \\ \gamma_{Lm}^{Tot}(1+Cos\theta_m) \end{bmatrix}_{mx1} + \begin{bmatrix} e_1 \\ e_2 \\ \dots \\ e_m \end{bmatrix} \quad \text{or,}$$

$$\mathbf{A\,x - B = E} \qquad \mathbf{(3.5)}$$

In equation (3.5), ***E*** is a column error matrix. Theoretically, ***E*** is a null matrix, however, due to experimental errors and over determinacy of the ***A*** matrix, it can have real non zero values. ***A*** matrix is known from the probe liquid surface free energy components and ***B*** is known from the measured contact angles. The unknown matrix **x** is determined by an iterative method to minimize the sum or squares of errors (elements of **E** matrix). The elements of the **x** matrix can then be squared to obtain the three surface free energy components of bitumen. Alternatively, equation 3.5 can be written as:

$$\mathbf{x = A^{-1}(B + E)} \qquad \mathbf{(3.6)}$$

When, **A** is not a square matrix, i.e. when m>3, which is true in this case, $\mathbf{A}^{-1}$ is substituted by $\mathbf{A}^{+}$ which is the Moore-Penrose inverse. The Moore-Penrose inverse matrix, $\mathbf{A}^{+}$, can be determined by singular value decomposition of the **A** matrix. An analytical method to compute the error in the calculated surface free energy components based on the errors in contact angle measurement was developed. Appendix B presents details of these analytical methods.

Results

Surface energies of nine different types of bitumen were measured in this research. These materials were obtained from the Strategic Highway Research Program, Materials Reference Library (MRL), Reno, Nevada. The selected bitumen, identified by a three letter alphabetic code, was from different sources and represents a range of different chemical compositions. As mentioned earlier, in order to increase the accuracy

and reliability of the calculated surface free energy components, it is desirable to have as many probe liquids as possible. However, based on the criteria for selection of probe liquids, only five liquids could be selected as probes for measuring contact angles. Table 3.1 presents the surface free energy components of these five probe liquids. Tables 3.2 and 3.3 present the advancing and receding contact angles, obtained using the Wilhelmy plate method.

Table 3.1. Surface Free Energy Components of Probe Liquids

Liquid	γ (Total)	γ^{LW}	γ^{+}	γ^{-}
Water	72.8	21.8	25.5	25.5
Glycerol	64.0	34.0	3.92	57.4
Formamide	58.0	39.0	2.28	39.6
Ethylene Glycol	48.0	29.0	1.92	47.0
Methylene Iodide	50.8	50.8	0.0	0.0

Table 3.2. Advancing Contact Angles using Wilhelmy Plate Method

Bitumen	Methylene-iodide		Glycerol		Ethylene Glycol		Water		Formamide	
	Avg.	CV	Avg.	CV	Avg.	CV	Avg.	CV	Avg.	CV
AAB	41.1	2	63.2	1	57.3	0	81.2	1	63.4	0
ABD	43.5	4	34.5	1	51.5	0	47.9	1	40.1	2
AAM	43.4	5	21.3	1	51.1	3	45.8	1	41.6	1
AAF	41.7	1	67.5	0	58.8	0	86.7	2	67.0	1
AAH	40.8	2	61.2	1	59.6	1	85.3	1	76.1	2
AAL	42.6	2	39.9	0	49.9	2	41.2	3	30.5	2
ABL	37.0	2	64.5	2	53.3	1	75.8	3	65.7	0
AAD	42.1	1	70.2	0	65.0	2	86.1	1	74.1	1
AAE	38.4	1	45.9	1	48.6	0	49.3	2	37.1	1

Table 3.3. Receding Contact Angles Using Wilhelmy Plate Method

Bitumen	Methylene-iodide		Glycerol		Ethylene Glycol		Water		Formamide	
	Avg.	CV	Avg.	CV	Avg.	CV	Avg.	CV	Avg.	CV
AAB	41.1	2	63.2	4	57.3	1	81.2	1	63.4	0
ABD	43.5	1	34.5	4	51.5	3	47.9	1	40.1	4
AAM	43.4	15	21.3	27	51.1	1	45.8	3	41.6	7
AAF	41.7	1	67.5	1	58.8	0	86.7	1	67.0	1
AAH	40.8	2	61.2	0	59.6	1	85.3	1	76.1	1
AAL	42.6	1	39.9	5	49.9	1	41.2	6	30.5	4
ABL	37.0	7	64.5	6	53.3	3	75.8	4	65.7	4
AAD	42.1	3	70.2	0	65.0	0	86.1	2	74.1	1
AAE	38.4	3	45.9	2	48.6	3	49.3	6	37.1	3

In order to validate the accuracy of results obtained from the Wilhelmy plate method using the Neumann criteria, a simple straight line was fit to between $\gamma_L Cos\theta$ versus γ_L for each bitumen type. Although a second degree polynomial is typically recommended to fit the data, in this case, contribution of the second order term was negligible. The square of the difference between ordinates of the measured point and the curve was used to quantify the deviation of each point (representing each probe liquid) from the curve. For seven bitumen out of nine, the deviation was highest for Formamide. For the other two bitumen (AAB and ABD) the deviation was very high for both diiodomethane and ethylene glycol. When these deviations were computed by excluding formamide the best fit parameters improved for all bitumen including AAB and ABD. Based on this analysis it is inferred that there might be some undesirable interactions between the selected bitumen and formamide. Therefore, contact angles measured using formamide were not included to calculate surface free energy components of the bitumen. Also, results from this analysis indicate that the contact angles measured using the Wilhelmy plate method corroborate well with the theoretical requirements for contact angle measurement recognized in the literature.

Advancing and Receding Contact Angle

Theoretically the advancing and receding contact angles must be the same for a given solid surface. Kwok et al. [37, 38] state that physical roughness of the solid surface and chemical heterogeneity are two possible causes for the hysteresis. If hysteresis is due to surface roughness, then contact angles obtained from the test are meaningless since they do not satisfy the basic requirement of a smooth solid surface to apply Young's equation. On the other hand, if hysteresis is due to chemical heterogeneity of the solid surface, then the measured advancing contact angle can still be considered as a good approximation of the equilibrium contact angle to calculate surface free energy components [37]. For the Wilhelmy plate test, the bitumen samples were prepared by coating a thin glass slide with hot molten bitumen. The sample preparation was done at high temperatures when the bitumen is in a liquid state. As the sample cools, the same fundamental forces that responsible for surface free energy will ensure that the surface area is minimized and the surface does not have any roughness. On the other hand, the chemical heterogeneity of bitumen is well established. Therefore it seems reasonable to attribute the hysteresis of bitumen contact angles to chemical heterogeneity rather than physical roughness.

The use of advancing contact angles to calculate the surface free energy components responsible for adhesion is supported by the literature [26, 39]. However, some work by other researchers [40, 41] indicates that the receding contact angles can also be used as an index of surface free energy. Considering both advancing and receding contact angle data in Tables 3.2 and 3.3, the coefficient of variation between 0 percent and 4.5 percent is seen, with the exception of receding angles obtained for bitumen AAM-1. Standard deviations in the order of 1˚ are considered excellent and attainable, while values up to 3˚ are not uncommon in the literature.

Reproducibility in terms of standard deviation of the contact angles was used as a measure of precision of the technique. The pooled standard deviations for both the receding and advancing angles for each probe liquid was estimated under the assumption of common precision for different materials. Table 3.4 presents this information and is valid for conditions of one operator and one laboratory.

Table 3.4. Pooled Standard Deviations in Degrees for Contact Angles

Mode	Water	Methylene Iodide	Ehtylene Glycol	Glycerol	Formamide
Advancing	1.4	1.9	0.9	0.5	0.9
Receding	1.1	2.9	0.8	2.9	1.5

Surface Free Energy Components and Interpretation

Tables 3.5 and 3.6 present the total and individual surface free energy components of the nine bitumen based on the advancing and receding contact angles, respectively. The surface free energy components and errors were calculated using the procedures described earlier and detailed in Appendix B. The four probe liquids used for calculation were water, diiodomethane, ethylene glycol, and glycerol. The range of total surface free energy of bitumen calculated using advancing contact angles varies from 13.6 to 32.4 ergs/cm^2. This range using the receding contact angles varies from 31.3 to 47.6 ergs/cm^2. Further, the main contribution to the total surface free energy is due to the LW component. This is in line with the fact that bitumen is primarily a non-polar material.

In some cases it was observed that the square root of a bitumen surface free energy component, typically the acid or base component, was still negative. However, the magnitude of the component in such cases was very small and could be neglected or considered to be equal to 0 for all practical purposes. Based on this observation, it was concluded that the negative results of large magnitude from the previous studies was largely due to inadequate selection of probe liquids. To avoid negative solutions, the minimization of last squares of errors was repeated with the constraint that the solutions must be non-negative. Differences between the results from the constrained and unconstrained least squares regression were minimal.

Table 3.5. Surface Free Energy Components Based on Advancing Contact Angles

No.	Bitumen	Surface Free Energy Components (ergs/cm^2)			Total (ergs/cm^2)	Standard Deviation (ergs/cm^2)		
		LW	Acid	Base		LW	Acid	Base
1	AAB	13.58	2.68	0.00	13.6	0.7	0.3	0.0
2	ABD	32.45	0.40	0.00	32.5	1.0	0.1	0.0
3	AAM	24.85	0.20	0.00	24.9	1.2	0.1	0.0
4	AAF	21.35	0.79	0.00	21.4	0.7	0.1	0.0
5	AAH	20.25	1.35	0.00	20.3	0.7	0.2	0.0
6	AAL	31.29	0.00	0.00	31.3	0.8	0.0	0.0
7	ABL	18.47	1.76	0.02	18.8	0.8	0.3	0.1
8	AAD	18.47	0.06	0.10	18.6	0.4	0.0	0.1
9	AAE	26.10	1.99	0.00	26.1	0.5	0.2	0.0

Table 3.6. Surface Free Energy Components Based on Receding Contact Angles

No.	Asphalt	Surface Free Energy Components (ergs/cm^2)			Total (ergs/cm^2)	Standard Deviation (ergs/cm^2)		
		LW	Acid	Base		LW	Acid	Base
1	AAB	38.08	0.00	6.60	38.1	0.7	0.0	0.6
2	ABD	37.67	0.80	30.57	47.6	0.6	0.1	1.4
3	AAM	31.25	0.00	51.04	31.3	1.6	0.0	2.5
4	AAF	38.38	0.01	3.52	38.8	0.5	0.0	0.5
5	AAH	37.43	0.34	5.52	40.2	0.7	0.1	0.7
6	AAL	38.04	0.00	44.50	38.0	0.6	0.0	2.7
7	ABL	40.32	0.00	8.96	40.3	1.2	0.0	1.6
8	AAD	35.45	0.00	10.45	35.5	0.7	0.0	1.2
9	AAE	42.41	0.04	43.07	45.0	5.0	0.1	3.2

A comparison between Tables 3.5 and 3.6 indicates that a very large difference in the acid component, γ^+, and the base component, γ^-, exists depending on whether the advancing or receding contact angle was used to calculate the value. The aim of surface free energy measurements is not merely to distinguish between different bitumen types but to distinguish between bond strengths with different aggregates in wet and dry condition. The surface free energy components from advancing contact angles are used for computing the adhesive bond strength of the bitumen with the aggregate. Most bitumen are regarded to contain weak acid and weak base functional groups. The small magnitude of acid and base components of surface free energy from the advancing contact angles is in agreement with this. Therefore, the polar components computed from the advancing contact angle can be considered as a better representation of the neat bitumen properties.

Figures 3.3 and 3.4 graphically illustrate the LW and acid components of surface free energy along with their standard deviations based on the advancing contact angles. The base component for these bitumen is negligible and is not shown. Data in the figures indicates that the methodology is sensitive to distinguish the components between different types of binders.

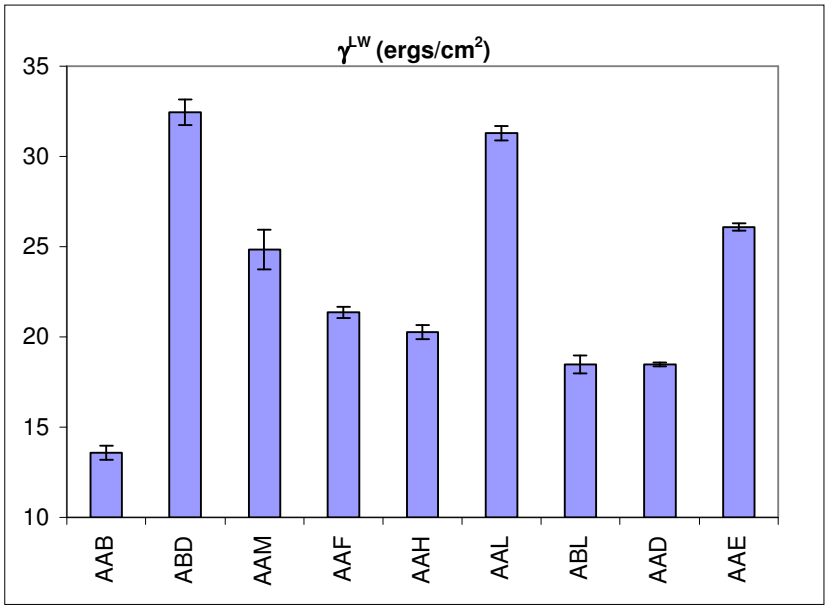

Figure 3.3. LW Component of Bitumen Surface Free Energy.

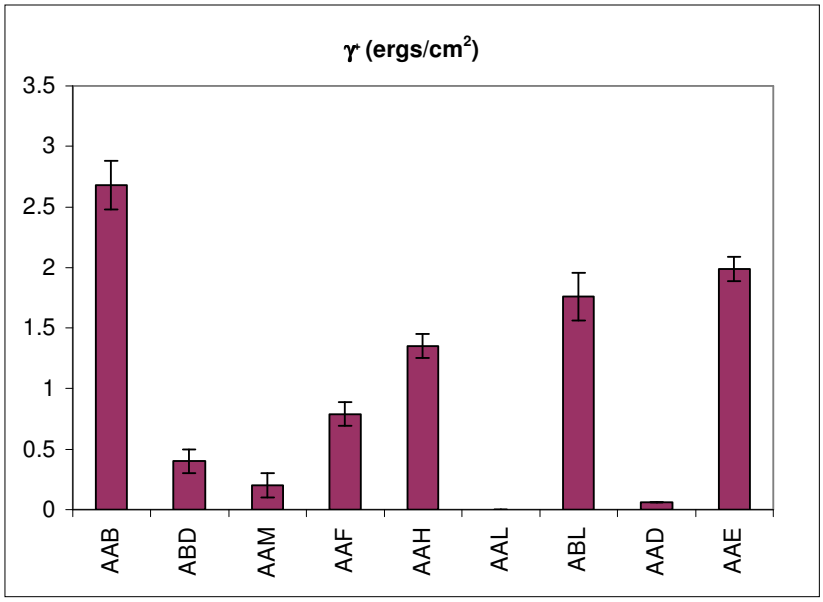

Figure 3.4. Acid Component of Bitumen Surface Free Energy.

Summary

Some of the problems associated with the use of Wilhelmy plate method from previous studies were as follows:

- Magnitude of the base component of bitumen surface free energy was very high.
- Square root of the surface free energy component was a large negative number in some cases.
- Computed surface free energy components were sensitive to the measured contact angles.
- Although precision of contact angles was determined the precision of computed surface free energy was not established.
- Accuracy of the data was not verified.

In this research, selection of appropriate probe liquids and its impact on the resulting surface free energy values is emphasized. Inclusion of more than three probe liquids helped reduce the sensitivity of the calculated surface free energy components and eliminate negative results of large magnitude. This also helped in validating the accuracy

of the measured contact angles based on various theoretical and experimental criteria stipulated in the literature concerning contact angle measurements. The surface free energy components of the bitumen calculated from the advancing contact angles in this research reconcile well with the general chemical properties expected for bitumen binders. Analytical methods to compute surface free energy components and the propagated errors from measured contact angles were developed using statistical methods described in detail in Appendix B. This improved the accuracy of the results and provided a means to estimate the precision of the surface free energy components and not just the precision of the measured contact angles.

CHAPTER IV

UNIVERSAL SORPTION DEVICE

Problem Description

Aggregates are a heterogeneous combination of various naturally occurring minerals. It is reasonable to regard aggregates as high energy solids, since the surface free energy of clean aggregates is typically higher than the surface free energy of any of the probe liquids that are commonly used. This eliminates the use of contact angle methods for measuring the surface free energy of clean aggregate surfaces and methods to measure properties such as spreading pressure must be resorted to. A gas sorption approach was used by Li [42] and Cheng [15] to determine surface energies of aggregates. Some of the results from Cheng [15] indicate the need for further refinement of this methodology for use as a test procedure for aggregates. For example, in some cases different probe liquids resulted in different specific surface area for the aggregate. Specific surface area is an important input in computing spreading pressures and eventually the surface free energy components. Therefore any discrepancy or error in specific surface areas of the aggregates is also reflected in the computed surface free energy components. Results from the previous studies were based on a limited number of aggregates that were tested manually and the accuracy of these results was not cross examined. Since measurement of adsorption isotherm is inherently a time consuming and sensitive procedure, manual control can lead to unwanted variability in the test results. In this research, a completely automated manifold was developed to facilitate testing and improve precision of the test method. Experimental and analytical methods to accurately measure and compute the surface free energy components were also developed.

Background and Theory

Spreading pressure, in the context of vapor adsorption on solid surface, is defined as the reduction in the surface free energy of the solid due to the adsorption of vapor molecules on its surface. Spreading pressure based on the equilibrium mass adsorbed at the maximum saturated vapor pressure is referred to as the equilibrium spreading pressure of the vapor with the solid, denoted by the symbol π_e. Based on this definition, equilibrium spreading pressure is expressed as:

$$\pi_e = \gamma_S - \gamma_{SV} \quad \textbf{(4.1)}$$

where, γ_S and γ_{SV} are the surface free energies of the solid in vacuum and in the presence of the vapor at maximum saturated vapor pressure, respectively.

The equilibrium spreading pressure of a vapor on a solid surface and their interfacial work of adhesion are related as follows (Refer Appendix A for a more detailed discussion and theoretical background of this equation):

$$W_{SL} = \pi_e + 2\gamma_{LV} \quad \textbf{(4.2)}$$

The above equation is valid for high energy materials such as aggregates. Further, using the Good-van-Oss-Chaudhury (GVOC) theory for the work of adhesion, the spreading pressure of the vapor on the solid surface and their surface free energy components are related as follows:

$$\pi_e + 2\gamma_{LV} = 2\sqrt{\gamma_S^{LW}\gamma_L^{LW}} + 2\sqrt{\gamma_S^{+}\gamma_L^{-}} + 2\sqrt{\gamma_S^{-}\gamma_L^{+}} \quad \textbf{(4.3)}$$

The surface free energy components of the solid are the three unknowns in equation (4.3). The surface free energy components of the liquid are known and the spreading pressure between the liquid vapor and solid is experimentally measured. Similar to the Wilhelmy plate method, in order to compute the three surface free energy

components of the solid using equation 4.3, its spreading pressure with at least three different liquid vapors must be measured experimentally.

The spreading pressure of a vapor over the aggregate surface is determined from its adsorption isotherm using equation (4.4) [43]:

$$\pi_e = \frac{RT}{MA}\int_0^{p_0}\frac{n}{p}dp \qquad \textbf{(4.4)}$$

where, *R*, is the universal gas constant, *T* is the test temperature, *n* is the mass of vapor adsorbed per unit mass of the aggregate at vapor pressure, *p*, *M* is the molecular weight of the probe vapor, p_0 is the maximum saturation vapor pressure of the liquid, and *A* is the specific surface area of the aggregate.

Specific surface area of the aggregate is calculated using the classical Branauer, Emmett and Teller (BET) equation [44] as shown below:

$$A = \left(\frac{n_m N_0}{M}\right)\alpha \qquad \textbf{(4.5)}$$

where, N_0 is the Avogadro's number, *M* is the molecular weight of the probe vapor, and α is the projected area of a single molecule of the probe vapor, and n_m is the monolayer capacity of the aggregate surface.

Monolayer capacity is the number of molecules required to cover the aggregate surface in a single layer. This is calculated using equation (4.6) from the slope 'S' and intercept 'I' of the best fit straight line between $\frac{p}{n(p_0 - p)}$ versus $\frac{p}{p_0}$, where p, p_0, and *n* are the partial vapor pressure, maximum saturation vapor pressure, and mass of vapor adsorbed on aggregate surface, respectively. The straight line fit is done only for partial vapor pressure, or $\frac{p}{p_0}$, ranging from 0 to 0.35, since the BET equation is valid only for this range.

$$n_m = \frac{1}{S + I} \qquad \textbf{(4.6)}$$

Figure 4.1 summarizes the analytical steps proposed in this research to obtain surface free energy components of an aggregate. Note that the specific surface area is determined using nHexane to calculate the spreading pressures from all three probe vapors. Detailed explanation for this is explained later in the section entitled "Experimental Variables".

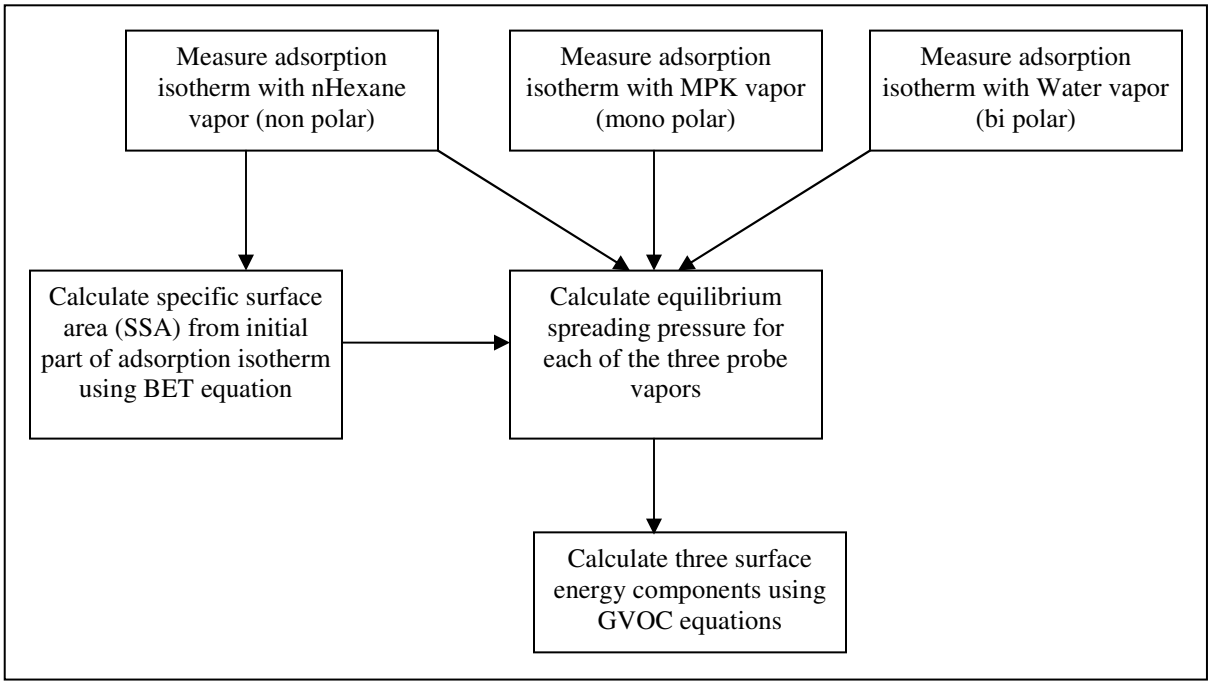

Figure 4.1. Flow Chart of Steps to Determine Aggregate Surface Free Energy.

Development of Test Method

Surface free energy components of aggregates are calculated from the spreading pressures of three probe vapors on the aggregate surface. Spreading pressure of a probe vapor is determined by measuring the full adsorption isotherm of the probe vapor on the aggregate surface. Therefore, the main experimental task to determine surface free

energy of aggregates is to measure its adsorption isotherm with different probe vapors.

To obtain a full adsorption isotherm, the aggregate was exposed to ten equal increments of partial probe vapor pressure from vacuum to maximum saturation vapor pressure. For each increment, the adsorbed mass was recorded after it reached equilibrium. Ten points were found to be sufficient to establish a good fit to the data within a reasonable test period. The time taken for the adsorbed mass to attain equilibrium was considerable for some aggregates and resulted in long overall test times. Furthermore, sensitivity of measurements and the human judgment required to determine if equilibrium was achieved, introduced variability and human error in the experiment. In order to avoid the influence of these factors on the test results, an automated test system capable of executing the entire test procedure with minimal operator effort and interference was developed. More details of the test method and set up are described in the following sub sections.

Sample Preparation

The aggregates to be tested were sampled from a representative stockpile. Aggregates passing ASTM sieve #4 and retained on ASTM sieve #8 were used for testing. The aggregates were sieved and cleaned with distilled water in the sieve. About 25 grams of the aggregate were required for one replicate test with each probe vapor. After cleaning the aggregate with distilled water, they were dried in an oven at 150°C for 6 hours and allowed to cool to room temperature inside a vacuum desicator for about 6 more hours. Once the sample was cleaned and ready to test it was placed in a wire mesh sample basket for testing.

Test Setup

The adsorption measurements were carried out in an air tight sorption cell. The sample basket was suspended in the cell from a hook connected to a microbalance via a magnetic suspension coupling. The magnetic suspension coupling enables accurate measurement of mass without the balance coming into any physical contact with the sample or vapors in the sorption cell. The sorption and micro balance together form the sorption apparatus manufactured by Rubotherm.

In order to automate the test procedure, a test manifold was developed and connected to the sorption apparatus. A software (SEMS, Surface Energy Measurement System) was developed to regulate the vapor pressure in the sorption cell and acquire mass, pressure, and temperature data as the test progresses. Figure 4.2 illustrates a schematic of the manifold and the sorption apparatus. Figure 4.3 shows a snapshot of the SEMS software for running the sorption test. The probe liquids were stored in air-tight cylinders connected to the manifold. The cylinders were degassed after connection to remove any trapped air and ensure the presence of only pure vapors from the probe liquid. The cylinders were connected to the sorption cell via a solenoid valve that was regulated by a computer to maintain the desired amount of vapor pressure in the sorption cell.

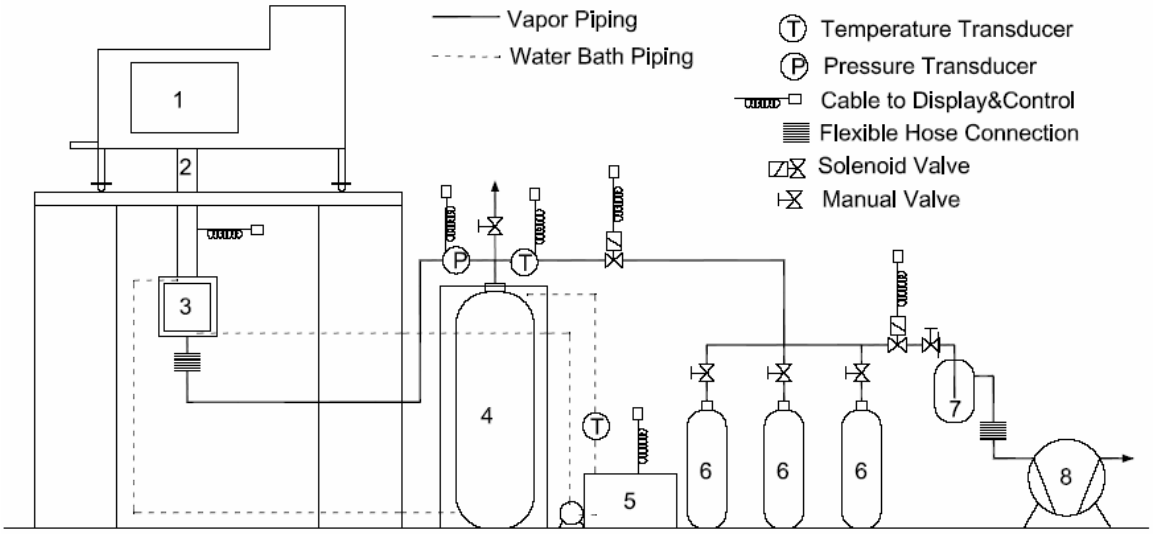

1. Microbalance
2. Magnetic suspension
3. Sample cell
4. Buffer Tank
5. Water bath
6. Probe liquid containers
7. Knock out tank
8. Vacuum pump

Figure 4.2. Layout of Universal Sorption Device System.

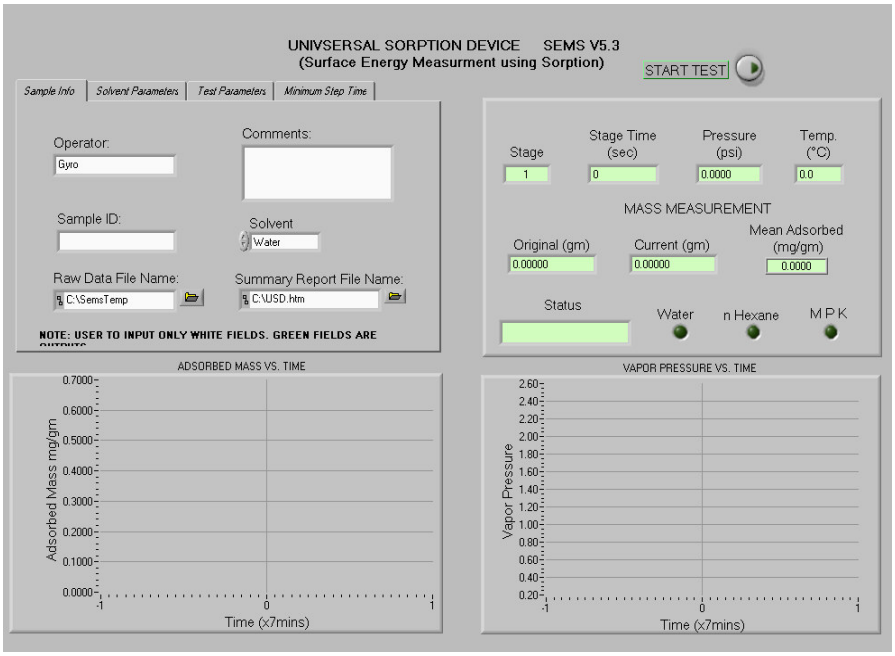

Figure 4.3. Snapshot of SEMS Software Used for Sorption Measurement.

Test Method

After the sample was suspended from the magnetic suspension hook, the sorption cell was sealed using a viton O-ring. The sorption cell was degassed using a mechanical vacuum pump. Degassing was carried out at 70°C under a vacuum of about 5 millitorr for a period of 2 hours followed by cooling to 25°C under vacuum for 4 hours. The temperature of the sorption cell was maintained using a water bath controlled by SEMS.

After completion of degassing, the adsorption isotherm of a probe vapor with the aggregate was obtained using SEMS. The following is a typical sequence of steps executed to obtain a full isotherm:

- Mass of the aggregate was measured after degassing under vacuum.
- Vapors from the probe liquid containers were dosed into the sorption cell to achieve a vapor pressure of approximately one-tenth the maximum saturated vapor pressure of the probe.
- Mass of adsorbed vapor was calculated as the difference between mass after exposure to vapor and the mass under vacuum when equilibrium is attained.
- The previous two steps were repeated by increasing the vapor pressure in

increments of approximately one-tenth of its maximum vapor pressure until saturated vapor pressure was achieved in the adsorption cell.

In order to determine whether the adsorbed mass has reached equilibrium, SEMS calculates the slope of the adsorbed mass versus time for the last five minutes of the test. If the slope is less than a pre-specified significant threshold value, the adsorbed mass is considered to have reached equilibrium and the next increment of partial vapor pressure applied. Correction for buoyancy is automatically applied to the measured mass as follows:

$$B = \frac{MpV}{RTz} \tag{4.7}$$

where, M is the molecular weight of the vapor, p is the partial vapor pressure at the time of measurement, V is the volume of the aggregate sample, R is the Universal gas constant, T is the test temperature, and z is the compressibility factor that can be calculated using empirical equations or obtained from physical tables [45].

Following completion of the test, the SEMS software uses equations (4.4), (4.5) and (4.6) to calculate the specific surface area of the aggregate and the spreading pressure of the probe vapor from the test data and presents a summary report. Equations (4.2) and (4.3) were used to determine the three surface free energy components of the aggregates based on the spreading pressures from the three probe vapors and specific surface area calculated using nHexane. The three probe vapors used in this research were nHexane, Methyl propyl ketone (MPK), and water. Table 4.1 presents the surface free energy components of these three probes.

Table 4.1. Surface Free Energy Components of Probe Vapors

Probe Vapor	γ^{LW} (erg/cm^2)	γ^{+} (erg/cm^2)	γ^{-} (erg/cm^2)	γ (erg/cm^2)
Water	21.8	25.5	25.5	72.8
Methylpropylketone	21.7	0	19.6	21.7
Hexane	18.4	0	0	18.4

Experimental Variables

Chemisorption versus Adsorption

Bond strength between two materials due to their surface energies is typically an order of magnitude or more smaller than the chemical bond strength. The main causes for the development of a bond between two materials are physical adsorption due to their surface energies and chemical adsorption or chemisorption due to formation of chemical bonds between the materials. For example, vapors physically adsorbed on a solid surface can be removed by degassing at normal temperatures, while chemisorbed vapor molecules bond more tenaciously to the solid surface and usually cannot be removed without the aid of very high temperature and vacuum. The methodology to measure surface free energy of aggregates is applicable only when the adsorbed mass is mostly due to physical adsorption and not chemisorption. In earlier experiments Cheng [15] determined that there was no appreciable difference in the adsorption and desorption characteristics of typical aggregates such as granite, limestone, and gravel using the same probe vapors. Based on this data and similar results from other studies [46], it is reasonable to consider that the adsorption of selected probe vapors on the aggregate surface is primarily physical in nature.

Specific Surface Area

Surface free energy is expressed in units of energy per unit area. Since the adsorption isotherm is measured in terms of mass of vapor adsorbed per unit mass of aggregate, specific surface area is an important input to compute the spreading pressure and surface free energy of aggregates. Equations (4.5) and (4.6) shown earlier are used to calculate the specific surface areas of aggregates from their adsorption isotherms. The physical interpretation of these equations is as follows. Equation (4.5) determines the number of molecules required to form a monomolecular layer over the aggregate surface. Thus, the total number of molecules forming a monolayer multiplied by the projected area of each molecule results in the specific surface area of the aggregate.

The projected cross sectional area of a probe vapor molecule is theoretically obtained using a liquid density equation that assumes the hexagonal packing model.

Adsorbed molecules of polar probes such as MPK and water may have a preferred orientation resulting in different projected cross sectional areas for different aggregates. As a result, using the theoretical cross sectional area of the molecule may result in inaccurate estimation of specific surface areas of the aggregates. The projected cross sectional area of nHexane (non polar probe) calculated based on liquid density formula is $36Å^2$. Gases such as nitrogen or argon are commonly used as probes to determine specific the surface area of solids on account of their relatively inert and non polar. Based on the comparison of specific surface areas of various standard materials using one or more probe vapors including inert gases, the projected area of nHexane molecules is estimated as $56Å^2$ [47], which is larger than the value calculated using the liquid density formula. In this research it is recommended that this value of projected area of nHexane molecules be used to determine the specific surface areas of the aggregates. This proposition is supported by experimental data presented later in this chapter.

Sample size and preconditioning

Although measuring adsorption isotherms is not a new technique, certain modifications were required in order to implement it for measuring aggregate surface energies. Most of the vapor sorption methods described in literature use very finely divided solids and a sample mass of about 1gm or less [43, 46, 48]. Further, most of these tests are based on measurement of relatively pure and homogenous solids and employ preconditioning temperatures as high as 250°C for time durations as long as 24 hours.

Aggregates used in hot mix asphalt are heterogeneous and are often combined from different size fractions to achieve a desired gradation. Surface free energy of an aggregate is an intrinsic material property and therefore must be independent of its geometry. This eliminates the requirement to test every size fraction of the same aggregate to obtain its surface free energy characteristics. This is true unless the size fraction is extremely fine such that differences in individual crystals become significant. Such fines are more likely to be considered as a part of the bitumen mastic rather than an aggregate bound by the bitumen. It is important to select a sample size and quantity that represents the mixture properties. Approximately 25 grams of aggregate passing the

ASTM #4 sieve and retained on the ASTM #8 sieve was found to be the most appropriate quantity and size for surface free energy measurements using the sorption apparatus. The quantity of the sample is determined by the range (5-100 grams) and sensitivity (10 micro grams) of the balance. For a given specific surface area and sample mass, a smaller aggregate size will result in a large total surface area and vice-versa. A large total surface area increases measurement precision because larger amounts of vapor mass are adsorbed, but this results in longer degassing and equilibrium times. On the other hand, a smaller total surface area reduces the test duration but at the expense of measurement precision. The size fraction, between the #4 to #8 sieves optimizes precision and test duration.

In this research, preconditioning of aggregates was done in two stages. In the first stage the aggregate sample was cleaned with distilled water to remove any physical or organic impurities from the surface. The sample was then heated in an oven at 150°C for 12 hours and allowed to cool to room temperature in a desiccator. Calcium sulfate crystals were added to the desiccator to lower humidity. In the second stage of preconditioning the aggregates were transferred into the sample basket and suspended in the sorption cell. A vacuum of about 5 millitorrs was applied for a period of two hours at a temperature of 70°C and the cell was allowed to cool back to test temperature under vacuum for three to four hours. The adequacy of this preconditioning procedure was determined in two ways. Firstly, the mass of aggregate was monitored during degassing and no appreciable change in mass was observed after about 2 hours of degassing indicating that there was no further significant desorption from the aggregate surface. Secondly, in another experiment isotherms of the same aggregate subjected to different durations of degassing were compared and found to be indifferent. Figure 4.4 illustrates this comparison for a gravel sample with MPK as a probe vapor. It is evident from the figure that the preconditioning procedure described above is adequate for testing this aggregate size fraction.

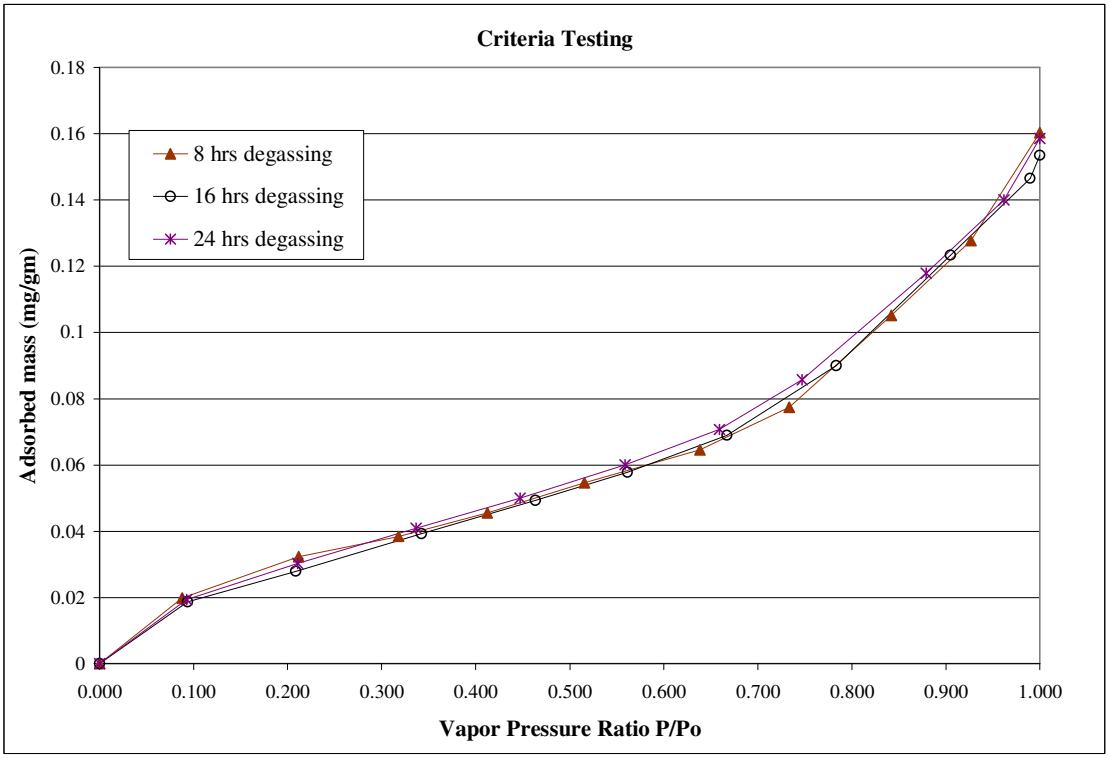

Figure 4.4. Evaluation of Preconditioning Time.

Test Results

Surface energies of five different aggregate types and four minerals were measured in this research. The aggregates were obtained from the Strategic Highway Research Program, Materials Reference Library (MRL), Reno, Nevada. These aggregates were from different sources and represent a range of mineral compositions. Three replicates of each aggregate were tested with each of the three probe vapors.

The SEMS software was used to carry out the adsorption test. Figure 4.5 shows a typical output from the SEMS software after completion of a test with a probe vapor. The specific surface area and spreading pressure for the aggregate with the probe vapor are calculated using equations (4.4) and (4.5), respectively. In order to calculate the surface free energy characteristics of the aggregate, spreading pressures from different probe vapors are combined using equations (4.2) and (4.3). Table 4.2 presents the spreading pressure measured using the USD and the coefficient of variation of the results

based on three replicate measurements. The specific surface areas of the aggregates were computed from the adsorption isotherm of nHexane and with a projected area of nHexane molecule as 56$Å^2$.

Table 4.2. Spreading Pressure

Aggregate	M P K		n Hexane		Water	
	Spreading Pressure (erg/cm^2)	**CV (%)**	**Spreading Pressure (erg/cm^2)**	**CV (%)**	**Spreading Pressure (erg/cm^2)**	**CV (%)**
RD	32.1	16.0	20.1	6.7	94.4	8.6
RL	69.7	7.2	28.3	14.1	293.2	4.0
RK	31.1	12.4	25.3	15.8	59.3	5.6
RA	20.3	17.0	23.9	5.5	124.5	16.4
RG	61.5	10.5	28.7	15.3	252.9	6.0
Quartz	8.7	10.9	22.8	5.1	142.7	8.6
Albite	28.4	1.9	23.4	9.0	85.6	6.5
Calcite	29.4	3.5	39.6	3.5	139.6	6.2
Microcline	18.4	3.9	20.0	1.3	72.7	3.7

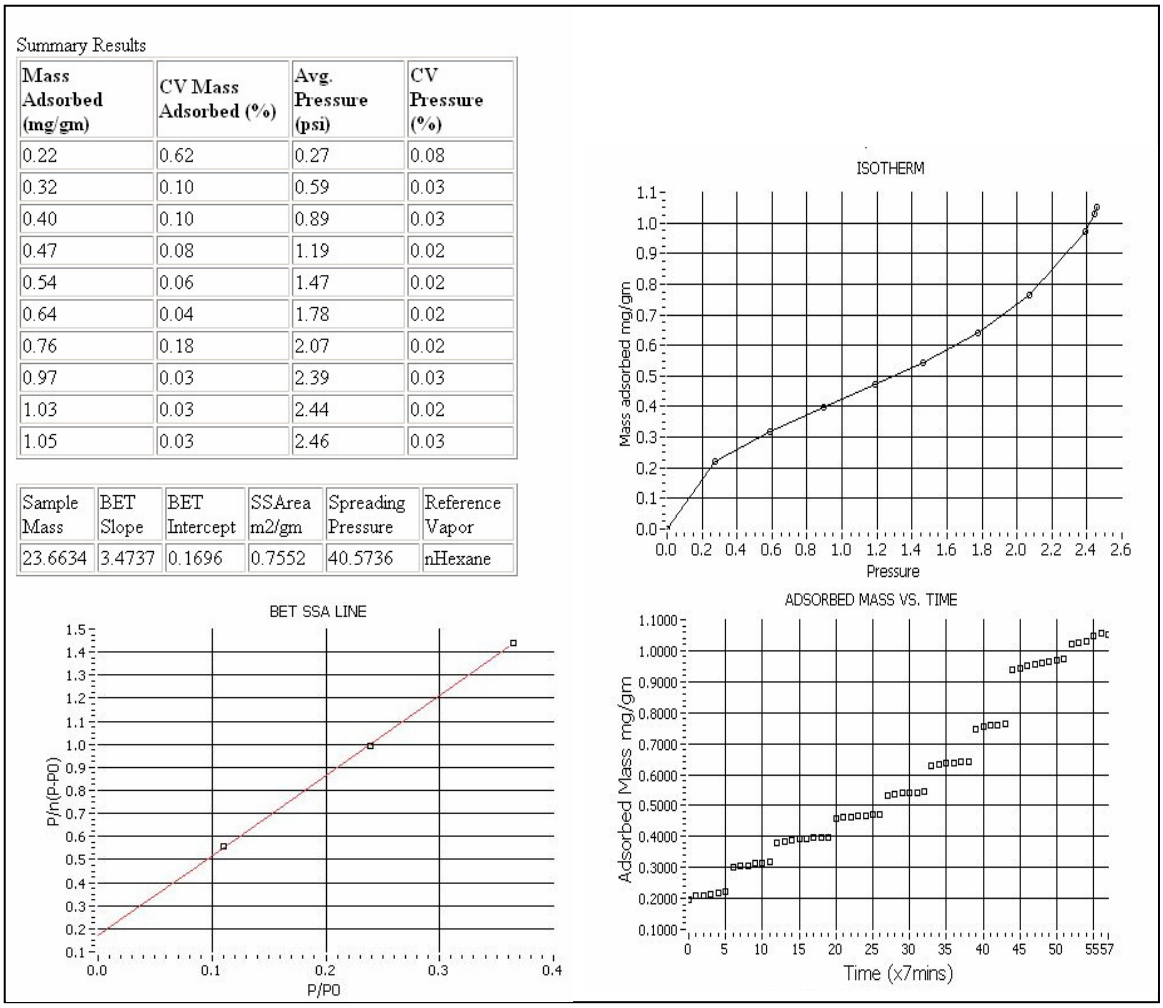

Figure 4.5. Typical Report Generated Using SEMS Software.

Table 4.3 summarizes surface free energy characteristics for the five aggregates and four minerals. Figures 4.6 through 4.8 illustrate the three surface free energy components of the aggregate and mineral that were tested along with their standard deviations. Results from these figures show that the last method can be used to determine the surface free energy components of the three aggregates with reasonable precision. Standard deviations for the surface free energy components are calculated using propagation of errors. Appendix C presents the analytical steps that were used to compute the surface free energy components and their standard deviations based on the replicate measurements of spreading pressures.

Table 4.3. Surface Free Energy Components

Aggregate	γ^{LW} (erg/cm^2)		γ^+ (erg/cm^2)		γ^- (erg/cm^2)		γ^{AB} (erg/cm^2)	γ^{Total} (erg/cm^2)
	Avg.	Std. Dev.	Avg.	Std. Dev.	Avg.	Std. Dev.		
RD: Limestone	44.1	1.25	2.37	1.08	259	18	49.57	93.6
RL: Gravel	57.5	4.09	23	4.15	973	39	299.2	356.8
RK: Basalt	52.3	4.77	0.64	0.74	164	10	20.5	72.8
RA: Granite	48.8	0.49	0		412	83	0	48.8
RG: Sandstone	58.3	4.52	14.6	4.01	855	34	223.2	281.5
Mineral: Quartz	37.2	1.0	0.0		525	32.2	48.3	96.6
Mineral: Albite	47.5	0.5	0.7	0.1	245	10.1	21.3	77.1
Mineral: Calcite	67.0	1.6	0.0		427	20.8	0	67.0
Mineral: Microcline	43.9	0.4	0.0		239	8.0	0	46.6

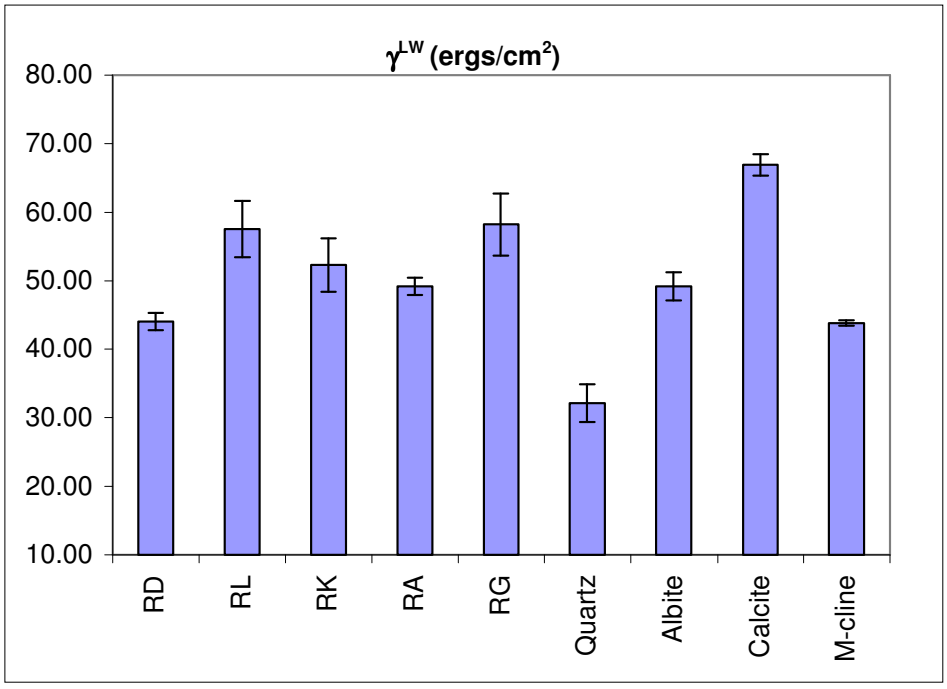

Figure 4.6. LW Component of Aggregates.

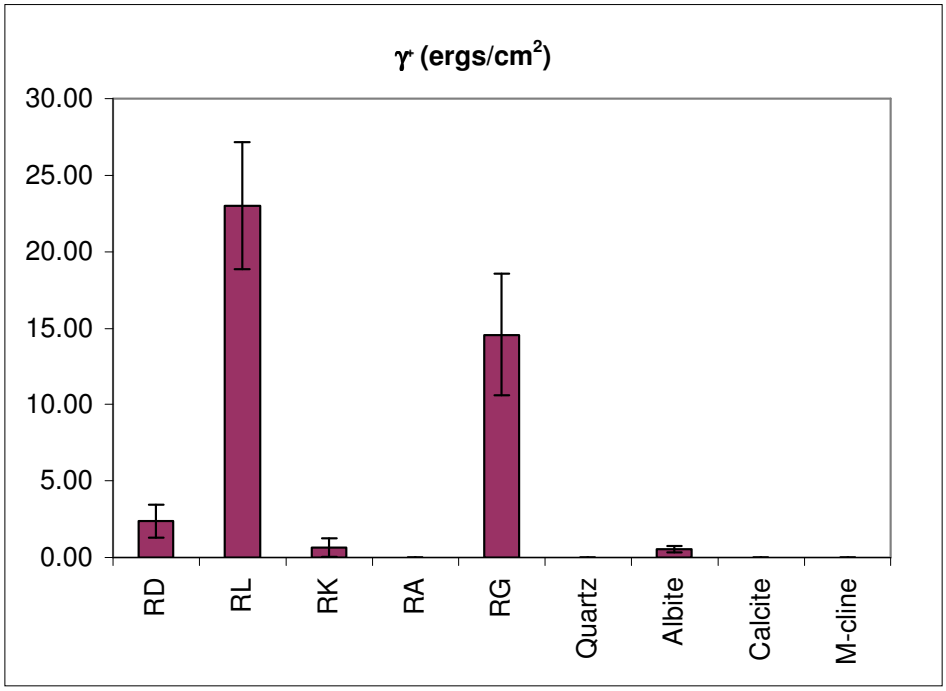

Figure 4.7. Acid Component of Aggregate.

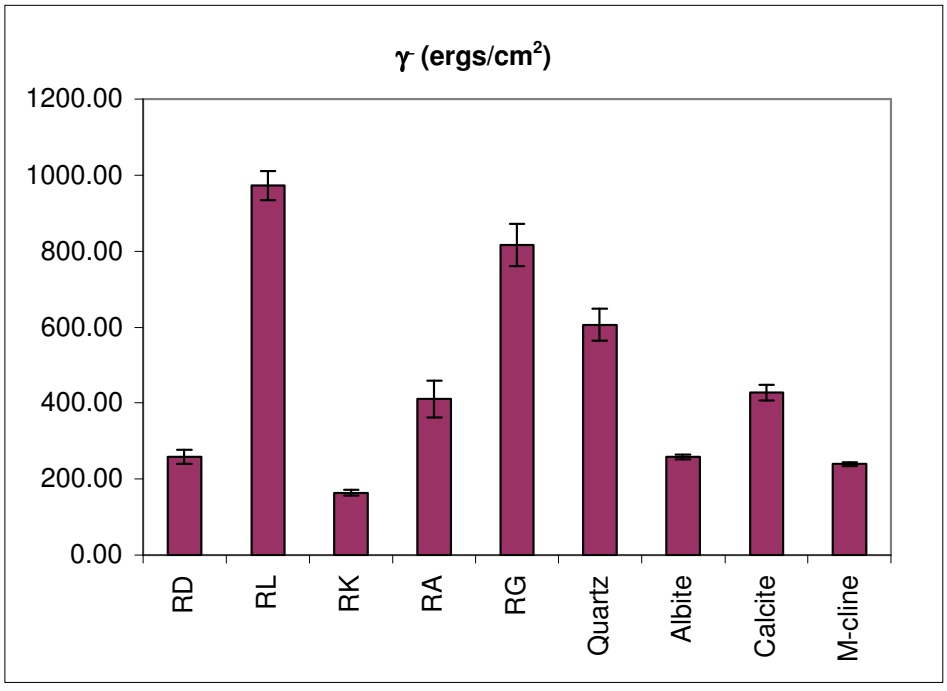

Figure 4.8. Base Component of Aggregate.

Validating Test Method Based on Specific Surface Area

Table 4.4 presents the specific surface areas of five different aggregates measured using the three probe vapors and considering the projected cross sectional area of the probe molecule based on the liquid density formula. Differences in cross sectional area determined using polar (MPK and water) and non-polar (nHexane) vapors are evident. The table also includes surface areas of aggregates calculated using nHexane but with a projected molecular cross sectional area of 56Å^2 as adopted from the literature [47]. It is proposed that nHexane must be used with a projected cross sectional area of 56Å^2 to compute the specific surface area of the aggregates since nHexane molecules are non-polar and therefore their orientation is not affected by different surface polarities of different aggregate surfaces. In order to validate this, the specific surface area of the same size fraction of two aggregates was measured using a commercially available standard Nitrogen sorption device manufactured by Micromeritics Inc. Data from Table 4.5 shows that the specific surface areas measured using this device agree well with the areas obtained using the adsorption equipment. This comparison also provides a limited validation of the accuracy of measurement of this test method

Table 4.4. Specific Surface Area of Aggregates

	Water[1] (10A^2)		**MPK[1] (35A^2)**		**Hexane[1] (39A^2)**		**Hexane[2] (52A^2)**
Aggregate	**SSA (m^2/gm)**	**CV(%)**	**SSA (m^2/gm)**	**CV(%)**	**SSA (m^2/gm)**	**CV(%)**	**SSA (m^2/gm)**
RD	0.17	4	0.23	10	0.18	5	0.26
RL	2.01	6	1.40	7	0.69	10	1.00
RK	4.15	12	6.49	7	7.20	8	10.38
RA	0.10	18	0.05	6	0.07	4	0.10
RG	1.62	4	0.99	10	0.51	7	0.74

Value in parenthesis is projected area of molecule used for calculation. [1] is value calculated using liquid density formula and [2] is value adopted from literature

Table 4.5. Specific Surface Area Using Different Methods

Aggregate	USD SSA (m^2/gm)	Micromeretics SSA (m^2/gm)
RK	10.38	10.10
RA	0.10	0.13

Surface Free Energy Components and Interpretation

The test results indicate that the sorption test controlled by the SEMS software measures spreading pressures of aggregates with reasonable precision. The Lifshitz-van der Waals (LW) or dispersive component of surface free energy varies from 44 to 58 ergs/cm^2 for different aggregates. Although differences in the dispersive component between aggregates is not large, it contributes significantly to adhesion keeping in perspective the dispersive component of bitumen surface free energy that typically varies from 12 to 35 ergs/cm^2. Also, from existing literature [48, 49, 50] the dispersive component of finely divided minerals commonly found in aggregates, such as quartz and calcite is reported to be between 35 to 80 ergs/cm^2. These values were determined using various other techniques such as Wicking method, micro calorimeter and inverse gas chromatography. The values obtained from USD measurements are in agreement with this range.

The magnitude of the acid component is very small, and the magnitude of the base component is very high and significantly different for all five aggregates. Also, from results shown in Chapter IV, most bitumen have a small acid component of surface free energy. The dry work of adhesion between the bitumen and aggregate is given by equation (2.2). From this equation it is evident that the acid and base interactions between the bitumen and aggregate are geometrically combined in a complimentary fashion (acid component of aggregate with base component of bitumen and vice-versa) to compute the total work of adhesion. Therefore, the large magnitude of base component of aggregates is a significant contributor to the adhesion between the bitumen and aggregate with the acid component of bitumen, although small, acting as a scaling factor. This is in concurrence with other adhesion theories that attribute adhesion between

bitumen binder and aggregate to the weakly acidic character of the bitumen and a basic character of the aggregate [28].

Summary

The test method developed in this research offers a convenient way to measure surface free energy components of aggregates that can be combined with the surface free energy components of bitumen to compute the dry work of adhesion, work of debonding and estimate the moisture sensitivity of asphalt mixes. Discrepancies in specific surface areas of aggregates reported by previous researchers were resolved. Precision of the test method was improved significantly by developing an automated test manifold controlled by a computer. Specific surface areas of aggregates measured using this test method compare well with specific surface areas measured using industry standard method and provide a limited validation for the accuracy of this device. Surface properties of pure minerals such as quartz and calcite measured using this method are also in reasonable agreement with similar data available in the literature based on other test methods.

CHAPTER V

SURFACE FREE ENERGY AND MOISTURE SENSITIVITY OF ASPHALT MIXES

General

The objective of measuring surface free energies of bitumen and aggregate is to be able to compute their interfacial work of adhesion and the reduction in free energy of the system (work of debonding) when water displaces bitumen from the aggregate-bitumen interface. These two parameters can be used to estimate the moisture sensitivity of asphalt mixes based on the principles of physical adhesion.

The conventional method of identifying moisture sensitive asphalt mixes during the mixture design process is by comparing results from mechanical tests on dry and moisture conditioned asphalt mixes. However, these tests are not always reliable and do not provide any information regarding the causes for good or poor performance of a particular mixture. This information is indispensable to a materials engineer who is often times required to modify the locally available materials, for economic reasons, to suit the design specifications. The motivation to develop tests that measure material properties related to the fundamental mechanisms that are responsible for moisture sensitivity of asphalt mixes is to fill this gap. Surface free energy of bitumen and aggregate and their concomitant bond energies are important material properties that influence the moisture sensitivity of asphalt mixtures.

This chapter presents results to compare the moisture sensitivity of asphalt mixes measured by laboratory tests with the bond energy parameters of their constituent materials. The chapter also presents results from another study that compares the moisture sensitivity of asphalt mixes based on field evaluation, with the bond energy parameters of their constituent materials. The surface energies and bond energy parameters in the latter study were computed using the experimental and analytical techniques developed in this research and described in Chapters III and IV.

Bond Energy Parameters Related to Moisture Sensitivity

The three parameters based on surface free energies of bitumen and aggregate that are related to the moisture sensitivity of an asphalt mix are,

- work of adhesion between the bitumen and aggregate,
- work of debonding or reduction in free energy of the system when water displaces bitumen from a bitumen-aggregate interface, and
- cohesive bond energy of the bitumen binder.

The first two parameters can be computed using equations (2.2) and (2.3), respectively, if the surface free energy components of these materials are known. The cohesive bond energy of the bitumen binder is the work done to create a new unit area by fracture in the neat bitumen phase. By extending equation (2.2) to a system where both phases are of the same material, it can be shown that the cohesive bond energy is simply twice the total surface free energy of the material.

For an asphalt mixture to be durable and less sensitive to moisture, it is desirable that the work of adhesion, W_{AB}, between the bitumen and the aggregate be as high as possible. Also, the greater the magnitude of work of debonding when water displaces bitumen from the bitumen-aggregate interface, W_{ABW}^{wet}, the greater will be the thermodynamic potential that drives moisture damage. Therefore it is desirable that the magnitude of work of debonding be as small as possible. Based on this reasoning, one of the parameters that can be used to combine the two energy terms, W_{AB}, and W_{ABW}^{wet}, to assess the moisture sensitivity of the asphalt mix, is their ratio given as follows:

$$ER_1 = \left| \frac{W_{AB}}{W_{ABW}^{wet}} \right| \qquad \textbf{(5.1)}$$

The value of the bond energy parameter, ER_1, can be computed and used to predict the moisture sensitivity of the asphalt mix by measuring the surface free energy components of the constituent bitumen and aggregate. The higher the value of ER_1, the less moisture sensitive the mix is likely to be.

Equation (5.1) proposes ER_1 as a parameter to estimate the moisture sensitivity of asphalt mixes based on the hypothesis that moisture sensitivity of an asphalt mix is directly proportional to the dry adhesive bond strength, and inversely proportional to the work of debonding or the reduction in free energy during debonding. The latter term is determined from equation (2.3), which is reiterated as follows:

$$W_{ABW}^{wet} = \gamma_{AW} + \gamma_{BW} - \gamma_{AB} \quad \textbf{(5.2)}$$

The term γ_{AB} in equation (5.2) refers to the interfacial bond energy between the bitumen and the aggregate. The magnitude of resistance of the bitumen-aggregate interface is accounted for when work for debonding, W_{ABW}^{wet}, is computed. Therefore, it can be argued that the numerator for the bond energy parameter, ER_1, is redundant since the strength of interfacial adhesion is already accounted for in the denominator. However, an important factor that is not accounted for in the ratio, ER_1, is the wettability of aggregate by the bitumen.

Although wettability and adhesion are both related to the surface free energy of materials, these are two different attributes. Wettability refers to the ability of one material to wet the surface of the other material. In other words, a material will wet the surface of another material if the cohesive bond energy of the former is less than the work of adhesion with the latter. Work of adhesion on the other hand measures the strength of adhesion at the interface of two materials. For example, a commercial epoxy glue might not wet a clean plastic surface, but may have a very good adhesive bond strength with the surface it is applied to. Wettability also determines the ability of a material to impregnate itself in to the micro textural features of the solid surface. Therefore, for a given aggregate surface, a bitumen with greater wettability will coat the aggregate surface more than a bitumen with lower wettability. Better coating of aggregate surface results in fewer locations for initiation of moisture damage and corresponds to lower moisture sensitivity of the mix. Therefore, it is also proposed that resistance of an asphalt mix to moisture damage is directly proportional to the wettability of the constituent bitumen

with the aggregate and inversely proportional to the reduction in free energy when water causes debonding. Mathematically, this is expressed as follows:

$$ER_2 = \left| \frac{W_{AB} - W_{BB}}{W_{ABW}^{wet}} \right| \quad \textbf{(5.3)}$$

where, W_{BB}, is the cohesive bond energy of the bitumen and other terms are as described before.

It is proposed that the two parameters, ER_1 and ER_2, that are derived using surface free energy of materials can be used to estimate the moisture sensitivity of asphalt mixes based on the principles of physical adhesion, when other mixture properties, loading conditions, and environmental conditions are controlled. The bond energy parameters were computed for the nine bitumen and five aggregate types that were used for surface free energy measurements in the previous chapters. In addition to these two bond energy parameters, it also proposed that moisture sensitivity of asphalt mixes will also be inversely related to the overall micro texture of the aggregate surfaces which can be approximated to be proportional to its specific surface area. In order to accommodate the influence of surface roughness at a micro level, two additional parameters are proposed. These are the product ER_1 with the specific surface area, and the product of ER_2 with the square root of the specific surface area. Square root of the specific surface area is selected for the latter case based on a principles of catalysis which states that rate of diffusion in micro porous materials is either proportional to the square root of the specific surface area or independent of it [51]. Since all asphalt mixes are cured at the mixing temperature for the same time duration before compaction, the amount of bitumen that wets different aggregate surfaces can also be approximated to be proportional to the square root of the specific surface area of the. The remainder of this chapter will present data that demonstrates the correlation between moisture sensitivity of asphalt mixes measured in the laboratory or from field performance with these four bond energy parameters.

Table 5.1 presents the cohesive bond strength, W_{BB}, for the nine bitumen types. Tables 5.2 and 5.3 present the work of adhesion and work of debonding for all possible combinations of the nine bitumen types with the five aggregates. Tables 5.4 and 5.5 present the values of the two bond energy parameters, ER_1 and ER_2. From the data in these tables it is evident that for a given aggregate type, changing the type of bitumen can result in a range of different energy parameters, and consequently a range of different predicted moisture sensitivities. Similarly, for a given type of bitumen, changing the type of aggregate can result in significantly different moisture sensitivities of the asphalt mix.

Table 5.1. Work of Cohesion for Different Binder Types

Bitumen	Work of cohesion (ergs/cm^2)
AAB	27.2
ABD	64.9
AAM	49.7
AAF	42.7
AAH	40.5
AAL	62.6
ABL	37.7
AAD	37.2
AAE	52.2

Table 5.2. Work of Adhesion Between Bitumen and Aggregates

Bitumen	RA	RK	RL	RD	RG
AAB	118*	95*	158*	102	150
ABD	105*	99*	126*	96	123
AAM	88	84	104	81	102
AAF	101	90	126	90	121
AAH	110	95	141	97	135
AAL	78	81	85	74	85
ABL	114	96	149	100	143
AAD	70*	69*	83*	66	82
AAE	129	110	165	113	159

* Indicates mixes included for testing

Table 5.3. Work of Debonding in Presence of Water

Bitumen	RA	RK	RL	RD	RG
AAB	-58*	-15*	-182*	-44	-154
ABD	-79*	-20*	-222*	-58	-189
AAM	-88	-27	-236	-65	-202
AAF	-76	-22	-215	-57	-184
AAH	-68	-18	-202	-51	-171
AAL	-99	-31	-256	-72	-220
ABL	-66	-18	-194	-49	-165
AAD	-101*	-36*	-251*	-74	-217
AAE	-58	-11	-185	-43	-156

* Indicates mixes included for testing

Table 5.4. Bond Energy Parameter – Lab Tests *(ER_1)*

Bitumen	RA	RK	RL	RD	RG
AAB	2.05*	6.34*	0.87*	2.32	0.97
ABD	1.34*	4.88*	0.57*	1.66	0.65
AAM	1.00	3.13	0.44	1.24	0.50
AAF	1.32	4.12	0.58	1.59	0.66
AAH	1.61	5.23	0.70	1.91	0.79
AAL	0.79	2.65	0.33	1.03	0.39
ABL	1.74	5.41	0.77	2.04	0.86
AAD	0.69*	1.90*	0.33*	0.88	0.38
AAE	2.23	9.87	0.89	2.63	1.02

* Indicates mixes included for testing

Table 5.5. Bond Energy Parameter – Lab Tests *(ER_2)*

Bitumen	RA	RK	RL	RD	RG
AAB	1.57*	4.53*	0.72*	1.70	0.80
ABD	0.51*	1.67*	0.27*	0.54	0.31
AAM	0.44	1.27	0.23	0.48	0.26
AAF	0.76	2.15	0.38	0.84	0.43
AAH	1.02	3.00	0.50	1.11	0.55
AAL	0.16	0.60	0.09	0.16	0.10
ABL	1.16	3.30	0.58	1.27	0.64
AAD	0.32*	0.87*	0.18*	0.38	0.20
AAE	1.32	5.19	0.61	1.42	0.68

* Indicates mixes included for testing

Moisture Sensitivity Based on Laboratory Performance of Mixes

The experiment to validate the correlation between energy parameters and moisture sensitivity of asphalt mixes based on laboratory tests comprised of three important steps. The first step was to select a set of asphalt mixes which would be

expected to have a range of different moisture sensitivities. This was done based on the energy parameters shown in Tables 5.4 and 5.5. The second step was to select a method to quantify moisture sensitivity of asphalt mixes by laboratory testing. This was done by dividing the compacted samples of selected asphalt mixes into two different groups. The first group of mixes was the control group (dry) and the second group of mixes was subjected to accelerated moisture damage (moisture conditioned). The ratio of the mechanical properties of the moisture conditioned mix to the dry mix was used to quantify the moisture sensitivity of the asphalt mixes. In the third step, correlation between moisture sensitivity of asphalt mixtures based on laboratory testing and bond energy parameters was determined. The following sub sections provide details of the aforementioned experiments.

Materials

Nine mixtures were selected for the mechanical tests using aggregates RA (granite), RK (basalt) and RL (limestone) and asphalt binders AAB, ABD and AAD. Amongst the nine neat asphalt binders measured using the Wilhelmy plate method, the asphalt AAB has the lowest cohesive bond energy of about 27 ergs/cm^2 and the asphalt ABD has the highest cohesive bond energy of about 65 ergs/cm^2. Amongst the 45 possible combinations of nine asphalt binders and five aggregates with known surface energies, the work of adhesion between AAB and RL was one of the highest and AAD and RA was one of the lowest. Similarly the calculated value of free energy released when water displaces asphalt from the asphalt-aggregate interface was one of the highest for the combination of AAD and RL and one of the lowest for the combination of AAB with RK. Another important factor that differentiated the three selected aggregates was their specific surface area. The specific surface areas of RA, RL and RK were of the order of 0.1, 1 and 10 m^2/gm, respectively. Therefore, selection of these three aggregates and bitumen provide a range of different values for the bitumen cohesion, bitumen-aggregate adhesion, and bitumen-aggregate debonding.

Mix Designs and Sample Preparation

Figure 5.1 shows the aggregate gradation used for all the nine mix designs. The optimum asphalt content was determined using the Superpave design method with a Superpave Gyratory Compactor (SGC) using 125 design gyrations at 4% air voids. The test samples were prepared using the SGC in a 101 mm diameter mold. Two of the mechanical tests included in this study were in the direct tension mode. Based on the literature, the minimum recommended aspect ratio (diameter : height) for samples subjected to direct tension tests is 1:2 [52]. Also the minimum diameter of the cylindrical sample must be at least four times the size of the largest aggregate in the mix. Based on this information, dimensions of the test specimen were selected as 75 mm in diameter and 150 mm in height. The finished specimen were obtained by coring and sawing a 100 mm diameter and 175 mm high sample compacted using the SGC. The number of gyrations of the SGC was adjusted to achieve a target air void of 7±0.5% for the finished sample (after coring and sawing). Samples with air voids that did not fall in this range were discarded. Extreme care was exercised during sawing and coring operations to ensure proper sample geometry.

Mechanical Tests and Parameters

Three types of mechanical tests were conducted on the dry and moisture conditioned asphalt mix samples. One of these tests was in compression and the other two were in a direct tension mode. The direct tension mode was selected since the effect of stripping would be most evident in this mode. At least two replicates of both dry and moisture conditioned samples were tested for each of the nine mix designs. All mechanical tests were conducted at a temperature of about 25±1°C. Aluminum plates with fixtures to connect them to the universal testing machine, were glued to both ends of the sample using epoxy glue to enable testing in direct tension mode. Each sample was attached with three linear variable displacement transformers (LVDTs) with a maximum range of 1.8mm to record permanent and resilient deformation. The LVDTs were mounted at a distance of 25 mm from either face of the sample with a total gauge length of 100 mm.

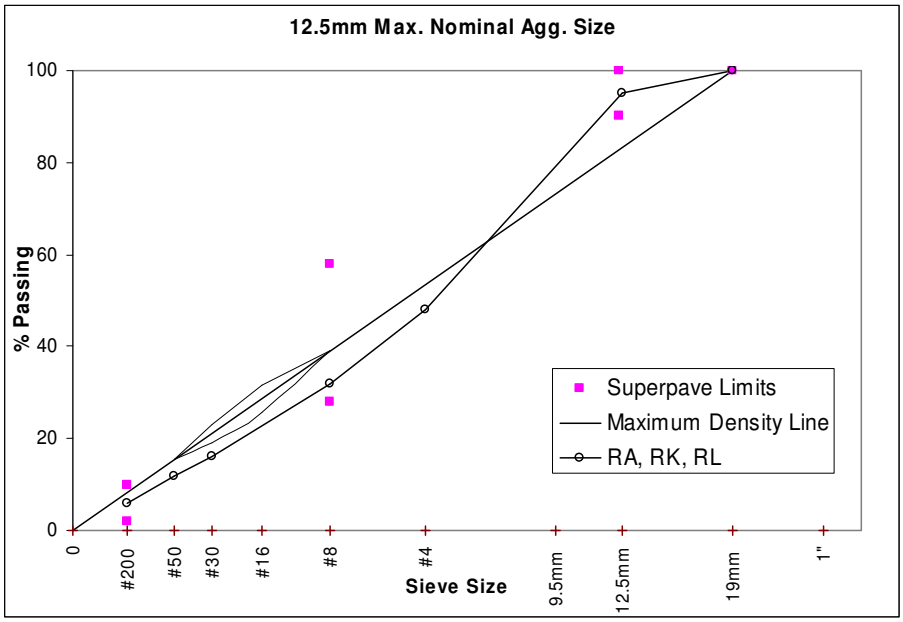

Figure 5.1. Aggregate Gradation for All Mixes.

The first mechanical test was the dynamic modulus test in compression. This test was conducted using a haversine loading with a frequency of 10 Hz. The stress level was kept to a minimum to avoid any permanent sample damage. Each sample was tested for 200 load repetitions. The samples were then allowed to rest for a minimum of 30 minutes prior to further testing. The parameter of interest from this test is the ratio of the dynamic modulus of the moisture conditioned sample to the dry sample.

The second type of test was the dynamic modulus test in tension. The sample was connected to the loading arm from the top and gripped using a mechanical chuck at the bottom via the aluminum end plates. Proper alignment of the sample was ensured during this process. The loading arm was continuously adjusted during the process of fixing the sample to ensure that the sample was not prestressed. The dynamic modulus in tension was also conducted using a haversine loading with a frequency of 10 Hz and 200 load repetitions. The parameter of interest from this test is the ratio of the dynamic modulus in tension of the moisture conditioned sample to the dry sample. The third test immediately followed the second test. In this test the dynamic haversine loading was continuously applied at a high stress level until the sample failed in tension. In most

cases failure of the sample was from the middle. Resilient strain and permanent deformation of the sample was continuously recorded during the test. Figures 5.2 and 5.3 show typical loading and response from the dynamic creep test in tension. The parameter of interest from this test is the ratio of the fatigue life of the moisture conditioned sample to the dry sample. Figure 5.4 shows the reduction in modulus of the mix with increasing number of load cycles normalized by the modulus of the first load cycle.

A good estimate of fatigue life is the number of load cycles that corresponds to the maximum value of:

$$N\frac{E_N^*}{E_1^*} \tag{5.4}$$

where, N is the number of load cycles, E_N^* is the shear modulus at the Nth load cycle, and E_1^* is the shear modulus at the 1st load cycle. Figure 5.4 also shows a plot of $N\frac{E_N^*}{E_1^*}$ versus the load cycles. Figure 5.5 shows the set up for conducting the tension tests with a sample that failed in tension after the dynamic creep test.

In dynamic creep the parameters of interest were the accumulated permanent strain in the sample as well as the reduction in modulus of the sample with increasing number of load cycles. In order to collect data for these parameters, LVDTs with smaller range and greater sensitivity were used. However, due to practical limitations, these LVDTs could not record data until complete sample failure for all samples. Therefore for this research, the fatigue life of the mix is defined as the number of load cycles required to attain 1% permanent strain. Table 5.6 provides a summary of the mechanical tests and relevant parameters used to quantify moisture sensitivity of asphalt mixes.

Table 5.6. Summary of Mechanical Tests Used to Estimate Moisture Sensitivity

Test Type	Test Parameters	Parameters to estimate moisture sensitivity	Sample Size
Dynamic Modulus (Compression)	Haversine loading in compression at 10Hz and 25°C at low stress level for 200 cycles	Ratio of wet to dry compression modulus of mix	Diameter: 75mm Height: 150mm Obtained by sawing & coring a 100mm diameter and 175mm high sample compacted using the Superpave gyratory compactor
Dynamic Modulus (Tension)	Haversine loading in tension at 10Hz and 25C at low stress level for 200 cycles	Ratio of wet to dry tension modulus of mix	
Dynamic Creep	Haversine loading in tension at 10Hz and 25C at high stress level until sample failure	Ratio of wet to dry number of load cycles required for 1% permanent microstrain	

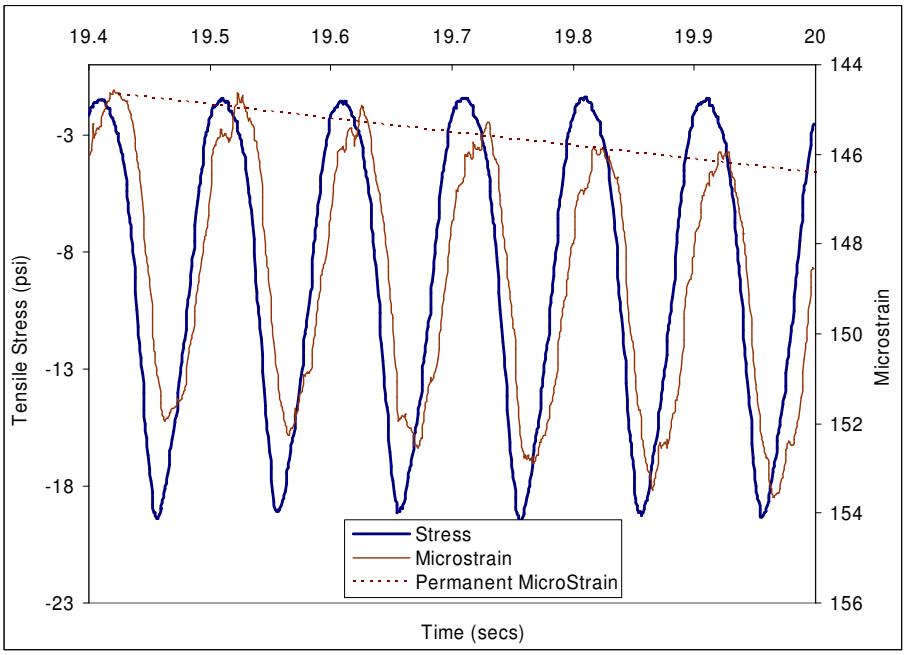

Figure 5.2. Typical Loading and Average Response from Dynamic Creep Test Without Rest Period.

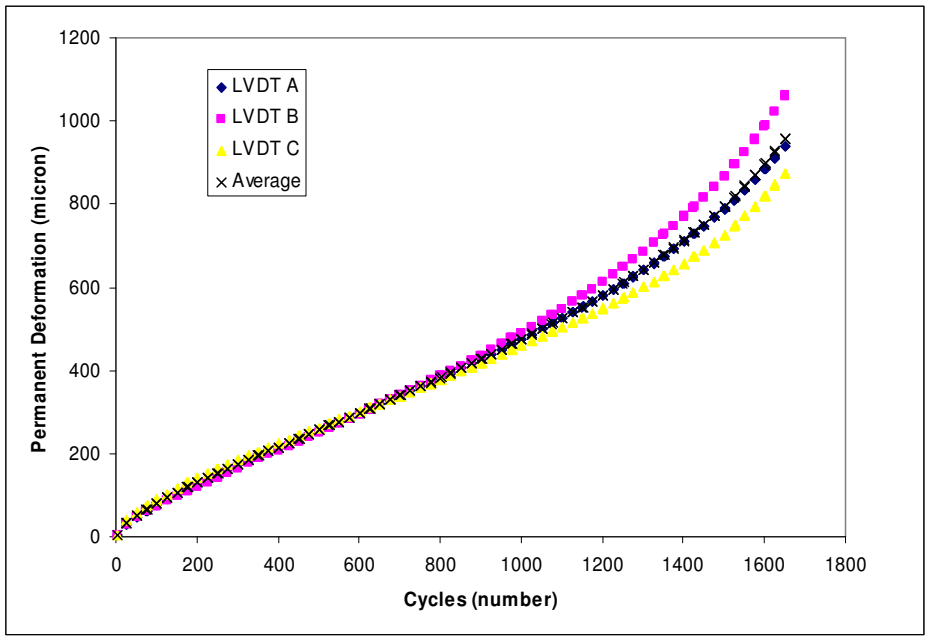

Figure 5.3. Curve Showing Accumulated Permanent Strain Versus Load Cycles.

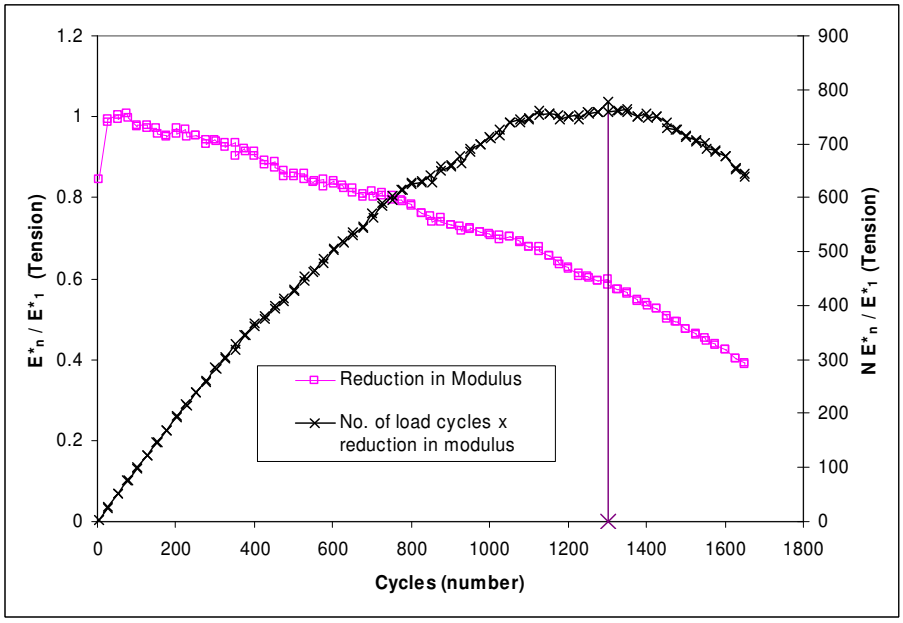

Figure 5.4. Reduction in Modulus from Dynamic Creep Test.

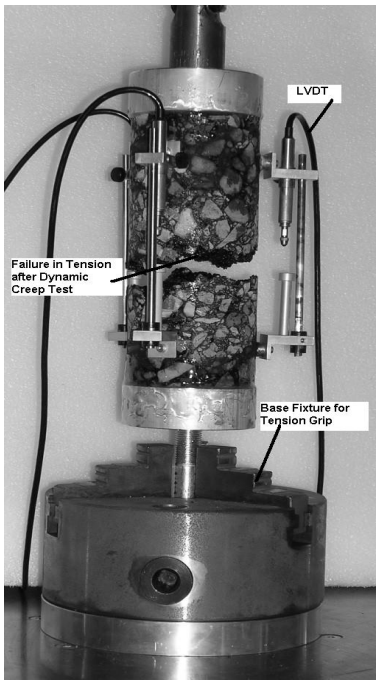

Figure 5.5. Test Set Up and Sample Failure for Dynamic Creep Test (Tension).

Moisture Conditioning

Samples were moisture conditioned by submerging them in deionized water under vacuum to achieve a saturation level between 70 to 80%. This took about two minutes in most cases. After achieving target saturation, the samples were kept submerged under deionized water for 24 hours at 50°C. The samples were then removed from the water and air dried for 24 hours prior to testing. The samples retained a saturation level between 25 and 30% at the time of testing. Testing of the moisture conditioned samples was completed within 24 to 36 hours after removal from the water. Figure 5.6 shows the failure plane of a moisture conditioned sample after a dynamic creep test in tension.

Figure 5.6. Failure Plane of Moisture Conditioned Sample After Dynamic Creep Test.

Results

Four bond energy parameters, ER_1, ER_2, $SSA\,x\,ER_1$, and $\sqrt{SSA}\,x\,ER_2$, are proposed as indicators of moisture sensitivity of asphalt mixes. Three different parameters are used to quantify the moisture sensitivity of asphalt mixes based on laboratory testing. These are the ratio of dynamic modulus in compression, ratio of dynamic modulus in tension, and ratio of load cycles for 1% permanent strain in tension of dry samples to moisture conditioned samples. Correlations between the four bond energy parameters and the three parameters from laboratory testing were determined. The ratio of dynamic modulus in compression did not show a significant correlation with any of the bond energy parameters. This was expected since the modulus of asphalt mixes in compression is a complex function of various other mechanical and material properties and the effect of debonding might not be significant in the compression mode. However the bond energy parameters showed different levels of correlation with the other two parameters from the mechanical tests. Figures 5.7 through 5.14 illustrate the correlation between each of the four bond energy parameters and the moisture sensitivity of asphalt mixes based on each of the two parameters from the direct tension tests.

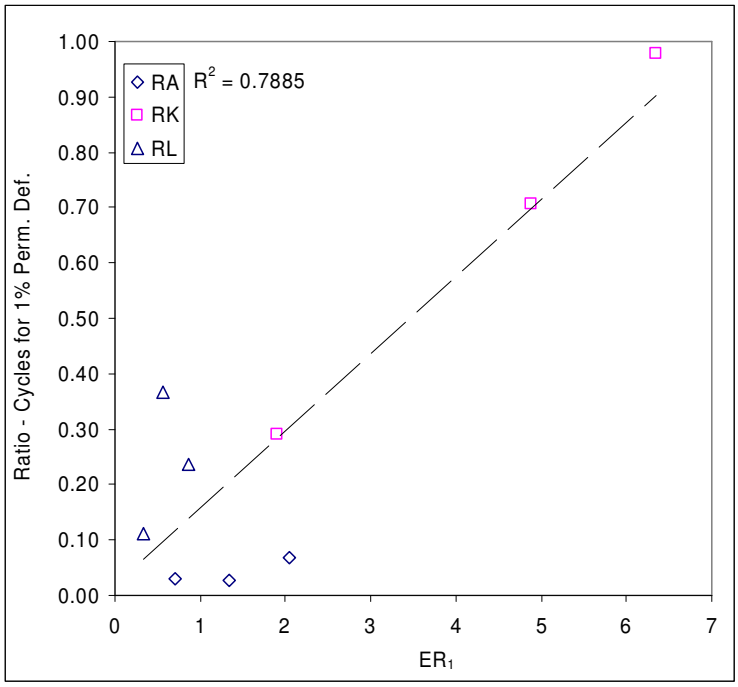

Figure 5.7. ER_1 vs. Wet to Dry Ratio of Fatigue Life.

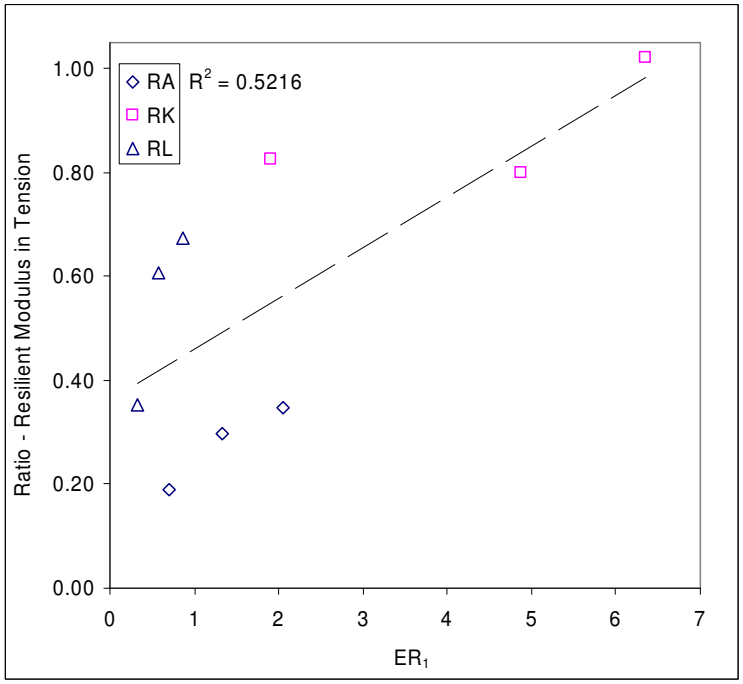

Figure 5.8. ER_1 vs. Wet to Dry Ratio of Resilient Modulus in Tension.

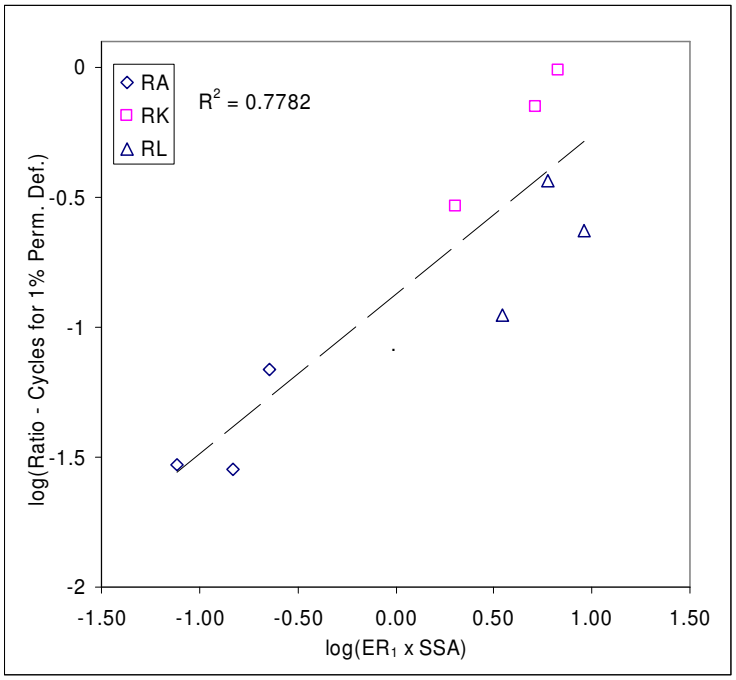

Figure 5.9. ER_1xSSA vs. Wet to Dry Ratio of Fatigue Life.

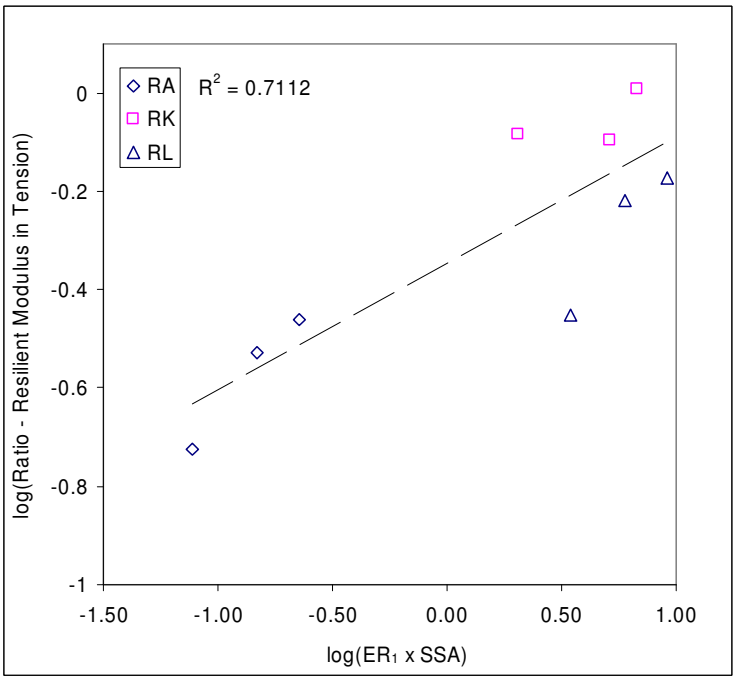

Figure 5.10. ER_1xSSAvs. Wet to Dry Ratio of Resilient Modulus in Tension.

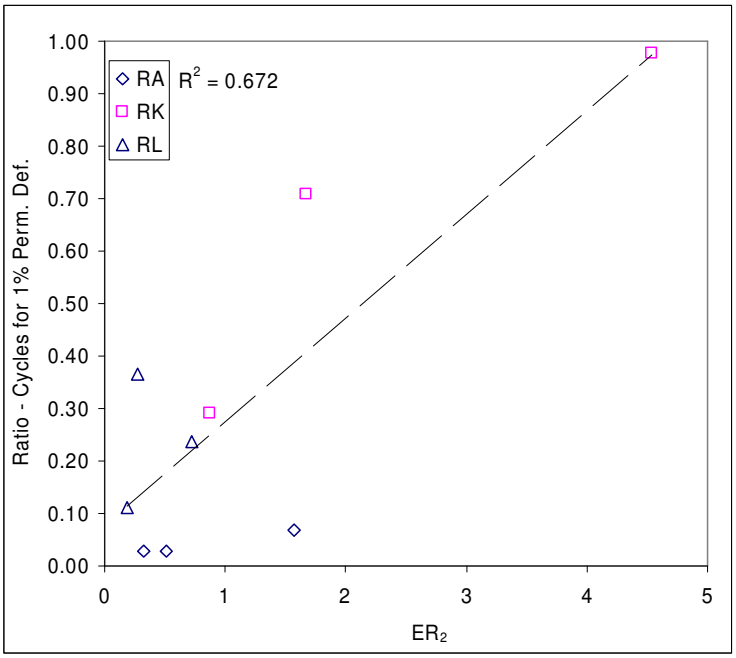

Figure 5.11. ER_2 vs. Wet to Dry Ratio of Fatigue Life.

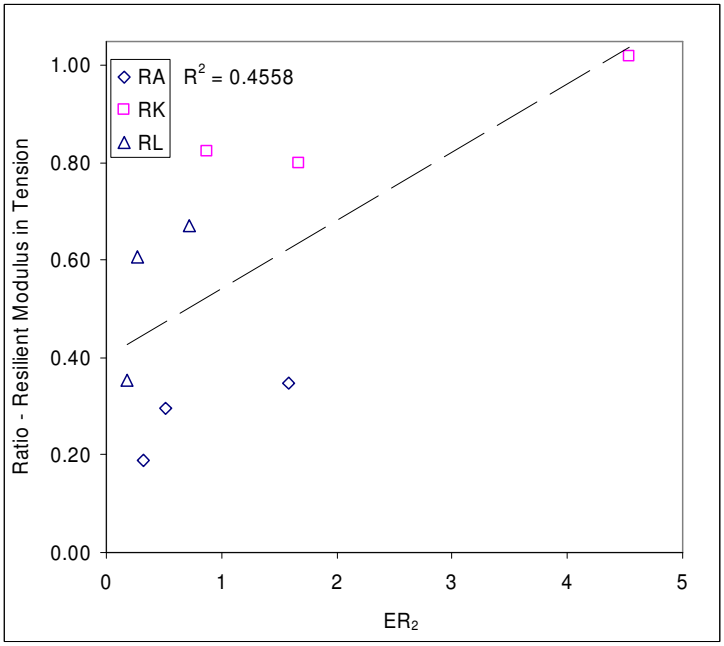

Figure 5.12. ER_2 vs. Wet to Dry Ratio of Resilient Modulus in Tension.

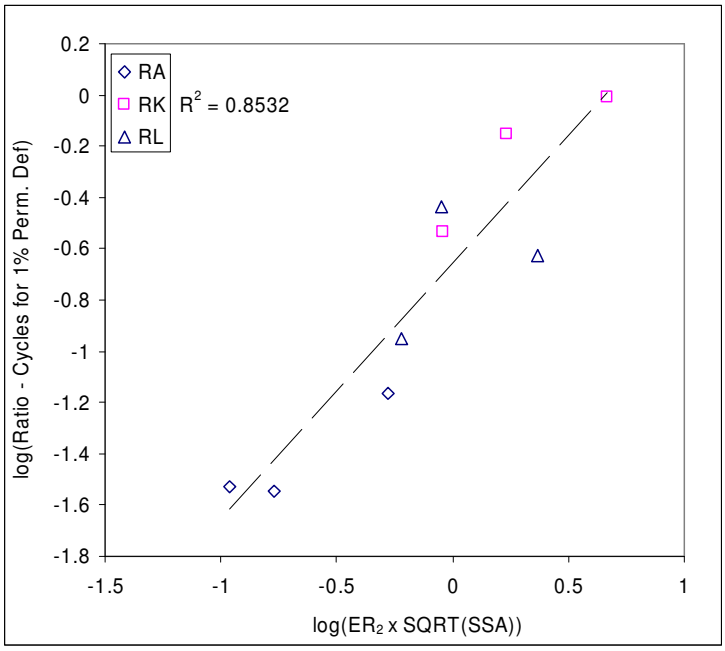

Figure 5.13. ER_2xSQRT(SSA) vs. Wet to Dry Ratio of Fatigue Life.

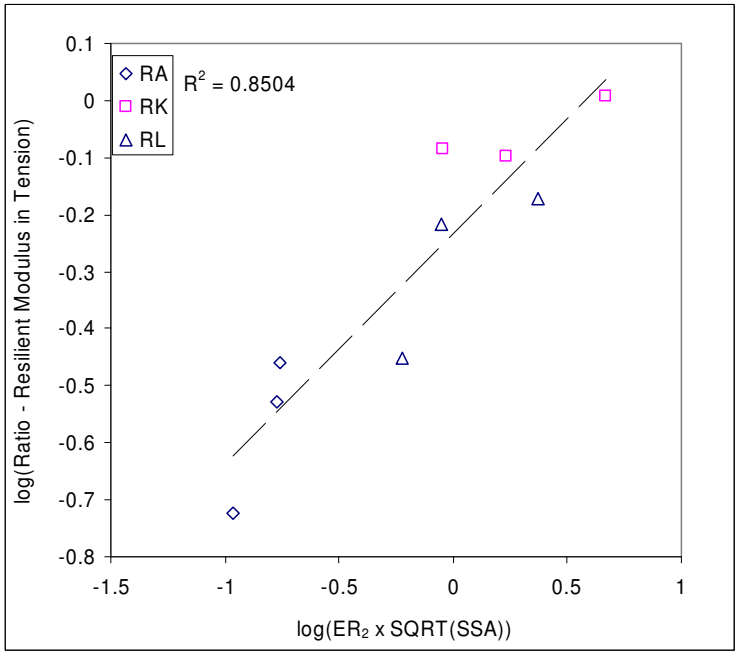

Figure 5.14. ER_2xSQRT(SSA) vs. Wet to Dry Ratio of Resilient Modulus in Tension.

Discussion

Correlation between the bond energy parameters multiplied with the specific surface area of the aggregates and the moisture sensitivity of the asphalt mixes was made on a log-log scale. This is because, the specific surface areas of the three aggregates increased by an order of magnitude from aggregate RA to RL to RK. The following can be inferred from the results:

- The correlation between bond energy parameters and moisture sensitivity of the mix based on ratio for cycles required for 1% permanent deformation was better than the correlation between bond energy parameters and moisture sensitivity of the mix based on ratio of resilient modulus in tension.
- The bond energy parameter of ER_2 (ratio of wettability to the work of debonding) correlates better than ER_1 (ratio of work of adhesion to the work of debonding) with the moisture sensitivity of the mixes estimated by laboratory testing.
- Product of square root of specific surface area and ER_2 gives the best correlation with moisture sensitivity of the mix estimated by laboratory testing.
- Use of wettability and specific surface areas in the bond energy parameters, as proposed earlier, is supported by these results.

Comparison of Field Performance of Mixes

One way to correlate the bond energy parameters with moisture sensitivity of asphalt mixes is by measuring the moisture sensitivity of the asphalt mixes using laboratory tests as discussed in the previous section. The advantage of using this methodology is that the experiments can be conducted on selected materials under well defined laboratory conditions. However, one of the reasons to investigate the use of bond energy parameters is the inefficiency of the mechanical tests in predicting moisture sensitivity of asphalt mixes. It is therefore desirable to establish a correlation of bond energy parameters with the moisture sensitivity of asphalt mixes based on their field performance. Unlike laboratory tests, it is difficult to control and quantify the moisture sensitivity of field mixes on a uniform scale owing to the differences in environmental

and field conditions of these mixes. Nevertheless, a qualitative assessment of moisture sensitivity of field mixes can still be made. The following sub sections present results from an independent study that correlates moisture sensitivity of field mixes with the four bond energy parameters proposed earlier. This independent study, uses the experiment and analytical techniques to measure surface energies and calculate bond energy parameters that were developed in this research [53].

Materials and Moisture Sensitivity

A total of eight field mixes from Texas and Ohio were included in this study. The moisture sensitivity was classified as "good" or "poor" these mixes based on inspection of pavements, field cores, and laboratory testing [53]. Table 5.7 lists the mix designs along with their rated resistance to moisture damage, constituent binder grades, and aggregate types. Similar binder grades or aggregate types with suffixes "A", "B" etc., indicate that these were obtained from different sources. The eight mix designs comprised of 6 different types of bitumen and 8 different types of aggregates. Some mixes had a combination of more than one type of aggregate. Surface energies for the bitumen and aggregates were determined using the Wilhelmy plate method and Universal Sorption Device as described in Chapters III and IV. The only difference was that ethylene glycol was not used as a probe liquid in measuring surface energies of the bitumen. Tables 5.8 and 5.9 list the surface free energy components for these materials, work of cohesion for bitumen, and specific surface areas for the aggregates.

Table 5.7. Summary of Mix Designs

Mix Design No.	Perfor-mance	Asphalt Grade	Aggregate Types	
1	Good	PG 76-22 A	Granite	
2	Poor	PG 76-22 B	Granite	
3	Good	PG 76-22 C	Quartzite	
4	Good	PG 76-22 C	Sandstone A	Sandstone B
5	Good	PG 76-22 C	Gravel A	Limestone A
6	Good	PG 76-22 D	Sandstone A	Sandstone B
7	Poor	PG 64-22	Limestone B	Gravel B
8	Poor	PG 64-28	Limestone B	Gravel B

Table 5.8. Surface Free Energy Components of Bitumen from Field Mixes

Asphalt Binder	Surface Free Energy (ergs/cm^2)				Work of cohesion (ergs/cm^2)
	LW	Acid	Base	Total	
PG 64-22	29.9	0.00	1.00	29.9	59.8
PG 64-28	17.9	0.13	2.88	19.1	38.2
PG 76-22 A	14.7	1.33	1.79	17.8	35.6
PG 76-22 B	24.2	0.07	1.31	24.7	49.4
PG 76-22 C	12.1	1.13	2.84	15.7	31.4
PG 76-22 D	21.8	0.63	0.65	23.1	46.2

Table 5.9. Surface Free Energy Components of Aggregates from Field Mixes

Aggregate	SSA (m^2/gm)	Surface Free Energy (ergs/cm^2)			
		LW	Acid	Base	Total
Granite	0.67	56.3	43.5	782.7	425.2
Gravel A	0.80	59.5	1.2	286.0	96.5
Gravel B	4.76	63.5	7.7	546.3	193.2
Limestone A	0.49	59.9	18.8	561.1	265.4
Limestone B	0.53	58.0	1.8	401.1	111.1
Quartzite	1.35	60.9	8.9	545.0	200.1
Sandstone A	0.83	62.5	2.0	222.6	105.0
Sandstone B	1.00	64.0	8.5	316.9	167.8

Surface free energy values were used to compute the work of adhesion, work of debonding, and the two bond energy parameters, ER_1, and ER_2. Since surface free energy components of bitumen and aggregates are measured individually, it is possible to compute the bond energy parameters for all possible combinations of bitumen and aggregate and not just the selected eight mixes. For mixes that contain more than one type of aggregate, the bond energy parameters were calculated for each bitumen-aggregate pair. It is reasonable to consider that the bitumen-aggregate combination that provides the poorest, or most critical values, of these parameters will govern the mixture performance. Tables 5.10 and 5.11 present the work of adhesion between the bitumen and aggregate in dry condition and work of debonding in presence of water. Tables 5.12 and 5.13 present values for the two bond energy parameters, ER_1, and ER_2.

Table 5.10. Work of Adhesion Between Bitumen and Aggregates

Bitumen	Quart-zite	Sand-stoneA	Granite	Gravel A	Sand-stoneB	Lime-stoneA	Lime-stoneB	Gravel B
76-22 C	114	92	134	93	103	119	100	115
76-22 D	115	100	125	101	108	117	105	116
76-22 B	96	89	103	87	94	98	88	97
76-22 A	122	99	140	101	110	126	108	122
64-22	91	89	95	87	93	93	86	93
64-28	93	82	106	81	90	97	83	93

Table 5.11. Work of Debonding in Presence of Water

Wet	Quart-zite	Sand-stoneA	Granite	Gravel A	Sand-stoneB	Lime-stoneA	Lime-stoneB	Gravel B
76-22 C	-139	-62	-200	-75	-95	-151	-101	-139
76-22 D	-138	-53	-208	-67	-90	-152	-96	-136
76-22 B	-158	-65	-230	-81	-104	-171	-113	-156
76-22 A	-132	-55	-195	-68	-89	-145	-94	-131
64-22	-163	-65	-239	-83	-106	-177	-116	-161
64-28	-160	-71	-228	-87	-108	-173	-118	-160

Table 5.12. Bond Energy Parameter – Field Mixes *(ER_1)*

ER1	Quart-zite	Sand-stoneA	Granite	Gravel A	Sand-stoneB	Lime-stoneA	Lime-stoneB	Gravel B
76-22 C	0.82	1.48	0.67	1.24	1.09	0.79	0.99	0.83
76-22 D	0.83	1.88	0.60	1.50	1.19	0.77	1.10	0.85
76-22 B	0.61	1.37	0.45	1.07	0.91	0.57	0.78	0.62
76-22 A	0.92	1.79	0.72	1.49	1.24	0.87	1.15	0.93
64-22	0.56	1.37	0.40	1.05	0.88	0.53	0.74	0.58
64-28	0.58	1.16	0.46	0.93	0.83	0.56	0.70	0.59

Table 5.13. Bond Energy Parameter – Field Mixes *(ER_2)*

ER_2	Quart-zite	Sand-stoneA	Granite	Gravel A	Sand-stoneB	Lime-stoneA	Lime-stoneB	Gravel B
76-22 C	1.69	1.03	1.95	1.21	1.32	1.73	1.48	1.67
76-22 D	2.01	0.99	2.63	1.23	1.47	2.16	1.63	1.95
76-22 B	3.42	1.65	4.28	2.16	2.31	3.52	2.92	3.31
76-22 A	1.54	0.87	1.87	1.04	1.19	1.61	1.29	1.51
64-22	5.17	2.20	6.75	3.09	3.17	5.30	4.45	4.90
64-28	2.94	1.61	3.37	2.04	2.08	2.94	2.62	2.89

Results

Figures 5.15 and 5.16 illustrate the comparison of field performance with the two bond energy parameters, ER_1 and ER_2. Figures 5.17 and 5.18 repeat these comparisons with the two bond energy parameters multiplied by the specific surface areas of the respective aggregates. A threshold value of the bond energy parameter in each case was derived based on the reported field performance of the asphalt mixes.

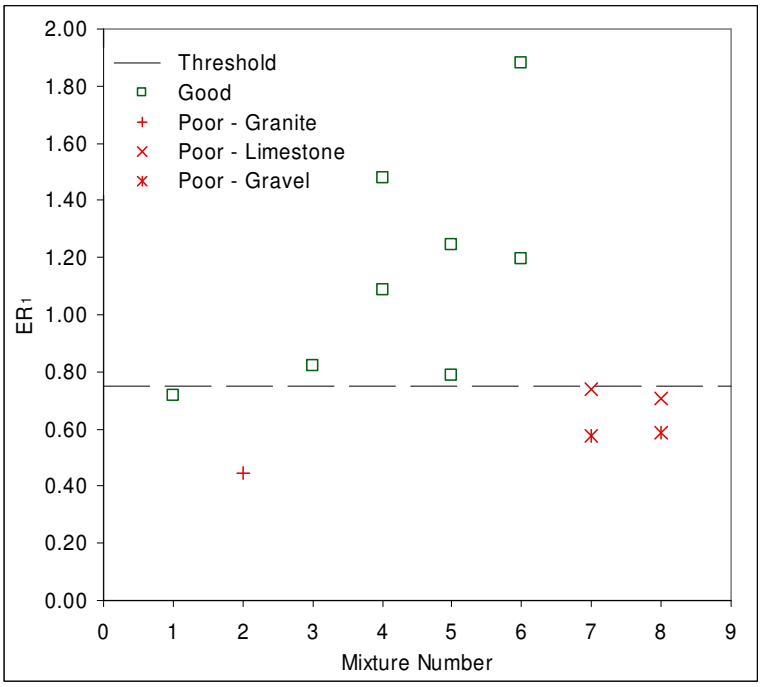

Figure 5.15. ER_1 vs. Field Evaluation of Moisture Sensitivity.

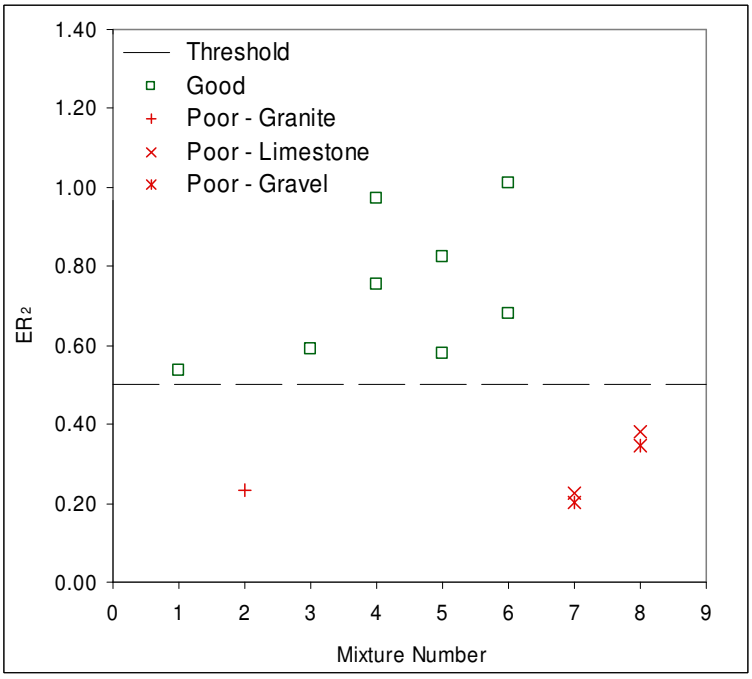

Figure 5.16. ER_2 vs. Field Evaluation of Moisture Sensitivity.

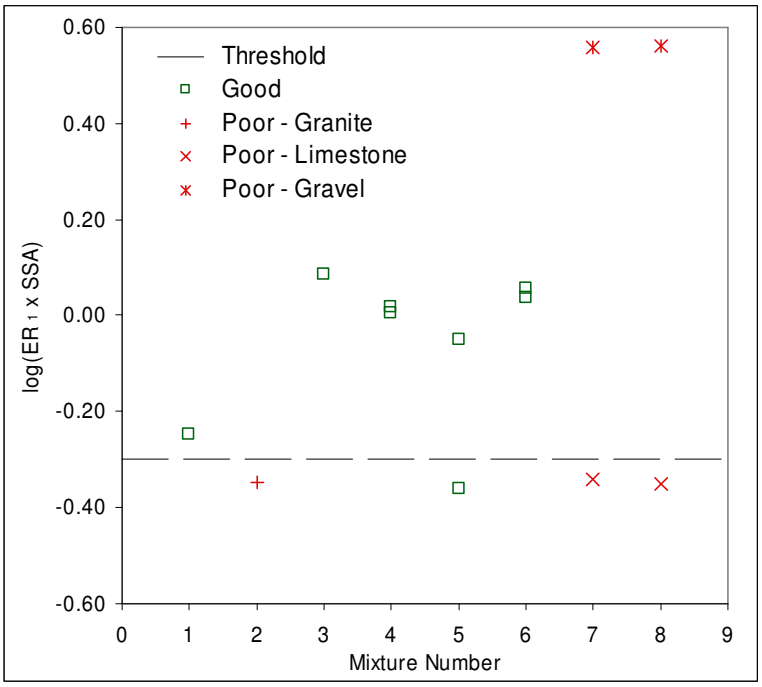

Figure 5.17. SSAxER$_1$ vs. Field Evaluation of Moisture Sensitivity.

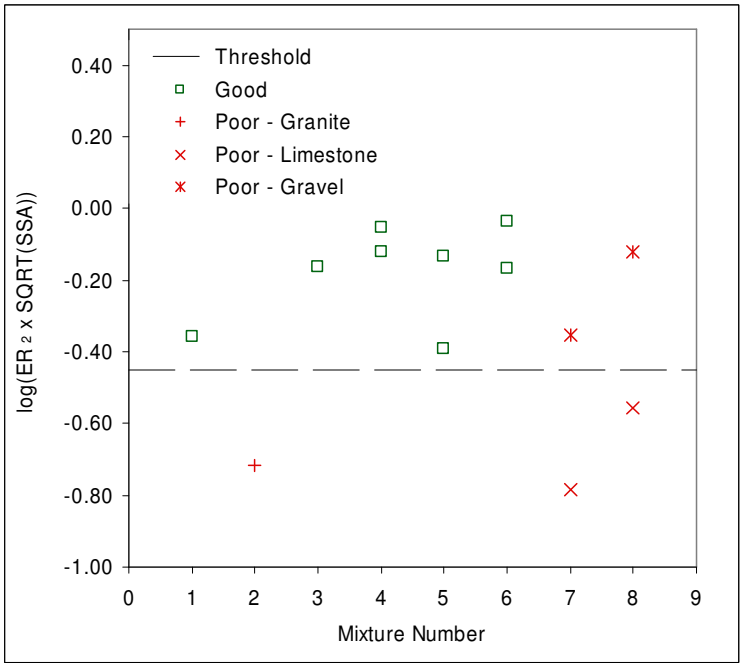

Figure 5.18. SQRT(SSA)xER$_2$ vs. Field Evaluation of Moisture Sensitivity.

Discussion

Mixes 7 and 8 contain more than one aggregate (limestone and gravel) and both are reported to be moisture sensitive based on field performance. Since both aggregates were present in significant percentages in the mix, it is reasonable to consider that failure of any one type of aggregate can render the entire mix as moisture sensitive. When only the bond energy parameters are considered, both aggregates appear to contribute approximately equally to moisture sensitivity of the mix. However, if the specific surface area of the aggregates are also considered by multiplying it with the bond energy parameters, it appears that limestone is the key contributor to moisture sensitivity of the mix and therefore it is the "weak link" that renders the entire mix to be moisture sensitive.

The threshold value for the bond energy parameters effectively differentiated mixes that were moisture sensitive in most cases, although the actual threshold value varied depending on the parameter used. From figure 5.17, it can be argued that mixture 5 must also be a poor performing mix when the bond energy parameter ER_1 x SSA is used to estimate moisture sensitivity of the mix, or that the bond energy parameter does not adequately differentiate moisture sensitive mixes in this case. Considering the limited data available, both the aforementioned arguments are possible. In these comparisons it must be borne in mind that there was no control over the traffic or environmental conditions which can contribute to significant variability in the results. Therefore, while a generalized conclusion can be made that bond energy parameters segregate mixes based on their moisture sensitivity, this data cannot be used for qualitative comparisons between various parameters.

CHAPTER VI

APPLICATIONS OF CALORIMETER

General

As described earlier, adhesion between bitumen and aggregate and debonding in the presence of water are key factors that influence the moisture sensitivity of an asphalt mix from a materials point of view. Mechanical interlocking, physical adhesion and chemical interactions are the three main mechanisms responsible for adhesion and debonding. The previous chapters described the development of tests to determine surface free energies of bitumen and aggregate and concomitant bond energy parameters. The use of bond energy parameters to identify moisture sensitive mixes was also demonstrated. However, these bond energy parameters are related to only physical adhesion between materials and also include mechanical interlocking to some extent when specific surface areas of the aggregates are combined with the bond energy parameters. However, when chemically active aggregates such as limestone are used or when active fillers such as hydrated lime or liquid anti strip agents are added to the bitumen, chemical interactions may contribute significantly to adhesion.

It is proposed that a micro calorimeter can be used in different ways to quantify the adhesion and debonding between the bitumen and aggregate. The three different ways of using the micro calorimeter explored in this research are as follows:

- To rapidly measure the enthalpies of immersion of aggregates with different probe liquids, which is then used to determine the surface free energies of aggregates.
- To measure the enthalpy of immersion of aggregates with water which is a direct measure of the total reduction of energy of the aggregate-water system when water coats the surface of a clean dry aggregate.
- To measure the enthalpy of immersion of aggregates with bitumen at mixing and compaction temperatures (approximately 150°C), which is a direct measure of the

total reduction of energy of the aggregate-bitumen system when bitumen coats the surface of a clean dry aggregate.

This chapter presents a description of the tests and results for the above three applications for a subset of materials used with the Wilhelmy plate method and USD. Comparisons between results based on surface free energy measurements and the results from the micro calorimeter indicate that this device can be used to measure various thermodynamic parameters related to the moisture sensitivity of the asphalt mixes with adequate sensitivity.

Surface Free Energy of Aggregates

When a clean solid (such as an aggregate) is immersed in a liquid, a new solid-liquid interface is formed and the clean solid surface is eliminated. This interaction is associated with a change in the total energy of the system and evolution of heat, referred to as the enthalpy of immersion. The enthalpy of immersion represents the strength of surface interaction at the solid-liquid interface. In the absence of any chemical reactions the enthalpy of immersion represents the reduction in total energy of the system due to the total surface energies of the two materials. If the interfacial surface free energy at the aggregate-liquid interface is represented by γ_{AL}, and surface free energy of the clean solid surface is represented by γ_A, then based on the above explanation, the change in free energy of the system due to immersion ΔG_{imm} is given by:

$$\Delta G_{imm} = \gamma_{AL} - \gamma_A \qquad \textbf{(6.1)}$$

The right hand side of equation (6.1), can be replaced by the surface free energy components of the solid and liquid using the GVOC theory. Further, based on the classic Gibbs free energy equation, ΔG_{imm}, can be replaced by the enthalpy of immersion ΔH_{imm}, and entropy of immersion ΔS_{imm}, to obtain the following equation:

$$\Delta H_{imm} - T\Delta S_{imm} = \gamma_L - 2\sqrt{\gamma_A^{LW}\gamma_L^{LW}} - 2\sqrt{\gamma_A^{+}\gamma_L^{-}} - 2\sqrt{\gamma_A^{-}\gamma_L^{+}} \qquad \textbf{(6.2)}$$

In equation (6.2) the subscript "A" refers to the aggregate, and "L" refers to the liquid and other terms are as described before.

Douillard et al [49] determined the heats of immersion and adsorption isotherms for various pure minerals with different probe liquids. Based on the comparisons of adsorption isotherms and heats of immersion, they demonstrate that the entropy term, ΔS_{imm}, in equation (6.2) can be approximated as 50% in magnitude of the enthalpy term, ΔH_{imm}. Since aggregates are composed of minerals which belong to the same class of materials used by Doullaard et al. it is reasonable to extend this approximation to heats of immersion with aggregates. If a calorimeter is used to measure enthalpy of immersion, ΔH_{imm} of a solid immersed in a probe liquid with known surface free energy components, and the approximation that the entropy term, ΔS_{imm}, is 50% in magnitude of the enthalpy term is used, then the only unknowns in equation (6.2) are the three surface free energy components of the solid. Just as with the Wilhlemy plate method and USD, measuring enthalpy of immersion with three probe liquids will generate a set of three equations that can be solved to determine the three surface free energy components of the aggregate.

Test Description

The micro calorimeter used in this study was an isothermal differential calorimeter manufactured by Omnical Inc.. The differential calorimeter comprises of two cells, a reaction cell and a reference cell. The net enthalpy is measured as the difference between the enthalpies of the reaction and reference cell using a series of thermocouples connected in series between the two cells. Figure 6.1 shows a schematic of the differential micro calorimeter.

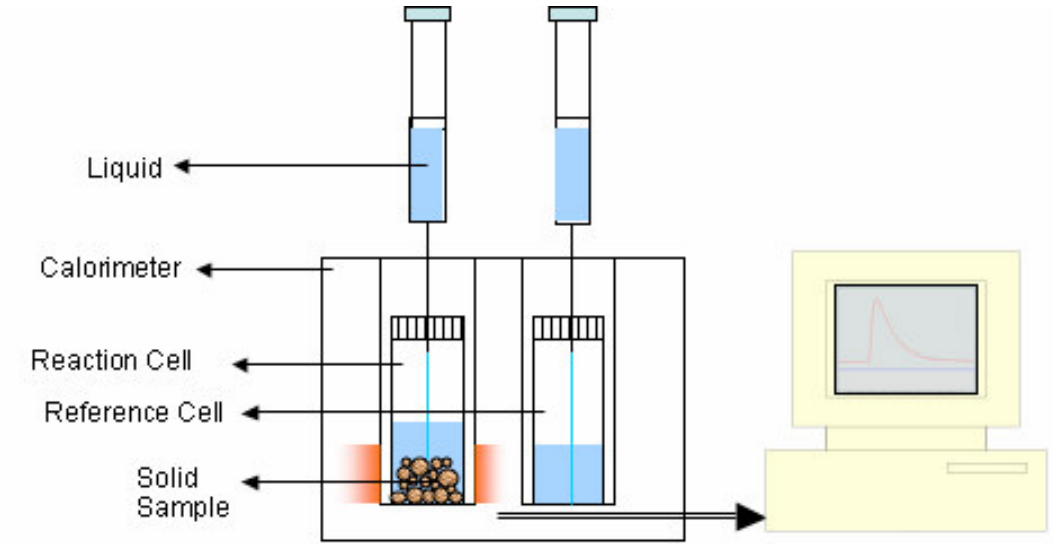

Figure 6.1. Schematic Layout of the Micro Calorimeter.

The aggregates included in this research were RD (limestone), RG (sandstone), RK (basalt), and RL (gravel). The three probe liquids used to measure the enthalpies of immersion were, heptane, benzene, and chloroform. These three probe liquids were selected because heptane is a non polar liquid and benzene and chloroform are mono polar liquids with a Lewis base and an Lewis acid character, respectively. Enthalpy of immersion of at least two replicates was measured in random order for each aggregate-probe pair.

Aggregates passing the #100 sieve and retained on the #200 sieve were found to be of suitable size for these tests. This was based on the minimum surface area required to generate heat that can be measured by the instrument with adequate precision. Crushed aggregates were sieved to obtain sufficient material of the desired size. The aggregates were then washed in the #200 sieve with distilled water and oven dried. About 8grams of the sample to be tested was placed in a 16ml capacity glass vial. The tare weight of the vial was recorded before filling it with the sample. The vials have a polypropylene open top cap sealed with a PTFE lined silicone septa. This vial was used in the reaction cell. Another empty vial sealed with a similar cap and septa was used in the reference cell. Prior to testing, both vials were preconditioned by heating at 150°C for four hours under vacuum below 300millitorr. Vacuum was drawn in both vials using

a 26 gauge syringe needle passing through the silicone septa. After completion og preconditioning the needle was quickly withdrawn allowing the silicone septa to seal itself retaining the contents of the vial under vacuum. The vials were then allowed to cool to the test temperature of 25°C. The test set up developed in this study enables preconditioning of four vials simultaneously. After the samples were preconditioned and cooled, the vial with the aggregate sample was weighed again to obtain the exact dry weight of the test sample and placed in the reaction cell. The empty vial was placed in the reference cell. Four syringes of 2ml capacity each were filled with the probe liquid. Two of these syringes were positioned on top of the reaction vial and the other two on top of the reference vial. An accompanying software with the micro calorimeter recorded the differential heat between the two cells within an accuracy of 10μwatts. As soon as thermal equilibrium was reached (typically 30 to 40 minutes) the syringes were pushed simultaneously piercing through the septa and the probe liquid was injected in both vials. Since differential heat between the two cells is recorded, heat generated due to the process of piercing and injection is compensated during measurement. The net heat measured in the reaction cell is due to,

(i) enthalpy of immersion in the reaction cell, and

(ii) difference in heat of vaporization of the probe liquid on account of the difference in free volume of the reaction and reference cell.

The latter is corrected by calculating heats of vaporization for the corresponding probe liquids.

Specific surface area of the aggregates is an important input for determining their surface free energy. In this research, the specific surface areas of the materials used were determined using adsorption measurements with the USD. In practice, this can be done using any commercial nitrogen adsorption equipment. The total enthalpy of immersion is divided by the mass of the sample to obtain the enthalpy of immersion in ergs/gm and then by the specific surface area to obtain the heat or enthalpy of immersion in ergs/cm^2. The surface free energy components of the aggregates were determined by solving the three simultaneous equations generated using each of the three probe liquids from equation 6.2.

Results and Discussion

Table 6.1 presents the average enthalpy of immersion of different aggregate-probe pairs and Table 6.2 presents the coefficient of variation for these measurements.

Table 6.1. Enthalpy of Immersion in ergs/cm^2

Aggregate	Liquid Probe		
	Benzene	**Chloroform**	**Heptane**
RD	159	345	108
RG	204	386	99
RK	63	137	38
RL	130	416	76

Table 6.2. Coefficient of Variation (%) for Measured Enthalpy of Immersion

Aggregate	Liquid Probe		
	Benzene	**Chloroform**	**Heptane**
RD	3	0	4
RG	0	1	5
RK	2	0	1
RL	7	2	4

Based on the data presented above it is evident that the micro calorimeter has very good repeatability. The device also has adequate sensitivity to differentiate between the heats of immersion of different aggregates with the same probe and heats of immersion of different probes with the same aggregate. Table 6.3 presents a comparison of the surface free energy components of the aggregates measured using the Universal Sorption Device and the micro calorimeter.

Table 6.3. Surface Free Energy Components of Aggregates in ergs/cm^2

Aggregate	Surface Free Energy Components					
	LW		Acid		Base	
	USD	MC	USD	MC	USD	MC
RD	44	52	2	11	258	469
RG	58	48	15	162	855	920
RK	52	18	1	16	162	154
RL	57	38	23	42	973	1652

Note: USD = Universal Sorption Device, MC = Micro Calorimeter

With the exception of the acid component of RG, the order of magnitude and trends in the surface free energy components derived from both methods are similar. Micro calorimeter appears to be more sensitive than the USD in differentiating between the Lifshitz-van der Waals (LW) component of surface free energy of different aggregates. Figures 6.2 through 6.4 present a graphical comparison of the three surface free energy components determined using the micro calorimeter and the USD.

The base component of surface free energy derived from the USD and the micro calorimeter show similar trends. The important application of determining aggregate surface free energy components is not to rank aggregates based on their surface free energy components, but to calculate the work of adhesion and work of debonding for different bitumen-aggregate combinations in order to predict the moisture sensitivity of different asphalt mixes.

Therefore it more reasonable to compare the work of adhesion and work of debonding obtained by combining surface energies from the USD and Wilhelmy plate, with these values obtained by combining surface energies from the micro calorimeter and Wilhelmy plate method. A total of 36 combinations of nine bitumen and four aggregates are included in this comparison. Figures 6.5 and 6.6 illustrate this comparison for the dry work of adhesion and wet work of debonding, respectively.

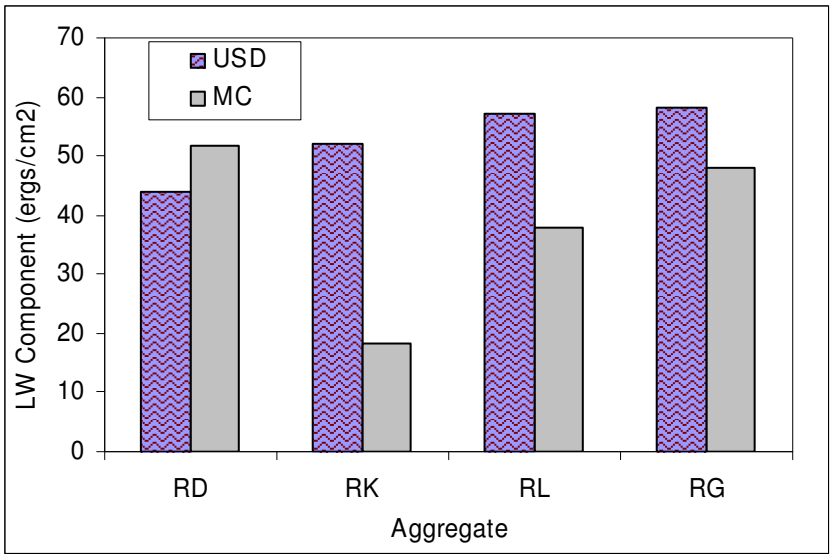

Figure 6.2. Comparison of the LW Component of Surface Free Energy.

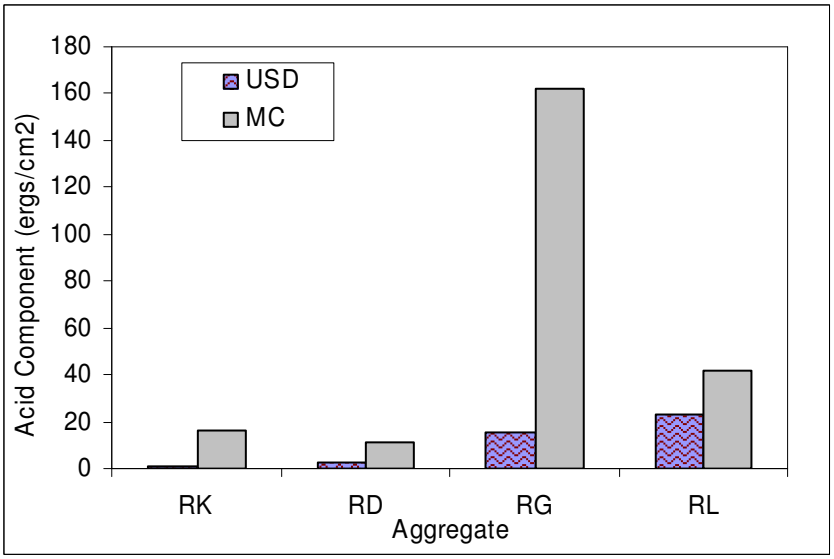

Figure 6.3. Comparison of the Acid Component of Surface Free Energy.

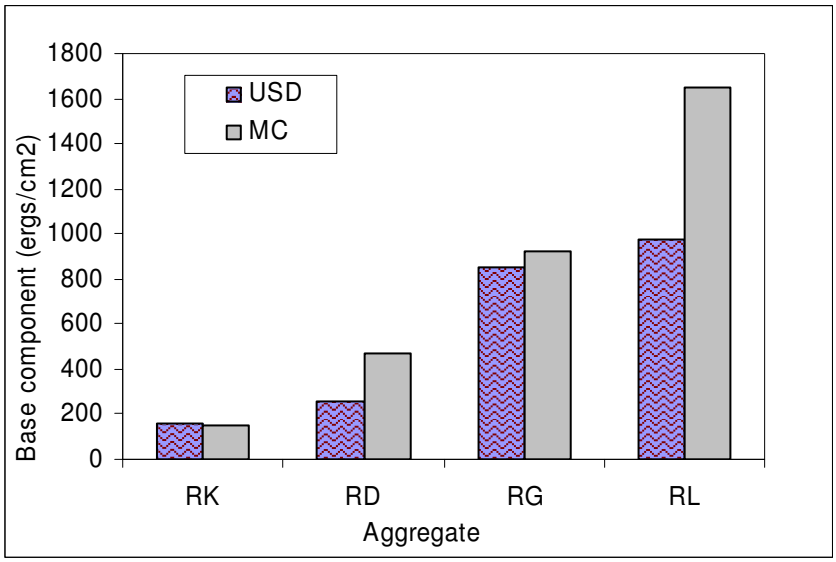

Figure 6.4. Comparison of the Base Component of Surface Free Energy.

The dry work of adhesion calculated using results from micro calorimeter compares well with the values calculated using results from the USD. The wet work of debonding calculated using results from the micro calorimeter correlates well with the values calculated using results from the USD, although there is a bias in the results.

In the preceding comparisons, results from the mirco calorimeter are compared with results from the USD. If the USD is used as a reference for accurate and true surface energies of aggregates then the bias and scatter between results from the micro calorimeter can be largely attributed to the assumption made for the contribution of the entropy term. However, both of these are indirect methods to measure surface free energy components of aggregates and there is no concrete evidence that results from the USD represent the “true values” for these components.

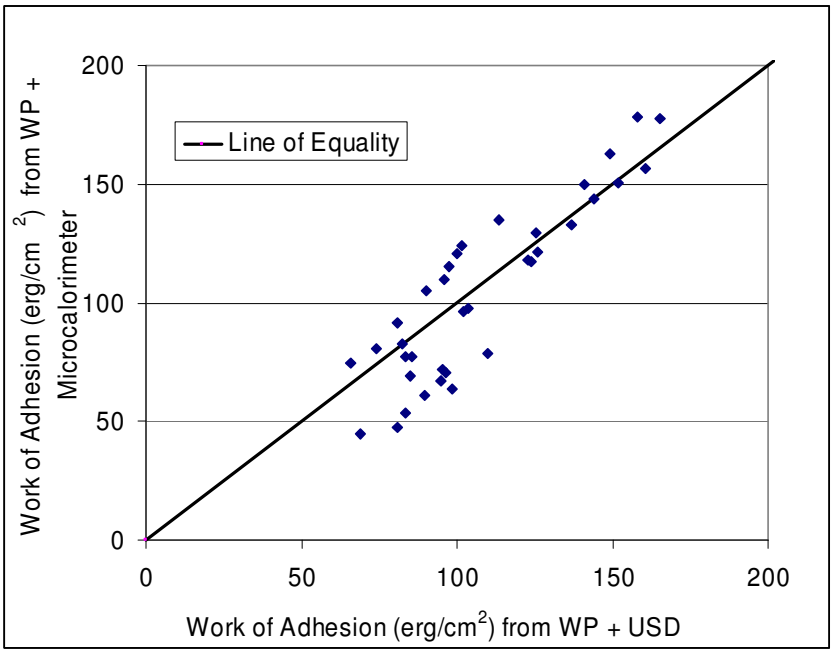

Figure 6.5. Comparison of Dry Adhesive Bond Strength between USD and Micro Calorimeter.

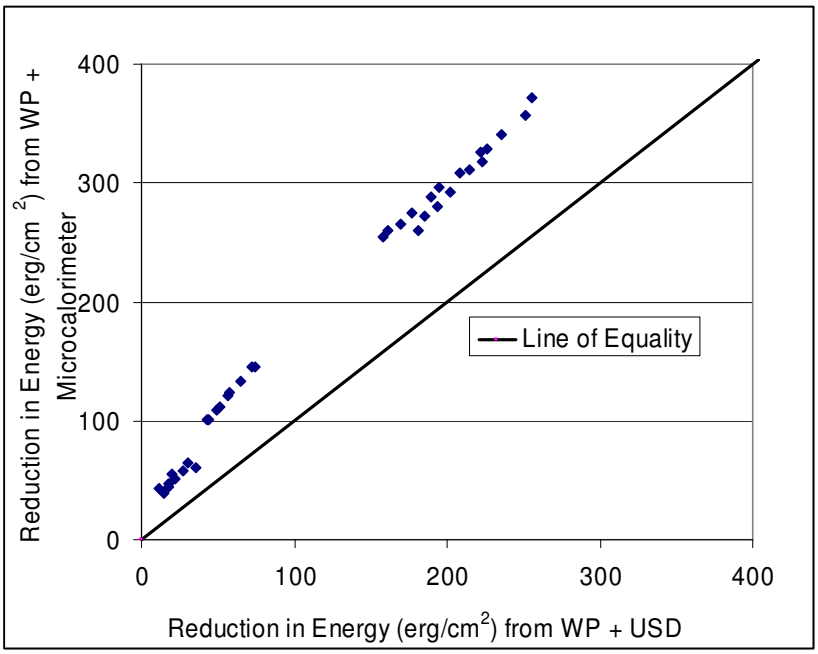

Figure 6.6. Comparison of Wet Adhesive Bond Strength between USD and Micro Calorimeter.

Hydrophilcity of Aggregates

The enthalpy of immersion of an aggregate in water can be used to quantify the hydrophilicity of different aggregates. In this context hydrophilicity of an aggregate is defined as the reduction in total energy of the system when water wets the surface of a clean dry aggregate. It can also be described as the thermodynamic drive for water to wet the surface of the aggregate or in a phenomenological sense it is the affinity of water molecules to the aggregate surface. The hydorphilicity of the four previously selected aggregates was measured as the heat of immersion of these aggregates with water. The test procedure was similar to the procedure used to measure heat of immersion of different aggregates with the probe liquids. Table 6.4 presents the values for heat of immersion of the four aggregates in water.

Table 6.4. Heats of Immersion in Water

Aggregate	Heat of Immersion	
	ergs/cm^2	ergs/gm
RD	348	515
RG	436	876
RK	373	7785
RL	977	4600

Results present in Table 6.4 show that the aggregates differ significantly in their affinity to water. The greater the hydrophilicity or the heat of immersion in water, the greater will be the thermodynamic drive for water to wet the surface of the aggregate. The hydrophilicity of an aggregate can also be theoretically computed if the surface free energy components of the aggregate and water are known. Mathematically this value is given by:

$$\left|\gamma_{AW} - \gamma_{A}\right| \qquad \textbf{(6.3)}$$

There are two major differences between the hydrophilicity estimated from these two different methods. Firstly, although both terms measure the reduction in energy of the system when water wets the aggregate surface, hydrophilicity derived from equation 6.3 is the reduction in free energy of the system whereas the hydrophilicty measured using the micro calorimeter is the reduction in total energy of the system. In other words, the latter term includes the enthalpy and entropy effect. For this class of materials it is reasonable to assume that the contribution of entropy will be a fixed percentage of the enthalpy of immersion. Therefore, although hydrophilicity derived by either method may not be equal due to the contribution of entropy, these two terms must at least be linearly correlated.

The second difference is that hydrophilicity determined using equation 6.3 takes into account only the physical interaction between the aggregate and water due to their surface free energies. According to the literature, electrostatic interactions between the aggregate and water also exist during the process of adhesion between these materials. These interactions are also associated with the change in pH of the water that comes into contact with the aggregate surface. Although, the contribution of electrostatic interactions themselves is a very small percentage of the total work of adhesion between the aggregate and water based on their surface free energy components [54], change in pH of the water can alter its surface free energy components which in turn can effect the magnitude of physical adhesion between the aggregate and the water. It is proposed here that the hydrophilicity of aggregates measured using the micro calorimeter is due to the cumulative effect of all these interactions, which otherwise would be difficult to quantify individually and combine.

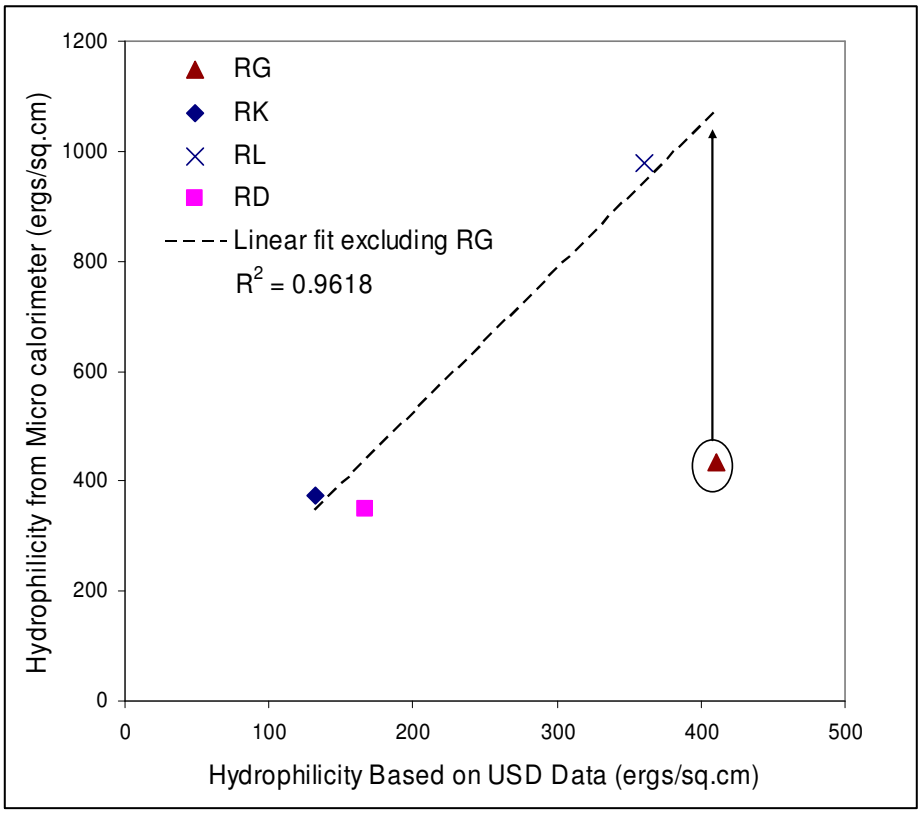

Figure 6.7 Hydrophilicity of Aggregates from USD vs. Micro calorimeter.

Figure 6.7 compares the hydrophilicity of aggregates based on equation 6.3 with the hydrophilcity of aggregates measured as the heat of immersion using the micro calorimeter. The correlation between hydrophilicity measured using both these methods for the three aggregates excluding RG, considering a straight line fit passing through the origin is significant. The bias of this straight line from 1:1 fit is due to the fact that the contribution of entropy is also included in the ordinate. This also explains the reason why the values of ordinate are generally higher compared to the values in the abscissa that includes only the free energy component of the total energy. The following paragraph explains the possible causes for deviation of RG from the general trend.

At first instance, the departure of RG from the general trend was attributed to the fact that the acid component of surface free energy of RG measured using the micro calorimeter was very high compared to the measured using the USD. However, this deviation did not improve when the graph was plotted by hypothetically increasing the

acid component of RG from the USD. The deviation is also not due to the entropy term since the relative contribution of entropy to the total energy of the system must be approximately the same for these materials. Eliminating these possible causes, the deviation of RG from the general trend can be explained based on the differences in electrostatic or other complex interactions associated with the change in pH of water after coming into contact with RG as compared to other aggregates. This provides a limited support to the proposition that the heat of immersion measured using the micro calorimeter is sensitive to the sum effect of different interactions that quantify the thermodynamic drive for water to wet the surface of the aggregate including the contribution from surface free energy of these materials. The following example further reinforces this proposition.

Consider moisture sensitivity of asphalt mixes with the two aggregates RG and RL. Data from the USD indicates that RG has a very high affinity for water (325 ergs/cm^2) based on the surface free energy terms alone. This is approximately the same as the affinity of RL to water (361 ergs/cm^2) compared to other aggregates (130 ergs/cm^2 for RK and 160 ergs/cm^2 for RD). Therefore the moisture sensitivity of RL aggregate must be approximately the same as that of the RG aggregate if hydrophilicity based on the surface free energies from the USD are considered. This is contradictory to data from other studies [55] which shows that RG is an aggregate with intermediate stripping tendency as compared to RL which has a very high tendency to strip. However, hydrophilicity of the two aggregates based on the heat of immersions measured by the micro calorimeter, corraborate well with these findings.

Total Energy of Adhesion Between Aggregates and Bitumen

Another application of the micro calorimeter is to measure the total energy of adhesion between different bitumen and aggregates at the mixing and compaction temperature. It is proposed that this instrument and method is sensitive to identify the presence of any chemical reaction that may contribute to the adhesion between the bitumen and aggregate. Earlier studies that report the measurement of work of adhesion between the bitumen and aggregate [32-34] were associated with several drawbacks. For

example, the post test equilibrium heat flow was generally much higher than the pre test equilibrium heat flow. This difference was attributed entirely to the reduction in free energy as multiple layers of bitumen built beyond the first monolayer on the aggregate surface during the adhesion process, whereas it is likely that a significant part of this difference is due to the differences in specific heats of the reaction and reference cell due to the mixing of the bitumen and the aggregate. Also, these studies did not attempt to use results from the micro calorimeter in conjunction with the heat of immersion with water and surface free energy components of bitumen and aggregate. The following paragraphs present a description of the test method to measure the total energy of adhesion between the aggregates and bitumen and a comparison of these results with the work of adhesion determined using the surface free energy of the bitumen and aggregate.

Materials and Test

The four aggregates used previously, RL, RK, RG and RD and two bitumen types, AAB and ABD were used in this experiment. This resulted in a total of eight bitumen-aggregate combinations. The micro calorimeter used was the same as before but with a different set up for holding the samples to conduct the tests at 150°C with bitumen in liquid form. Figure 6.8 shows the sample set up used for the high temperature experiments. The test procedure was similar to the heat of immersion experiments described earlier. The reaction vial (bitumen + aggregate) and reference vial (blank cell + aggregate) were placed in their respective cells. The aggregates were used immediately after oven drying them at 160°C for 16 hours. The system was allowed to come to equilibrium at 150°C, which usually took about 4 hours. During the equilibration time, aggregates in the glass columns are separated from the reaction vial with the bitumen or the blank vial using a filter paper. After equilibrium is reached, the glass columns are lowered by about 5 mm, puncturing the filter paper and allowing the aggregates to drop into the vial. Aggregates in the reaction vial readily mixed with the bitumen in the liquid form. This resulted in a reduction of free energy of the system that is associated with the release of heat and is measured by the micro calorimeter. The amount of heat given out is the total energy of adhesion between the bitumen and the aggregate.

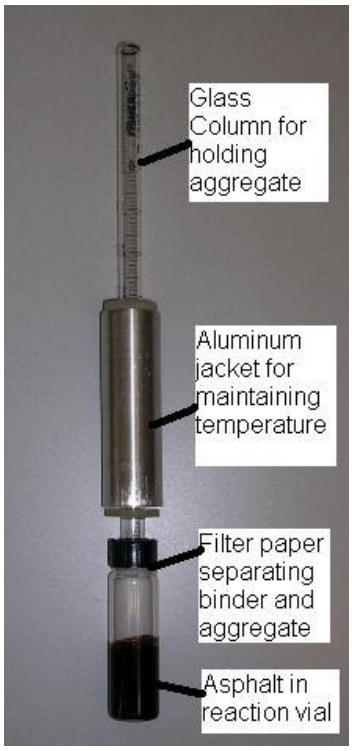

Figure 6.8. Reaction Vial to Conduct Immersion Experiments at High Temperatures with Micro calorimeter.

Results and Discussion

At least two replicate measurements were made for the heat of immersion for each bitumen-aggregate combination. Figures 6.9 and 6.10 present a comparison of the heats of immersion measured for the four aggregates using bitumen AAB and ABD, respectively, with the theoretical work of adhesion between these aggregates and the bitumen calculated using their surface free energy components from the Wilhelmy plate method and the USD.

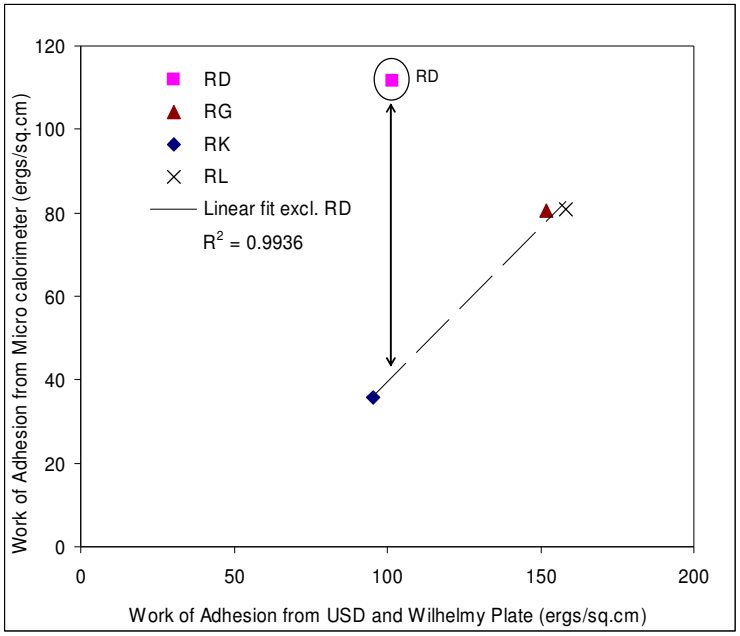

Figure 6.9. Measured Total Energy of Adhesion vs. Work of Physical Adhesion for AAB.

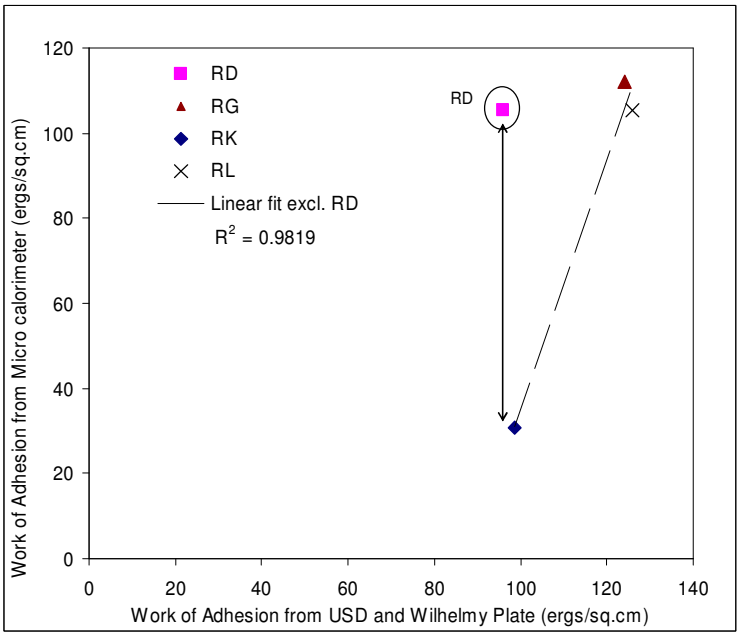

Figure 6.10. Measured Total Energy of Adhesion vs. Work of Physical Adhesion for ABD.

There are three possible reasons for the differences between the values measured using the micro calorimeter and the theoretical values calculated from the surface energies using the Wilhelmy plate method and the USD. Firstly, as mentioned before, the value computed from the surface energies is related to the free energy of adhesion, whereas the value measured using the micro calorimeter is due to the total energy of adhesion. However, under the assumption that the proportion of entropy does not change significantly for this class of materials when comparing one bitumen-aggregate combination with another, it is reasonable to expect that entropy will not affect the positive linear trend between the work of adhesion and total energy of adhesion. The second reason for difference between the two values is that the work of adhesion was computed based on surface free energy values of the bitumen and aggregate at 25°C, whereas the total energy of adhesion was measured using the micro calorimeter at 150°C. Since the rate of decrease in surface free energy of materials with temperature for these materials is usually small and similar, this difference will also not significantly affect the positive linear trend between the work of adhesion at 25°C and the total energy of adhesion at 150°C. The third and most important reason is that the work of adhesion based on the surface free energy components of bitumen and aggregate quantifies only the physical adhesion between these two materials. In contrast, the total energy of adhesion measured by the micro calorimeter is due to all possible physical and chemical interactions that occur between the aggregate and the bitumen. This difference is not necessarily constant for all aggregates. As a result chemical interactions can cause deviations in any expected positive correlation between work of adhesion based on surface free energy and total energy of adhesion based on heats of immersion.

Figures 6.9 and 6.10 show that the total energy of adhesion for RD is significantly greater than that expected for other aggregates based on the theoretical work of adhesion. Based on the above explanation, it is expected that there are significant chemical interactions associated with RD as compared to other aggregates. This is substantiated by the fact that while RD is predominantly a limestone, other aggregates are predominantly siliceous. Other studies suggest that the presence of calcium ions on the aggregate surface promote the formation of chemical bonds with functional groups such as carboxylic acids from the bitumen. Further, the heat dissipation curves for RD were

predominantly exothermic but inevitably showed a small endotherm before finally achieving the post mixing equilibrium. This endotherm was more significant for RD than for other aggregates. Typically chemisorption is preceded by physical adsorption and in some cases there is a small energy barrier that needs to be overcome before chemisorption follows physical adsorption. It is suggested that low intensity chemical interactions continue even after wetting of the aggregate surface by bitumen and the endotherm prior to equilibrium is associated with the energy absorbed during the transition from physical adsorption to chemisorption. From these results, it is inferred that the micro calorimeter can be used to quantify the total energy of adhesion between aggregate and bitumen including effects of physical and chemical bonding. Also, this method used in conjunction with surface energies measured using the Wilhelmy plate method and the USD can be used to identify presence of any chemical bonding that contributes to adhesion.

CHAPTER VII

CONCLUSIONS AND RECOMMENDATIONS

General

Moisture sensitivity of asphalt mixes is one of the forms of pavement distresses that results in high maintenance and rehabilitation costs of pavements. Therefore it is important to identify and eliminate materials or material combinations during the mix design process that can render the asphalt mix susceptible to premature moisture induced damage. Research in this field in the past five decades has focused on mechanical tests on whole asphalt mixes to estimate their moisture sensitivity. These tests do not always accurately predict the moisture sensitivity of asphalt mixes in field. Also, these tests do not provide information that can explain the causes for the moisture sensitivity or resistance to moisture damage of asphalt mixes. This information is important to modify mixes that do not meet moisture sensitivity requirements, by using locally available materials.

Moisture sensitivity of any asphalt mix in field is due to the combined action of material properties, mix design properties such as air void structure, external loads, and environmental conditions. Selection of proper materials is the first step to ensure that the resulting asphalt mix will not be moisture sensitive. This is possible by measuring material properties that are closely related to the mechanisms responsible for adhesion between bitumen and aggregate and debonding between these materials in presence of water. Examples of such properties are, physical adhesion due to surface free energies of bitumen and aggregate, and chemical interactions between these materials.

The use of Wilhelmy plate method and Universal Sorption Device (USD), was introduced in earlier studies to measure the surface free energies of bitumen and aggregate and use these values to quantify the work of adhesion between these materials in dry condition and the work of debonding in presence of water. However, results from these studies do not corroborate well with known physical and chemical properties of bitumen and aggregate. In this research, significant changes to these test methods were

made to enable measurement of bitumen and aggregate surface energies. The surface free energy components of the bitumen and aggregate were computed using analytical techniques that use the results from the Wilhelmy plate method and the USD. Precision of the surface free energy components was established using statistical methods for propagation of errors based on the precision of the experimentally measured parameters from these tests. Accuracy of the measurements from the Wilhelmy plate method was assessed by comparing the contact angles measured using this method with the theoretical requirements for advancing contact angles proposed in the literature. Accuracy of the USD was assessed by comparing the specific surface areas of aggregates measured using this device with the areas measured using a standard method based on nitrogen adsorption. Surface free energy components of some minerals measured using this method also corroborate well with surface free energy components of similar minerals reported in the literature using different test methods.

The work of cohesion in the bitumen, work of adhesion between bitumen and aggregate, and work of debonding between bitumen and aggregate in presence of water, were computed using the surface free energy of bitumen and aggregate. Different energy parameters based on these thermodynamic quantities and specific surface areas of aggregates were proposed to assess the moisture sensitivity of asphalt mixes. Moisture sensitivity of different asphalt mixes measured in the laboratory and based on field records correlate well with most of these energy parameters.

While physical adhesion due to surface free energy is the significant contributor to total adhesion in most bitumen-aggregate systems, there are also material combinations in which adhesion due to chemical reactions is important. For example, when a chemically active mineral aggregate such as limestone is used in the asphalt mix or when active fillers such as hydrated lime or liquid anti strip agents are added to the mix to improve its performance. The use of a micro calorimeter to measure the combined effects of physical and chemical adsorption of bitumen with aggregate and water with aggregate was demonstrated. It was also shown that this method can be used with the Wilhelmy plate method and USD to differentiate and identify the presence of any significant chemical interactions. Use of the micro calorimeter as a faster method to estimate the surface free energy components of aggregates was also demonstrated.

Conclusions and Discussion

Surface Free Energy of Bitumen and Aggregates

Based on development of the Wilhelmy plate method and the USD to measure the surface free energy components of the bitumen and aggregates, respectively, the following conclusions can be made:

- The Wilhelmy plate method and the USD can be used to measure the surface free energy components of bitumen and aggregates with adequate precision and accuracy.
- Most bitumen have a low Lifshitz-van der Waals (LW) component and very low acid and base components. This corroborates well with the known fact that bitumen are low surface energy materials with a weak acid-base character.
- Most aggregates have a similar magnitude of the LW component, and a small magnitude of the acid component. However, the base component of surface free energy varies significantly from one aggregate to another and is typically one or two orders of magnitude higher than any other component of aggregate or bitumen. Consequently, when the work of adhesion is computed, the geometric mean of the acid component of bitumen and base component of aggregates are significant contributors.

The following cautions must be exercised in interpreting the results from these methods:

- The magnitudes of acid and base components are computed using the surface free energy components of probe liquids from the GVOC scale which assumes that the acid component of water is equal to the base component of water. This assumption is disputed by some in the literature [36]. Therefore, the magnitude of acid and base components of different materials derived from these tests must not be interpreted too literally, since these magnitudes are relative on a scale that assumes that the acid component of water is equal to its base component.
- When bitumen slides are prepared for testing with the Wilhelmy plate method, a glass substrate is cleaned and immersed in the hot liquid bitumen. As soon as the

slide is removed from the liquid bitumen, it cools and attains its room temperature consistency within a short period of time. Representation of the polar functional groups from the bulk of the material on such a surface will be based on random distribution. When the surface free energy components of the bitumen are measured by immersing the slide in a probe liquid, the acid and base character of the bitumen will be established by the nature and concentration of different functional groups on the surface. However, in real mixes, when liquid bitumen is mixed with aggregates, there is a substantial amount of time that allows polar species to migrate from the bulk of the bitumen to the aggregate-bitumen interface. It is probable that the concentration of polar species at the bitumen aggregate interface will be more than the concentration of the polar species on the bitumen slide that is prepared for testing with the Wilhelmy plate method. Therefore, in interpreting the small acid and base values of the bitumen it must be remembered that these values can be significantly magnified due to kinetics of the polar molecules in real mixes.

- The Wilhemy plate method and the USD measure the surface free energies of the bitumen and aggregate which are related to the physical adhesion between these materials. Any possibility of chemical reactions between these two materials can influence the work of adhesion computed based on the surface free energies of these materials.

Surface Free Energy and Moisture Sensitivity of Asphalt Mixes

Different combinations of the thermodynamic parameters based on the surface free energy of bitumen and aggregate were proposed to rationally explain and assess the moisture sensitivity of asphalt mixes. The energy parameter that incorporates wettability of the aggregate by the bitumen, work of debonding in the presence of water, and the specific surface area of the aggregate, correlates best with the moisture sensitivity of asphalt mixes based on laboratory and field performance of asphalt mixes. This parameter is given as follows:

$$\left|\frac{W_{AB} - W_{BB}}{W_{ABW}^{wet}}\right|\left(\sqrt{SSA}\right) \quad \textbf{(7.1)}$$

The following must be noted while using the above or other thermodynamic parameters to assess moisture sensitivity of asphalt mixes:

- There are two possible applications for the thermodynamic parameters derived from the surface free energy measurements. Firstly, parameters such as the one shown in the expression (7.1) may be used on their own as a material selection and screening tool, as demonstrated in this research. Secondly, these thermodynamic parameters can be combined with other material and mixture properties and used with mechanistic models based on continuum mechanics to predict performance of pavements.
- The application of this parameter needs further investigation when binders that are modified chemically by addition of active fillers, liquid anti strip agents or any other active agent such as polyphosphoric acids.

Applications of Micro Calorimeter

The use of a micro calorimeter to measure thermodynamic properties related to moisture sensitivity of mixes was proposed. Results show that the micro calorimeter can be used to measure,

- surface free energy components of aggregates,
- total energy of adhesion between the bitumen and aggregate including the cumulative effects of physical adsorption and chemisorption, and
- total energy of adhesion between aggregate and water including effects of physical adsorption and effects due to electrostatic and other interactions.

The aforementioned properties measured using the micro calorimeter are directly related to the adhesion and debonding mechanisms between bitumen and aggregate and hence to the moisture sensitivity of the asphalt mixes.

Important advantages of using a micro calorimeter are:

- lower capital cost of the equipment,
- excellent repeatability combined with adequate sensitivity,

- shorter test times as compared to adsorption methods,
- preconditioning of samples can be done independent of the equipment saving on sample preparation time, and
- less operator skill required to operate the device and conduct tests.

Recommendations for Future Work

Based on the work done in this research the following recommendations for future work are made:

- The combined use of Wilhelmy plate method, USD and the micro calorimeter must be made to identify the material characteristics of aged bitumen, bitumen modified using active fillers, and bitumen modified using liquid anti strip agents.
- Application of thermodynamic parameters from surface free energy measurements in conjunction with other material and mixture properties using continuum damage models to predict performance of pavements subjected to various modes of distress.
- Laboratory and field tests to compare the moisture sensitivity of mixes with active fillers, and liquid anti strip agents with the thermodynamic parameters measured using the micro calorimeter.
- Immersion experiments of aggregates with bitumen and aggregates with probe liquids must be conducted using the micro calorimeter at different temperatures to quantitatively establish the effects of entropy.
- Immersion experiments of relatively homogenous aggregates representing the commonly used minerals, with probe liquids doped with chemicals that represent various functional groups in bitumen must be performed using the micro calorimeter. This information will be useful in understanding the relative adsorption of different functional groups from the bitumen to the aggregate surface, which can in turn be used to modify the locally available materials to reduce moisture sensitivity of asphalt mixes.

REFERENCES

1. U.S. Department of Transportation, Research and Innovative Technology Administration, *National Transportation Statistics 2005,* Washington , D.C. www.bts.gov/publications/national_transportation_statistics/2005. Accessed January 15, 2006.
2. Rice, J. M. Relationship of Aggregate Characteristics to the Effect of Water on Bituminous Paving Mixtures. In *Effect of Water on Bituminous Paving Mixtures*, ASTM STP No. 240, Philadelphia, Pa, 1958, pp. 17-34.
3. Ishai, I., and J. Craus. Effect of Filler on Aggregate-Bitumen Adhesion Properties in Bituminous Mixtures. *Journal of Association of Asphalt Paving Technologists,* Vol. 46, 1977, pp. 228-258.
4. Scott, J. A. N. Adhesion and Disbanding Mechanisms of Asphalt Used in Highway Construction and Maintenance. *Journal of Association of Asphalt Paving Technologists,* Vol. 47, 1977, pp. 19-48.
5. Taylor, M. A., and N. P. Khosla. Stripping of Asphalt Pavements: State of the Art. In *Transportation Research Record: Journal of the Transportation Research Board, No. 911,* TRB, National Research Council, Washington D.C., 1983, pp. 150-158.
6. Terrel, R. L., and S. Al-Swalilmi. *Water Sensitivity of Asphalt Aggregate Mixes: Test Selection.* Publication SHRP-A-403. Strategic Highway Research Program, National Research Council, Washington D.C., 1994.
7. Kanitpong, K. and H. U. Bahia. Role of Adhesion and Thin Film Tackiness of Asphalt Binders in Moisture Damage of HMA. *Journal of Association of Asphalt Paving Technologists,* Vol. 72, 2003, pp. 611-642.
8. Little, D. N., D. R. Jones, and S. Logaraj. Chemical and Mechanical Mechanisms of Moisture Damage in Hot Mix. Presented at National Seminar on Moisture Sensitivity, San Diego, CA, 2002.
9. Pocius, A.V. *Adhesion and Adhesives Technology*. Hanser/Gardner Publications Inc., Columbus, OH, 1997.

10. Tarrar, A. R. and V. P. Wagh. *The Effect of the Physical and Chemical Characteristics of the Aggregate on Bonding*. Publication SHRP-A/UIR-91-507. Strategic Highway Research Program, National Research Council, Washington, D.C., 1992.
11. Masad, E., T. Al-Rousan, J. Button, D. N. Little, and E. Tutumluer. *Test Methods for Characterizing Aggregate Shape, Texture and Angularity.* Publication NCHRP 4-30A. National Cooperative Highway Research Program, National Research Council, Washington, D.C., 2005.
12. Petersen, J. C., H. Plancher, E. K. Ensley, R. L. Venable, and G. Miyake. Chemistry of Asphalt-Aggregate Interaction: Relationship with Pavement Moisture-Damage Prediction Test. In *Transportation Research Record: Journal of the Transportation Research Board, No. 843,* TRB, National Research Council, Washington D.C., 1982, pp. 95-104.
13. Jamieson, I. L., J. S. Moulthrop, and D. R. Jones. SHRP Results on Binder-Aggregate Adhesion and Resistance to Stripping. In *Asphalt Yearbook 1995*, Institute of Asphalt Technology, Surrey, U.K., 1995.
14. Majidzadra, K. and F. N. Brovold. *State of the Art: Effect of Water on Bitumen-Aggregate Mixtures*. Highway Research Board, Special Report No. 98., Washington, D.C., 1968.
15. Cheng, D., *Surface Free Energy of Asphalt-Aggregate Systems and Performance Analysis of Asphalt Concrete Based on Surface Free Energy*. Ph.D. dissertation. Texas A&M University, College Station, 2002.
16. Kim, Y. R., D. N. Little, and R. L. Lytton. Effect of Moisture Damage on Material Properties and Fatigue Resistance of Asphalt Mixtures. In *Transportation Research Record: Journal of the Transportation Research Board, No. 1891,* TRB, National Research Council, Washington D.C., 2004, pp. 48-54.
17. Lottman, R. P. Laboratory Test Method for Predicting Moisture-Induced Damage to Asphalt Concrete. In *Transportation Research Record: Journal of the Transportation Research Board, No. 843,* TRB, National Research Council, Washington D.C., 1982, pp. 88-95.

18. Plancher, H., G. Miyake, R. L. Venable, and J. C. Petersen. A Simple Laboratory Test to Indicate the Susceptibility of Asphalt-Aggregate Mixtures to Moisture Damage During Freeze-Thaw Cycling. *Proc., Canadian Technical Asphalt Association Meeting*, Vol. 25, pp. 246-264.

19. Al-Swailmi, S., and R. L. Terrel. Evaluation of Water Damage of Asphalt Concrete Mixtures Using the Environmental Conditioning System (ECS). *Journal of Association of Asphalt Paving Technologists,* Vol. 61, 1992, pp. 405-445.

20. American Association of State Highway and Transportation Officials. Resistance of Compacted Asphalt Mixtures to Moisture-Induced Damage, Test Method T283-02, *Standard Specifications for Methods of Sampling and Testing – Part II,* AASHTO, Washington D.C., 2003.

21. American Society for Testing and Materials. Standard Practice for Effect of Water on Bituminous-Coated Aggregate Using Boiling Water, D3625-96. *Road and Paving Materials,* ASTM International, 2005.

22. American Association of State Highway and Transportation Officials. Standard Method of Test for Coating and Stripping of Bitumen-Aggregate Mixtures, Test Method T182-84, *Standard Specifications for Methods of Sampling and Testing – Part II,* AASTHO, Washington D.C., 2002.

23. Aschenbrener, T., R. B. McGennis, and R. L. Terrel. Comparison of Several Moisture Susceptibility Tests to Pavements of Known Field Performance. *Journal of Association of Asphalt Paving Technologists,* Vol. 64, 1995, pp. 163-208.

24. Tarrar, A. R., and V. P. Wagh. Innovative Tests to Predict the Strength and Type of Asphalt-Aggregate Bonds. *Fuel Science and Technology International*, Vol. 10, 1992, pp. 457-474.

25. Van Oss, C. J., M. K. Chaudhury, and R. J. Good. Interfacial Lifshitz-van der Waals and Polar Interactions in Macroscopic Systems. *Chemical Reviews*, 1988, Vol. 88, pp. 927-941.

26. Van Oss, C.J. *Interfacial Forces in Aqueous Media*, Marcel Dekker, Inc., NY, 1994.

27. Curtis, C. W., Y. W. Jeon, and D. J. Clapp. Adsorption of Asphalt Functionalities and Oxidized Asphalts on Aggregate Surfaces. *Fuel Science and Technology International*, Vol. 7, No. 9, 1989, pp. 1225-1268.

28. Petersen, J. C., E. K. Ensley, and F. A. Barbour. Molecular Interactions of Asphalt in the Asphalt-Aggregate Interface Region. In *Transportation Research Record: Journal of the Transportation Research Board, No. 516,* TRB, National Research Council, Washington D.C., 1974, pp. 67-78.

29. Petersen, J. C. Quantitative Functional Group Analysis of Asphalts Using Differential Infrared Spectrometry and Selective Chemical Reactions. In *Transportation Research Record: Journal of the Transportation Research Board, No. 1096,* TRB, National Research Council, Washington D.C., 1986, pp. 95-104.

30. Plancher, H., S. M. Dorrence, and J. C. Petersen. Identification of Chemical Types in Asphalts Strongly Adsorbed at the Asphalt-Aggregate Interface and Their Relative Displacement by Water. *Journal of Association of Asphalt Paving Technologists,* Vol. 46, 1977, pp. 151-175.

31. Curtis, C. W., D. J. Clapp, Y. W. Jeon, and B. M. Kiggundu. Adsorption of Model Asphalt Functionalities, AC-20, and Oxidized Asphalts on Aggregate Surfaces. In *Transportation Research Record: Journal of the Transportation Research Board, No. 1228,* TRB, National Research Council, Washington D.C., 1989, pp. 112-127.

32. Ensley, E. K., J. C. Petersen, and R. E. Robertson. Asphalt-Aggregate Bonding Energy Measurments by Microcalorimetric Methods. *Thermochimica Acta*, Vol. 77, 1984, pp. 95-107.

33. Ensley, E. K. A Study of Asphalt Aggregate Interactions and Asphalt Molecular Interactions by Microcalorimetric Methods : Postulated Interaction Mechanism. *Journal of the Institute of Petroleum,* Vol. 570, No. 59, 1973, pp. 279-289.

34. Ensley, E. K. and H. A. Scholz. A Study of Asphalt Aggregate Interactions by Heat of Immersion. *Journal of the Institute of Petroleum,* Vol. 560, No. 58, 1972, pp. 95-101.

35. Adamson, A. W. and A. P. Gast. *Physical Chemistry of Surfaces.* John Wiley and Sons, New York, 1997.

36. Della Volpe, C., S. Siboni. Some Reflections on Acid Base Solid Surface Free Energy Theories. *Journal of Colloid and Interface Science*, Vol. 195, 1997, pp. 121-136.

37. Kwok, D. Y., T. Gietzelt, K. Grundke, H. J. Jacobasch, and A. W. Neumann. Contact Angle Measurements and Contact Angle Interpretation. 1. Contact Angle Measurements by ADSA and a Goniometer Sessile Drop Technique. *Langmuir*, Vol. 13, 1997, pp. 2880-2894.

38. Kwok, D. Y., A. Leung, C. N. C. Lam, A. Li, and R. Wu. Low-Rate Dynamic Contact Angles on Poly(methyl methacrylate) and the Determination of Solid Surface Tensions. *Journal of Colloid and Interface Science,* Vol. 206, 1998, pp. 44-51.

39. Della Volpe, C., S. Siboni. Acid Base Surface Free Energies of Solids and the Definition of Scales in the Good van Oss Chaudhury Theory. *Journal of Adhesion Science and Technology*, Vol. 14, 2000, pp. 235-272.

40. Jacobasch, H. J., K. Grundke, S. Schneider, and F. Simon. Surface Characterization of Polymers by Physico-Chemical Measurements. *Journal of Adhesion*, Vol. 48, 1995, pp. 57-73.

41. Chibowski, E. Surface Free Energy of a Solid from Contact Angle Hysteresis. *Advances in Colloid and Interface Science*, Vol. 103, 2003, pp. 149-172.

42. Li, W. Evaluation of the Surface Energy of Aggregate Using the Cahn Balance. Unpublished Manuscript, Chemical Engineering Department, Texas A&M University, College Station, 1997.

43. Jura, G. and W. D. Harkins. Surfaces of Solids XI. Determination of the Decrease of Free Surface Energy of a Solid by an Adsorbed Film. *Journal of American Chemical Society*, Vol. 66, 1944, pp. 1356-1361.

44. Gregg, S. J. and K. S. W. Sing. *Adsorption, Surface Area and Porosity*, Academic Press, New York, 1967.

45. Pitzer, K. S. and L. Brewer. *Thermodynamics*, McGraw-Hill Book Company, New York, 1961.

46. Chen, C. H. and N. H. Dural. Chloroform Adsorption on Soil. *Journal of Chemical Engineering Data,* Vol. 47, 2002, pp. 1110-1115.

47. McClellan, A.L. and H. F. Harnsberger. Cross-sectional Areas of Molecules Adsorbed on Solid Surfaces. *Journal of Colloid and Interface Science*, Vol. 23, 1967, pp. 577-599.

48. Bilinski, B. and L. Holysz. Some Theoretical and Experimental Limitations in the Determination of Surface Free Energy of Siliceous Solids. *Powder Technology*, Vol. 102, 1999, pp. 120-126.

49. Douillard, J. M., T. Zoungrana, and S. Partyka. Surface Gibbs Free Energy of Minerals: Some Values. *Journal of Petroleum Science and Engineering*, No. 14, 1995, pp 51-57.

50. Bilinski, B., and E. Chibowski. The Determination of the Dispersion and Polar Free Energy of Quartz by the Elution Gas Chromatography Method. *Powder Technology,* No.35, 1983, pp. 39-45.

51. Thomas, J. M., W. J. Thomas. *Principles of Heterogeneous Catalysis.* Wiley VCH, New York, 2005.

52. Chehab, G. R., E. O'Quinn, and Y. R. Kim. Specimen Geometry Study for Direct Tension Test Based on Mechanical Tests and Air Void Variation in Asphalt Concrete Specimens Compacted by SGC. In *Transportation Research Record: Journal of the Transportation Research Board, No. 1723,* TRB, National Research Council, Washington D.C., 2000, pp. 125-1332.

53. Zollinger, C. *Application of Surface Energy Measurements to Evaluate Moisture Susceptibility of Asphalt and Aggregates.* Master's thesis. Texas A&M University, College Station, 2005.

54. Hefer, A. W., D. N. Little, and R. L. Lytton. A Synthesis of Theories and Mechanisms of Bitumen-Aggregate Adhesion Including Recent Advances in Quantifying the Effects of Water. *Journal of Association of Asphalt Paving Technologists,* Vol. 74, 2005, pp. 139-196.

55. Western Research Institute. *Fundamental Properties of Asphalts and Modified Asphalts, Volume 1: Interpretive Report.* Publication FHWA-RD-99-212, WRI, Laramie, WY, 2001.

56. Michales, A. S. Fundamentals of Surface Chemistry and Surface Physics. *Proc., Symposium on Properties of Surfaces*, ASTM Materials Science Series – 4, Los Angeles, CA, 1962, pp. 3-24.

57. Cottrell, A. H. *The Mechanical Properties of Matter*. John Wiley and Sons, New York,1964.

58. Kuznetsov, V. D. *Surface Energy of Solids.* Her Majesty's Stationery Office, London, 1957.

59. Beilby, C. *Aggregation and Flow in Solids.* The Macmillan Co., London, 1921.

60. Dupre, A. *Theorie Mecanique de la Chaleur*, Gauthier-Villars, Paris, 1869.

61. Harkins, W. D. and Y. C. Cheng. The Orientation of Molecules in Surfaces. VI. Cohesion, Adhesion, Tensile Strength, Tensile Energy, Negative Surface Energy, Interfacial Tension, and Molecular Attraction. *Journal of the American Chemical Society*, Vol. 43, 1921, pp. 35-53.

62. Young, T. *Miscellaneous Works.* Edited by G. Peacock and J. Leitch. J. Murray, London, Vol. I, 1855.

63. Bangham, D. H. The Gibbs Adsorption Equation and Adsorption on Solids. *Transactions of Faraday Society,* Vol. 88, 1937, pp. 805.

64. Griffalco, L. A. and R. J. Good. A Theory for the Estimation of Surface and Interfacial Energies I. Derivation and Application to Interfacial Tension. *Journal of Physical Chemistry*, Vol. 61, 1957, pp. 904-909.

65. Fowkes, F. M. Determination of Interfacial Tensions, Contact Angles and Dispersion Forces in Surfaces by Assuming Additivity of Intermolecular Interactions in Surfaces. *Journal of Physical Chemistry*, Vol. 66, 1962, pp. 382.

66. Fowkes, F. M. The Relation of the Attractive Forces at Interfaces to Wetting, Spreading, Adsorption, and Long-Range Attractive Forces. *Proc. of the Second Symposium on Fundamental Phenomena in the Materials Science*, Boston, MA, 1966, pp. 139-164.

67. Harkins, W. D. *The Physical Chemistry of Surface Films.* Reinhold, New York, 1952.

68. Dann, J. R. Forces Involved in the Adhesive Process I. Critical Surface Tensions of Polymeric Solids as Determined with Polar Liquids. *Journal of Colloid and Interface Science*, Vol. 32, 1970, pp. 302-320.

69. Berg, J. C. Role of Acid-Base Interactions in Wetting and Related Phenomenon. In *Wettability,* (J.C. Berg, ed.), Marcel Dekker, New York, 1993, pp. 75-148.

70. Lee, L. H. Correlation Between Lewis Acid-Base Surface Interaction Components and Linear Solvation Energy Relationship Solvatochromic Alpha and Beta Parameters. *Langmuir*, Vol. 12, 1996, pp. 1681-1687.

71. Kamlet, M. J., J. M. Abboud, M. H. Abraham, and R. W. Taft. Linear Solvation Energy Relationships. 23. A Comprehensive Collection of the Solvatochromic Parameters, α, π, β, and γ, and Some Methods for Simplifying the Generalized Solvatochromic Equation. *Journal of Organic Chemistry,* Vol. 48, 1983, pp. 2877-2887.

72. Condor, J. and Young, C. *Physicochemical Measurement by Gas Chromatography*, John Wiley and Sons, London, UK, 1979.

73. Skoog, D.A., and J. J. Leary. *Principles of Instrument Analysis.* 4th Edition, Saunders College Publishing, New York, 1992.

74. Hefer, A., *Adhesion in Bitumen-Aggregate Systems and Quantification of the Effects of Water on the Adhesive Bond*. Ph.D. dissertation. Texas A&M University, College Station, 2004.

APPENDIX A

BACKGROUND OF CONCEPTS RELATED TO SURFACE FREE ENERGY

Background

The intermolecular forces that determine the existence of matter in a solid or liquid state are also responsible for the special properties of the surface [56]. Figure A.1 shows the hypothetical layout of molecules and the intermolecular forces of a material in vacuum.

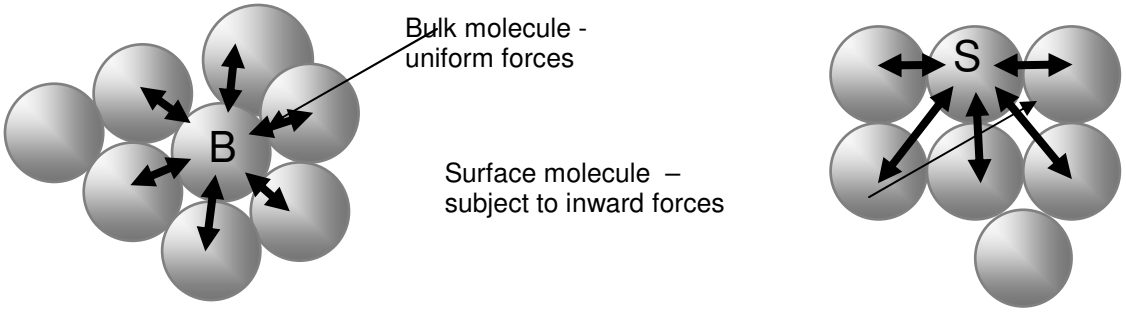

Figure A.1. Differences in intermolecular forces of surface molecules versus bulk molecules

The molecule in the bulk, 'B' is subjected to intermolecular forces that are evenly distributed from all sides, whereas, the molecule 'S' on the surface is subjected to intermolecular forces from all sides, except from the side exposed to vacuum. This misbalance of forces has two outcomes. Firstly, molecules at the surface have free energy which is approximately equal to its missing share of bond energy compared to the molecules in the bulk. Secondly, the material will try to minimize the number of molecules on the surface with free energy by drawing into its bulk as many molecules from the surface as possible. This also explains the tendency of liquids to contract to a spherical shape on a molecular basis.

The presence of excess energy of surface molecules also suggests that energy must be supplied to extend the surface of a material. The total energy thus supplied to extend the surface by unit area, E_s, can be approximated by the heat of vaporization per unit volume of the material [57]. Further, surface free energy is defined as the work required to create unit area of a new surface of the material in vacuum, commonly denoted by the greek letter γ. The term "free energy" is used in this context since the definition is based on work done, and is different from the total excess energy E_s. The terms surface tension and surface free energy are used interchangeably. The former was originally introduced to explain the capillary action of liquids. This term is misleading if one attempts to explain the surface properties of liquids by considering the presence of a surface layer that is subjected to tension. It must be emphasized that the primary source of surface energy or surface tension is the inward pull on the surface molecules at the surfaces from the bulk and not forces that are parallel to the surface creating some kind of a tension.

Special Characteristics of Surface Free Energy of Solids

The phenomenon of reduction in surface area of a material due to its surface free energy is readily visualized for liquids. For example, in the absence of gravity, liquids try to minimize the total surface area for a given volume by assuming the shape of a sphere. However, in case of solids, reduction in surface area is not evident. This does not mean that the forces involved on the solid surfaces are absent or less as compared to the liquids. The reason why solids do not contract is due to the limited mobility of molecules.

Unlike liquids, the limited mobility of molecules on a solid surface is also responsible for heterogeneity of surface free energy even for pure solids. For example, different faces of crystals can have different surface energies. Kuznetsov [58] provides a detailed account that explains the differences in surface free energies of different faces of the same crystal and how it influences the cleavage shape when a crystal is fractured. For example, molecules at the free edge of a crystal are likely to have more free energy as compared to molecules on the face of a crystal. However the effect of free edges on the

surface energy of the solid is likely to be significant only if the solid particles are extremely small or have a very large surface area [35]. Other, factors such as crystal defects and size can significantly alter the surface free energy of the solid surface. The type of surface finishing also affects the surface free energy of the solid. For example, even after very fine grinding, a crystalline solid might have distinct crystal features on the surface. During this process the total surface area of the solid may be reduced due to the reduction in roughness but the surface free energy might remain largely unaffected. However, if the surface is prepared by polishing it with a yielding substance (eg. leather) the top few layers of the surface, (upto 50Å), can be rendered as amorphous significantly altering its surface free energy [59].

Interfaces

The explanation and definition of surface free energy is based on the consideration of a material in vacuum. In real life applications, materials are rarely exposed to vacuum. In fact, most surfaces exist in the form of an interface with another material. Various types of interfaces that are commonly seen are liquid-liquid interface, liquid-vapor interface, solid-liquid interface, and solid-vapor interface. Surface free energy of materials is especially useful in explaining a variety of physical phenomena such as adhesion, wetting, and adsorption, at these interfaces. This section presents a discussion on some of these physical phenomena.

Work of Adhesion and Cohesion

When two materials are brought together to form a new interface, the surface free energy of these materials causes them to physically adhere with each other. Therefore, the work required to separate these two materials is referred to as the work of adhesion. Dupre [60] expressed the work of adhesion between two materials, W_{AB}, in terms of their respective surface energies and interfacial energy as:

$$W_{AB} = \gamma_{AV} + \gamma_{BV} - \gamma_{AB} \qquad \textbf{(A.1)}$$

where, γ_{AV} and γ_{BV} are the surface free energies of 'A' and 'B' when they are separated in a vapor medium 'V', and γ_{AB} is the interfacial energy between these materials.

Similar to the work of adhesion, the work of cohesion of a liquid is defined as the work required to separate a column of the liquid of unit area into two [61]. This definition can be extended to solids as well. From the definition of surface free energy it can be shown that the total work of cohesion of a material is:

$$W_{AA} = 2\gamma \qquad \textbf{(A.2)}$$

where, γ is the surface free energy of the material. Comparison of the work of adhesion between any two materials with their individual work of cohesion can be used to estimate how the two materials interact at their interface. For example, if the work of cohesion of a liquid is significantly greater than its work of adhesion with another solid, then the molecules of the liquid will have more affinity to itself than to the solid surface. This will result in limited wettability of the solid by the liquid. Similarly if work of cohesion of the liquid is significantly less than its work of adhesion with the solid, then the liquid will wet the surface of the solid. In this context, wettability of a solid, A, by a liquid, B, can be quantified as follows:

$$\text{Wettability of A by B} = W_{AB} - W_{BB} \qquad \textbf{(A.3)}$$

Contact Angles

Contact angles are commonly used to measure the surface free energy of solids. When a drop of liquid is placed on a clean smooth horizontal surface, it either spreads over the solid surface or takes the shape of a drop with a finite contact angle between the solid and liquid phases (Figure A.2).

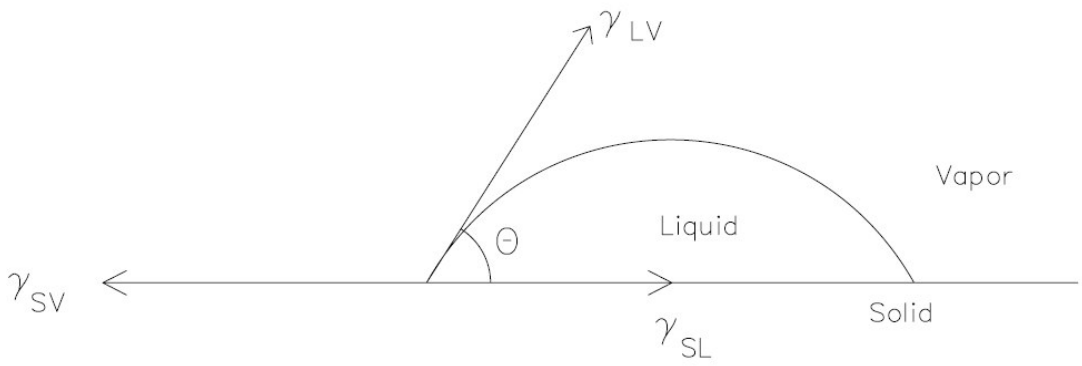

Figure A.2. Contact Angle of Liquid on a Solid Surface

If a finite contact angle is formed by the liquids on the solid surface, then the relationship between the contact angle, θ, and the surface free energies of the solid and liquid is given by:

$$\gamma_{SV} = \gamma_{SL} + \gamma_{LV} \cos\theta \qquad \textbf{(A.4)}$$

where, γ_{SL} is the interfacial energy between the solid and the liquid, γ_{SV} and γ_{LV} are the surface free energies of the solid and liquid in presence of the vapor V. Equation (A.4) is due to Young [62], although it was not proven for several years after he first proposed it. Equations (A.1) and (A.4) can be combined to give the following equation:

$$W_{SL} = \gamma_{LV}(1 + \cos\theta) \qquad \textbf{(A.5)}$$

The above equation is referred to as the Young-Dupre equation and is a very important relationship commonly used to determine surface free energies of solids.

Spreading Pressure

Spreading pressure is defined as the reduction in the surface free energy of the solid due to the adsorption of vapor molecules on its surface. Based on this definition, spreading pressure is mathematically expressed as:

$$\pi_p = \gamma_S - \gamma_{SVp} \qquad \textbf{(A.6)}$$

where, π_p is the spreading pressure of a vapor at partial vapor pressure p, and γ_S and γ_{SVp} are the surface energies of the solid in vacuum and in the presence of the vapor at partial vapor pressure p, respectively.

Further, equation (A.7) presents a direct application of the Gibbs free energy equation relating spreading pressure of the vapor at partial pressure, p, to the mass of vapor adsorbed and its vapor pressure [43, 63]:

$$\pi_{p1} = \frac{RT}{MA}\int_0^{p1}\frac{n}{p}dp \qquad \textbf{(A.7)}$$

where, R is the universal gas constant, T is the test temperature, and other terms are described before. The spreading pressure based on the equilibrium mass adsorbed at the maximum saturated vapor pressure is referred to as the equilibrium spreading pressure of the vapor with the solid, denoted by the symbol π_e. Equation (A.7) is rewritten as follows for equilibrium spreading pressure:

$$\pi_e = \gamma_S - \gamma_{SV} \qquad \textbf{(A.8)}$$

Using equation (A.1) we can define work of adhesion between a solid and a liquid, W_{SL} as:

$$W_{SL} = \gamma_S + \gamma_L - \gamma_{SL} \qquad \textbf{(A.9)}$$

Substituting the values of the interfacial tension γ_{SL} from equation (A.4) , π_e from equation (A.8), and considering the total surface tension of the liquid saturated in its own vapor to be the same as the surface tension of the liquid, we get a more general form of the equation for work of adhesion:

$$W_{SL} = \pi_e + \gamma_{LV}(1+\cos\theta) \quad \textbf{(A.10)}$$

For solid surfaces with very low surface energy, such as polymers, the spreading or film pressure is small and the approximation $\pi_e \approx 0$ can be made. This assumption typically holds good for all liquids that form a finite contact angle with the clean solid surface. Therefore equation (A.10) reduces to the form of equation (A.5) as described earlier. This approximation is not valid for solids with very high surface energies. However, for such solids, the contact angle is typically 0, and therefore the work of adhesion can be expressed as:

$$W_{SL} = \pi_e + 2\gamma_{LV} \quad \textbf{(A.11)}$$

This relationship between the work of adhesion and equilibrium spreading pressure of the vapor is very important in determining the surface free energy of solids.

Theories Related to Surface Free Energy

Thus far, the term surface free energy or surface tension of a solid or liquid was expressed as a single quantity, γ. This section describes the origin and modeling of surface free energy of materials from the molecular interactions point of view. This discussion is important as it can be applied to theoretically calculate and predict work of adhesion between two different materials based on their individual surface energies, determine the interfacial energy of various types of interfaces, and to measure the surface free energy of unknown materials indirectly using the principles of work of adhesion.

Background for the Development of Theories Related to Surface Free Energy

One of the earliest theories to explain surface free energy and interfacial energy of materials was given by Good and Griffalco [64]. They used the Berthlot relation for the

attractive constants between like molecules A_{aa} and A_{bb}, with attractive constant of unlike molecules A_{ab}:

$$\frac{A_{ab}}{\sqrt{A_{aa}A_{bb}}} = 1 \qquad \textbf{(A.12)}$$

to determine the relationship:

$$\gamma_{ab} = \gamma_a + \gamma_b - 2\Phi\sqrt{\gamma_a\gamma_b} \qquad \textbf{(A.13)}$$

where, Φ is characteristic constant for the system being studied.

They also demonstrate that the theoretical value of Φ under idealized conditions is close to unity. However, the true experimental value of Φ ranges from 0.31 to 1.15 for combinations of water with mercury and isobutyl alcohol respectively. They experimentally demonstrate that the deviation of Φ from 1 is more when the predominant forces in one phase are different from the predominant forces in the second phase. For example, the predominant forces in case of mercury are metallic bonds as compared to hydrogen bonds in water.

Fowkes [65] introduced the idea that the total surface free energy of a material is actually made up of two components, namely the dispersion forces and forces related to specific interactions such as hydrogen bonding. He also proposed that the total surface free energy or surface tension is a linear combination of these interactions expressed as follows:

$$\gamma^{Total} = \gamma^{Dispersive} + \gamma^{Specific} \qquad \textbf{(A.14)}$$

This method to model the surface free energy of materials into its components is also referred to as the two-component theory and is still in use today.

Fowkes [66] also revalidated the work of Griffalco and Good regarding the use of geometric mean based on the Berthelot relationship. He also showed that this

relationship is valid as long as there is no substantial difference between the sizes of molecules being used. The assumption of setting Φ as 1 was successful in the experimental work since only dispersive component of surface energies was being investigated using saturated hydrocarbons. Saturated hydrocarbons in general do not have any bonds that can contribute to specific interactions and the specific component for this class of materials is set to 0.

Harkins [67] demonstrated the relationship between the surface energies of a solid, liquid, their interfacial energy and equilibrium spreading pressure as follows:

$$\pi_e = \gamma_s - (\gamma_L + \gamma_{SL}) \quad \textbf{(A.15)}$$

Fowkes used this relation to show that:

$$\pi_e + 2\gamma_L = 2\sqrt{\gamma_S^d \gamma_L^d} \quad \textbf{(A.16)}$$

He uses equation (A.16) with adsorption data from other researchers to show how dispersive component of surface free energy can be obtained using adsorption measurements. He also demonstrates how heat of immersion and heat of adsorption are related to surface free energy of these materials based on these equations. In another series of experiments he determines the value of the following expression using polar liquids:

$$\gamma_{12} - \gamma_1 - \gamma_2 + 2\sqrt{\gamma_1^d \gamma_2^d} \quad \textbf{(A.17)}$$

In the absence of any polar interactions, Fowkes verified that the value of the above expression was zero. However, when polar liquids were used, the expression always has some positive value indicating that there was some excess energy due to the polar interactions. This reinforced the idea that the total surface free energy of a solid or liquid is not equal to its dispersive component but also has an additional component due to the specific or polar interactions between various molecules. Dann [68] demonstrated

that this additional component due to polar interactions was a function of properties of both the materials.

More Recent Developments in Theories Related to Surface Free Energy

The specific component of surface free energy, $\gamma^{specific}$, from equation (A.14) is attributed to the polar interactions on the material surface and dispersive component to Lifshitz van der Waals (LW) type of interactions. Van Oss, Chaudhury and Good [25] explain that all polar interactions in the term $\gamma^{specific}$, including hydrogen bonding, can be explained as a type of electron acceptor-electron donor interactions. An important aspect of the electron acceptor-electron donor interactions, or Lewis acid-base interactions is that unlike the dispersive component, these interactions are asymmetrical. They use the term γ^{AB} in place of $\gamma^{specific}$ in equation (A.14) to represent the polar or acid – base component of surface free energy. This theory is also known as the Good – van Oss – Chaudhury (GVOC) theory or the acid-base theory of surface free energy. The electron acceptor and electron donor parameters of the acid-base component were represented as γ^+ and γ^-, respectively. On account of the asymmetry of these parameters, they proposed the following expression for the contribution of polar interactions between two materials represented by subscripts '1' and '2':

$$2\sqrt{\gamma_1^+\gamma_2^-} + 2\sqrt{\gamma_1^-\gamma_2^+} \qquad \textbf{(A.18)}$$

and the relationship between the acid-base component of the surface free energy of a material with its individual acid and base components as:

$$\gamma^{AB} = 2\sqrt{\gamma^+\gamma^-} \qquad \textbf{(A.19)}$$

Therefore, the total surface free energy of any material can be expressed in terms of its three surface free energy components as:

$$\gamma^{Total} = \gamma^{LW} + \gamma^{AB} = \gamma^{LW} + 2\sqrt{\gamma^+\gamma^-} \qquad \textbf{(A.20)}$$

Based on this theory, the interfacial tension between two materials denoted by subscripts '1' and '2' is given as:

$$\gamma_{12} = \gamma_1 + \gamma_2 - 2\sqrt{\gamma_1^{LW}\gamma_2^{LW}} - 2\sqrt{\gamma_1^{+}\gamma_2^{-}} - 2\sqrt{\gamma_1^{-}\gamma_2^{+}} \qquad \textbf{(A.21)}$$

Note the similarity between equations (A.17) and (A.21) and the changes due to the development of the acid-base theory. Equation (A.1) and (A.21) can also be combined to give the work of adhesion between two materials based on the acid-base theory as:

$$W_{12} = 2\sqrt{\gamma_1^{LW}\gamma_2^{LW}} + 2\sqrt{\gamma_1^{+}\gamma_2^{-}} + 2\sqrt{\gamma_1^{-}\gamma_2^{+}} \qquad \textbf{(A.22)}$$

Surface Free Energy Components of Some Liquids

Determining the three surface free energy components of solids based on the GVOC theory is of particular interest in various physical chemistry applications. A common methodology for this is to measure the work of adhesion of the solid with a suite of at least three different liquids with known surface free energy components (referred to as the probe liquids). This generates three linear equations based on equation (A.22), which can be solved to determine the surface free energy components of the solid. The surface free energy components of at least three probe liquids must be known a priori in order to be able to use this methodology successfully. It is evident that any error in the surface free energy components of the probe liquids will be inherited by the surface free energy components of the solid. As of date there is still general disagreement about the "true" values of the surface free energy components. Different values for the three surface free energy components of the same liquid are available in the literature. Therefore, a brief discussion of the causes and consequences of this discrepancy is justified in this context.

GVOC and coworkers first presented the three surface free energy components of various pure homogenous liquids. The split of total surface free energy between the dispersive or LW component and the polar or acid – base component for various liquids was determined by comparing results from experiments that measured their interfacial tension with non polar liquids such as alkanes. Once the LW component is known, the

acid-base component, γ_1^{AB}, can be determined using equation (A.20). GVOC realized that the further breakup of the acid-base components into acid and base components was not possible mathematically. This led them to make the assumption that the acid and base components for water are equal. In other words, the ratio of acid to base component of water was assumed to be 1. Using this assumption and equation (A.20) the acid and base component of water was each determined to be 25.5 ergs/cm^2. The three surface free energy components of water were then used to determine the surface free energy components of other liquids by measuring interfacial tensions. Based on their work and this assumption, GVOC present the three surface free energy components for approximately 60 liquids.

This approach has been under criticism by various other researchers in this field. Some of the reasons that instigated this criticism are as follows. Firstly, the Lewis base component of surface free energy for several materials such as polymers always seemed to be consistently much higher than the Lewis acid component [69]. Secondly, there appeared to be no rational justification for the assumption of considering the acid base component ratio for water to be equal to 1 since it has been argued that water tends to be more acidic than basic [36, 39].

In order to reconcile these differences, use of a reference material with all three known surface free energy components is inevitable. It has been suggested that if the reference material to be used is water, then it must be regarded as a stronger Lewis acid than a Lewis base [36, 70]. In other words, the ratio of acid to base component of water must be greater than 1 as opposed to the assumption made by GVOC. Various values have been proposed in the literature for this ratio. For example Taft and co-workers [71] consider the ratio of acid to base character of water as 1.17/0.18 = 6.5. Although these values refer to the parameters that are used to quantify the electron donor and electron acceptor characteristics of water based on a “solvatochromic scale”, it still suggests that the assumption made by GVOC maybe in error. Della Volpe demonstrate that if the ratio of 6.5 is used to compute the three surface free energy components of various liquids, a totally new set of numbers emerge. It is evident that the surface free energy components of any solid determined using these liquids and values as a reference will inherit these assumptions and accordingly care must be taken in interpreting such results.

Summary of Theories Related to Surface Free Energy

In summary, currently there are two main theories used to explain the surface free energy of solids and liquids. These are the two component theory, in line with equation (A.14) proposed by Fowkes, and the three component or acid-base theory, according to equation (A.20) proposed by GVOC. The three surface free energy components of various liquids were determined by GVOC and co workers based on the assumption that the ratio of acid to base component of water is 1. However, some other researchers argue that the scale of surface free energy components based on this ratio is inaccurate since the actual ratio of acid component to base component of water is much higher than 1. Based on this argument, surface free energy components of various liquids have been proposed in literature using different values for the acid base ratio of water. Despite this criticism, the scale proposed by GVOC is still very popular amongst various users. However, surface free energy components of materials derived using this scale must be interpreted with caution considering the fact that the resulting values are only a relative measure with respect to the acid and base components of water.

Determining Surface Free Energy of Solids

Various direct and indirect methods to measure surface free energy of solids have been used in the literature. One of the earliest method to estimate surface free energy of solids was to measure the surface tension of the solid in liquid form at various temperatures above its melting point and then extrapolate its surface tension at room temperature. Several direct methods to measure surface free energy of crystalline solids have also been reported [58]. However, most of these methods are applicable for crystalline materials that undergo brittle fracture and are often useful only from a fundamental research point of view. Also, these methods have rarely been used to derive the three surface free energy components of solids.

Direct measurement of surface free energy components of solids is rarely feasible. However, it is possible to measure the work of adhesion of the solid as it interacts with various liquids and gases. Examples of interactions between solids and liquids or gases are, formation of contact angles, vapor adsorption, evolution of heat when solids are

immersed in a liquid etc. Various methods have been used to measure surface free energy of solids such as the contact angle approach, gas adsorption method, inverse gas chromatography, etc. Some of these methods will be discussed in this sub section.

The basic algorithm for determining the surface free energy components of an unknown solid is similar for all these methods. The work of adhesion between two materials, the solid (unknown surface free energy components) and the probe liquid or vapor (known surface free energy components) is determined experimentally. The work of adhesion is related to the surface free energy components of the solid and probe as follows:

$$W_{XP} = 2\sqrt{\gamma_X^{LW}\gamma_P^{LW}} + 2\sqrt{\gamma_X^{+}\gamma_P^{-}} + 2\sqrt{\gamma_X^{-}\gamma_P^{+}} \qquad \textbf{(A.23)}$$

where, W_{XP} is the work of adhesion between the probe liquid or vapor denoted by the suffix P, and the solid denoted by the suffix X. The work of adhesion of the solid with at least three different probe liquids or vapors must be measured to generate a set of three linear equations that can then be solved to determine the three unknown surface free energy components of the solid.

Some of the methods to measure surface free energy components of solids are based on measuring work of adhesion in the form of contact angles, adsorption isotherms, heats of immersion and retention times. The Wilhelmy plate method and sessile drop methods can be used measure dynamic and static contact angles of different probe liquids with the solid. The Universal Sorption Device (USD), micro calorimeter, and inverse gas chromatography are instruments used to measure the adsorption isotherms, heats of immersion and retention times, for different probes with the solid, respectively. Details for the Wilhelmy plate method, USD and micro calorimeter are presented in Chapters III, IV, and VI, respectively. The other two methods are discussed in the following sub sections.

Contact Angle Approach

The contact angle approach is applicable to solids that form a finite contact angle with various liquids. Usually such solids are referred to as low energy solids. Examples

of such solids include polymers such as PMMA, and polyethylene. By combining equations (A.5) and (A.23) one can relate the contact angle of the probe liquid with the solid to their surface free energy components as follows:

$$\gamma_P(1+\cos\theta) = 2\sqrt{\gamma_X^{LW}\gamma_P^{LW}} + 2\sqrt{\gamma_X^{+}\gamma_P^{-}} + 2\sqrt{\gamma_X^{-}\gamma_P^{+}} \qquad \textbf{(A.24)}$$

In equation (A.24), γ_P, without any superscript is the total surface free energy of the probe. Therefore, if the surface free energy of the probe liquid and its components are known, and the contact angle of the probe liquid with the solid is measured experimentally, then the only three unknowns in equation (A.24) are the three surface free energy components of the solid. Contact angles with three or more probe liquids and their surface free energy components can be used with equation (A.24) to generate a set of linear equations that can be solved to determine the unknown surface free energy components of the solid. Some of the general considerations for the use of this approach are that:

- the spreading pressure of vapors from the probe liquid on the solid surface must be negligible (this is generally true in case of low energy solids),
- the surface of the test specimen must be very smooth,
- the surface free energy of the probe liquids must be greater than the expected surface free energy of the solid, and
- the probe liquids must not interact chemically with the solid (eg dissolve the solid).

Two popular experimental methods to measure the contact angles of liquids with low energy solids are the Wilhelmy plate method and the sessile drop method. While the former is a dynamic method to measure contact angles, the latter is a static method. In the sessile drop method, a drop of the liquid is dispensed using a micro syringe on a smooth solid surface. The shape of the drop is captured by a camera and the contact angle of the liquid with the solid surface is calculated either manually or by using an image processing software. Figure A.3 shows a schematic of the set up for measuring contact angles using the sessile drop method. More refined techniques such as axisymmetric drop shape analysis can also be used to compute precisely the shape and contact angle of the drop by using computer analysis to fit the observed shape of the drop using

theoretical models [38]. The sessile drop method can also be used in an advancing mode by slowly adding more volume of liquid to the dispensed drop and causing its boundary to expand. Surface and interfacial phenomenon such as the change in contact angle of the drop with time can also be observed using this set up.

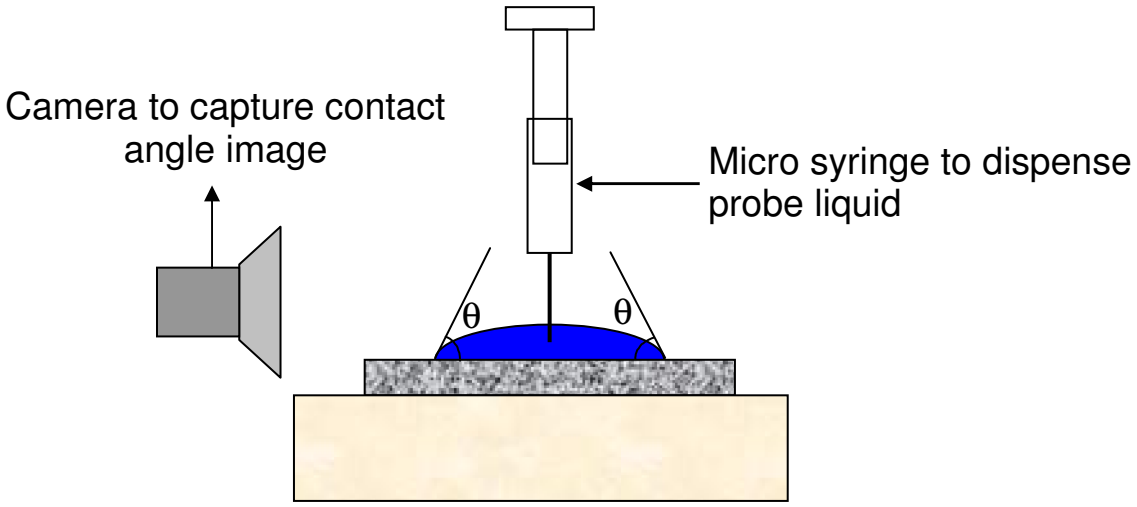

Figure A.3. Schematic for the sessile drop method

Inverse Gas Chromatography

Conventional gas chromatography is used to separate or investigate a mixture of gases that are passed through a column of known material using an inert carrier gas. The gas passing through the column interacts with the standard material in it. The total time of interaction results in different retention times or travel time for the gas from one end of the column to another. The time of interaction, also referred to as the retention time, is characteristic of the gas (unknown phase) and the material in the column (known phase). The principle of inverse gas chromatography is very similar to gas chromatography with the exception that in this case the known phase is probe vapors carried using the inert gas and the unknown phase or material under investigation is filled in the column. Although the basic principles remain the same, use of inverse gas chromatography to determine the surface free energy components of a solid deviates slightly from the basic algorithm described earlier.

In a typical experiment, the solid material to be investigated is filled in the column of the gas chromatograph. Typically gas chromatograph columns are capillary columns made of fused silica with 0.25mm diameter and about 15m in length. The material to be tested can be dissolved using a volatile solvent. The solution is then flushed through the capillary column followed by a dry inert gas purge that dries the solvent and leaves behind a film of the solid material on the inside walls of the capillary column. In case it is not feasible to prepare a solution of the solid sample, one can use a larger column made of silanzed glass with diameters of about 2-3mm and length of about 30cm and fill it with the solid in a powder form. Silanized glass wool can be used on either slide to plug the column and retain the sample in place.

Typically the tests using the IGC are conducted in an infinitely diluted condition, that is extremely small volumes of the probe gas are injected with the carrier gas to pass through the column. This is necessary to allow the consideration of the probe as an ideal gas. In the IGC experiments it is assumed that methane has negligible interaction with the solids in the column, and the retention time for methane is approximated as zero. Therefore the net retention time of other vapors is measured as the difference of their travel time with the travel time for methane. The free energy of adsorption is proportional to the retention volume based on the following equation:

$$-\Delta G_a \propto RT \ln(V_N) \qquad \textbf{(A.25)}$$

where,

$$V_N = \frac{j}{m} F t_N \frac{T}{273.15} \qquad \textbf{(A.26)}$$

In equations (A.25) and (A.26) T is the column temperature, m the sample mass, F the exit flow rate at 1 atm and 273.15K, t_N is the net retention time calculated as the difference between the travel time for the probe vapor with the travel time of methane, j is the James-Martin correction, which corrects the retention time for the pressure drop in the column bed [72, 73].

The free energy of adsorption is also be related to the work of adhesion as follows:

$$-\Delta G_a = aN_A \Delta G_a^{LW} + aN_A \Delta G_a^{AB} = aN_A \left(2\sqrt{\gamma_X^{LW}\gamma_P^{LW}} + 2\sqrt{\gamma_X^{+}\gamma_P^{-}} + 2\sqrt{\gamma_X^{-}\gamma_P^{+}}\right) \quad \textbf{(A.27)}$$

Combining equations (47) and (49) we get:

$$RT\ \ln(V_N) = aN_A \left(2\sqrt{\gamma_X^{LW}\gamma_P^{LW}} + 2\sqrt{\gamma_X^{+}\gamma_P^{-}} + 2\sqrt{\gamma_X^{-}\gamma_P^{+}}\right) + C \quad \textbf{(A.28)}$$

When a series of non polar liquids are used, the above equation reduces to:

$$RT\ \ln(V_N) = \sqrt{\gamma_X^{LW}} \left(aN_A 2\sqrt{\gamma_P^{LW}}\right) + C \quad \textbf{(A.29)}$$

The above equation is in the form of a straight line. Retention volumes for a series of non polar probe vapors with known values of surface energies, example alkanes, can be plotted based on equation (A.29). The slope of the resulting straight line corresponds to the $\sqrt{\gamma_X^{LW}}$. Thus the LW component of the solid can be determined. If retention times corresponding to polar probes are also included in the plot, then the values corresponding to the polar probe will lie above the straight line from the non polar probes. The deviation from the straight line is a measure of the polar or acid-base interactions between the probe and the solid, ΔG_a^{AB}. Figure A.4 illustrates this principle. Once the LW component is known, the acid and base components of surface free energy of the solid can be determined by measuring the retention time of monopolar probes (probes that have either the acid component zero or the base component zero) and using it with equation (A.28).

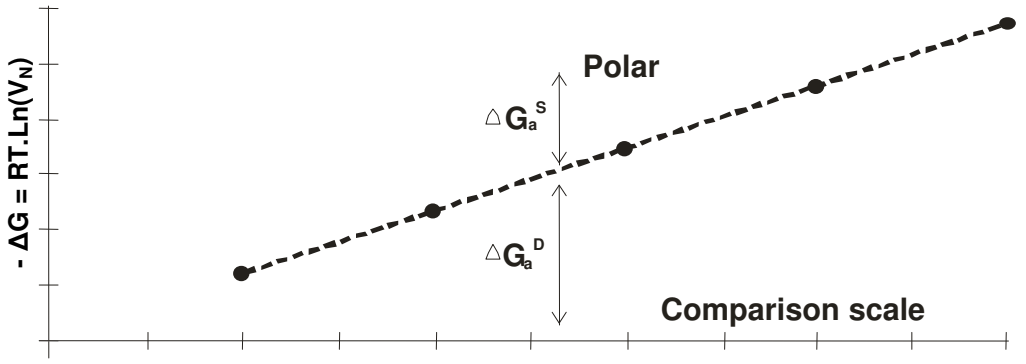

Figure A.4. Retention time versus liquid properties [74]

Any conventional gas chromatograph can be retrofit with suitable columns to function as an IGC. Commercially available IGC's are also available that are specifically designed for these kinds of experiments. Dry helium is typically used as a carrier gas. A mixture of alkanes (non polar probes) is injected in the IGC using a gas tight syringe. Ethylacetate and toluene are examples of monopolar probe vapors that are basic in nature (the acid component is zero) and DCM and chloroform are examples of probe vapors that are acidic in nature (the base component is zero). The time taken for the vapors to travel through the column is determined using a flame ionization detector at the other end of the column. Figure A.5 illustrates a typical output from the chemstation software.

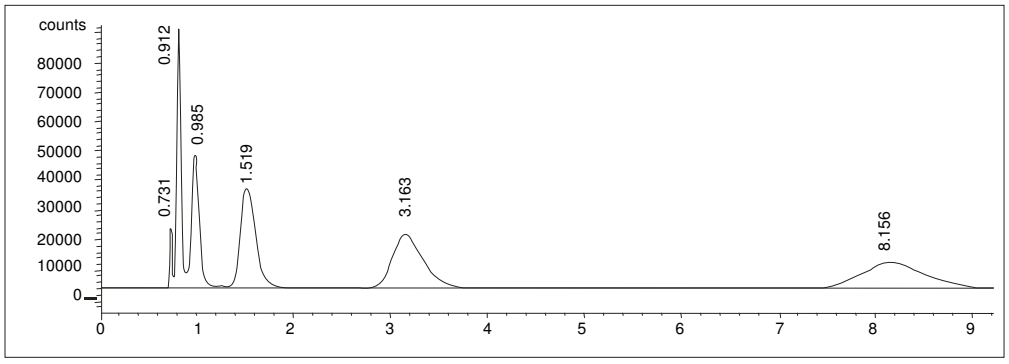

Figure A.5. Typical retention times from the chemstation software [74]

APPENDIX B

COMPUTING SURFACE ENERGIES FROM CONTACT ANGLES

Equations for Work of Adhesion

Based on the Young-Dupre equation (neglecting the spreading pressure) work of adhesion can be expressed as follows:

$$w = W_{adhesion} / 2 = 0.5\gamma(1 + Cos\theta) \quad \textbf{(B.1)}$$

where, γ is the total surface free energy of the probe liquid, and θ is the contact angle of the probe liquid on the surface of the solid being investigated.
For a set of liquids, this equation can be expressed as:

$$0.5\gamma_{li}(1 + Cos\theta_i) = \sqrt{\gamma_{li}^{LW}\gamma_s^{LW}} + \sqrt{\gamma_{li}^{+}\gamma_s^{-}} + \sqrt{\gamma_{li}^{-}\gamma_s^{+}} \quad \textbf{(B.2)}$$

where, γ is the total surface free energy, γ^{LW} is the Lifshitz-Van der Waals component of surface free energy, γ^{-} is the Lewis base component of surface free energy, γ^{+} is the Lewis base component of surface free energy, subscript li refers to the i^{th} liquid, where i is equal to the number of probe liquids being used, and subscript s refers to the solid surface.

If the actual number of liquids used is 'm' then the system of linear equations generated based on the above equations is shown below:

$$\mathbf{A\ x = B}, \quad \textbf{(B.3)}$$

where,

$$A = \begin{bmatrix} \sqrt{\gamma_{l1}^{LW}} & \sqrt{\gamma_{l1}^{+}} & \sqrt{\gamma_{l1}^{-}} \\ ..... & ..... & ..... \\ \sqrt{\gamma_{lm}^{LW}} & \sqrt{\gamma_{lm}^{+}} & \sqrt{\gamma_{lm}^{-}} \end{bmatrix}_{mx3}, \quad \textbf{(B.4)}$$

$$x = \begin{bmatrix} \sqrt{\gamma_{s}^{LW}} \\ \sqrt{\gamma_{s}^{-}} \\ \sqrt{\gamma_{s}^{+}} \end{bmatrix}_{3x1}, \quad \textbf{(B.5)}$$

$$B = 0.5 \begin{bmatrix} \gamma_{li}(1+Cos\theta_1) \\ ..... \\ \gamma_{li}(1+Cos\theta_m) \end{bmatrix}_{mx1} \quad \textbf{(B.6)}$$

Three distinct cases can occur:

Case 1: When m < 3 the number of equations generated is less than the number of unknowns and hence the set of equations becomes indeterminate,

Case 2: When m = 3 the number of equations is exactly equal to the number of unknowns and the equations can be solved. In this case the matrix A is a square matrix and the vector 'X' containing the square roots of the unknown components of the solid can be solved if **A** is non-singular as follows:

$$\mathbf{X} = \mathbf{A}^{-1}\mathbf{B} \quad \textbf{(B.7)}$$

Case 3: When m > 3 then the number of equations available are more than the unknowns and the system becomes over determinate. It is easy to see that the matrix A would no longer be a square matrix and it will not be possible to directly inverse the matrix. Other tools to get the best solution for this scenario will have to be used and are discussed later.

Sensitivity to Choice of Liquids

If the component properties of the liquids are very close to each other the calculated surface free energy components will become unduly sensitive to the measured contact angles. This is more important in cases when only a limited set of liquids are being used to estimate the surface energies of the solid. A simplified demonstration of a similar effect is given as follows.

Consider a case where a value 'y' is measured using different probes with characteristic 'x'. The calculated parameter of interest is the slope of y vs. x. If two probes with very similar values of x are selected then the measured value of y might not be very different. This theoretically small difference is compounded by experimental error which could be relatively large. As a result the calculated value of slope can have a large variability. This can be seen from Figure A.1 where probes 1 and 2 with values of 'x' as 1 and 2 respectively are used to measure parameter 'y'. With only these two points on the graph the variability in the slope can be very large. However, if a third probe is used with the value of 'x' as 10 which is significantly different from the values of the other two probes, and assuming that the variability of the measured parameter 'y' is same in this range, it can easily be seen that the variability in the calculated slope is reduced. Mathematically this scenario can be represented as follows:

$$Slope = \frac{y_2 - y_1}{x_2 - x_1} \qquad \textbf{(B.8)}$$

It is evident that if x_2-x_1 is very small its reciprocal would be very large, in turn which implies that the error in measuring y_2 and y_1 is amplified by a very large number.

The above illustration is a simplification of what could happen as a consequence of a poor choice of liquids especially when a limited set of liquids are to be used to determine the surface properties. In the present case, liquids must be selected so that the calculated surface energies would represent reasonable estimates of the true value with minimum error. A mathematical measure of this is the condition number of the selected set of liquids. The smaller the condition number the less sensitive are the calculated

results to the experimental error. More about condition number is discussed in the later sections.

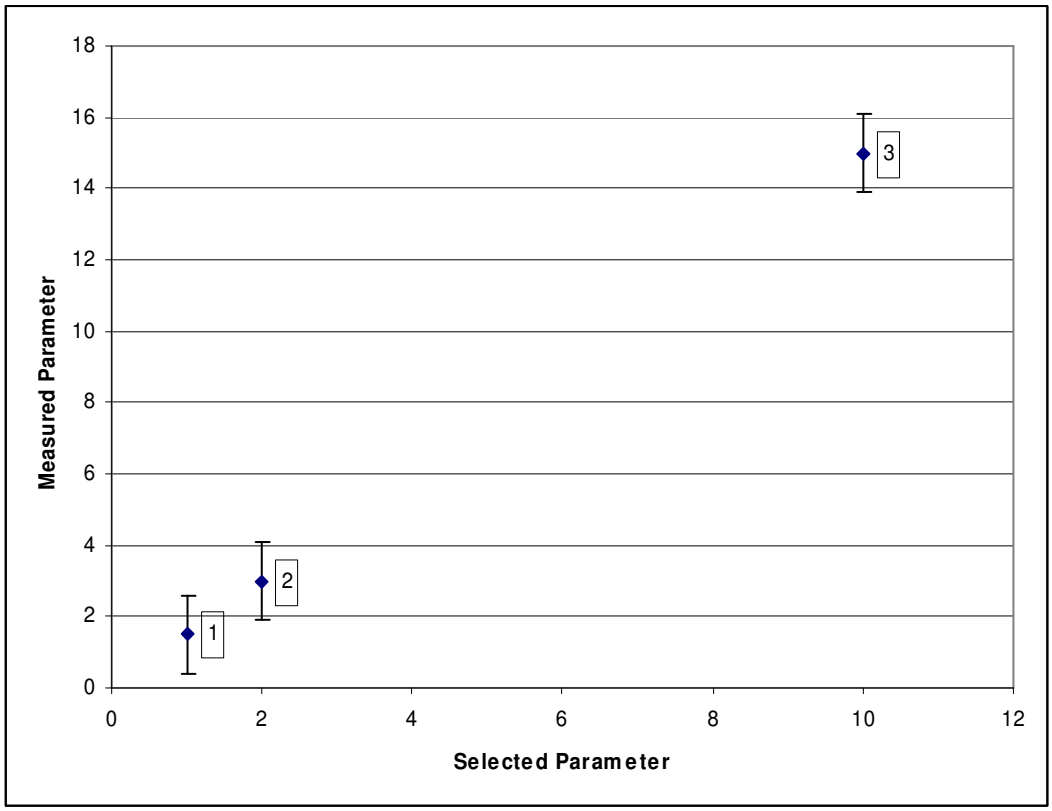

Figure B.1. Demonstration of Effect of Choice of Probes on Calculated Values

Error Propagation

As given in equation (B.1), 'w' is a function of 'γ' and 'θ'. By the propagation of error formulas, an estimate $\hat{w}$ of the true value of *w*, and the standard deviation of $\hat{w}$ can be obtained as follows:

$$\hat{w} = 0.5\gamma\left(1 + \cos\bar{\theta}\right) \qquad \textbf{(B.9)}$$

$$\mathrm{var}(\hat{w}) = \sigma_{\hat{w}}^2 = \sigma_{\gamma}^2\left[\frac{\partial w}{\partial \gamma}\right]^2 + \sigma_{\bar{\theta}}^2\left[\frac{\partial w}{\partial \theta}\right]^2 + 2\sigma_{\gamma\theta}\left[\frac{\partial w}{\partial \gamma}\right]\left[\frac{\partial w}{\partial \theta}\right] \quad \textbf{(B.10)}$$

$$\sigma_{\hat{w}} = \sqrt{\mathrm{var}\left(\hat{w}\right)} \quad \textbf{(B.11)}$$

where, γ is the total surface free energy value of the liquid available from literature, $\bar{\theta}$ is the average contact angle from "*r*" replicate measurements, $\sigma_{\Gamma}{}^2$ is the variance of γ, $\sigma_{\bar{\theta}}{}^2$ is the variance of $\bar{\theta}$, $\sigma_{\Gamma\bar{\theta}}$ is the covariance of γ and $\bar{\theta}$, and the square brackets denote that the derivatives within the brackets are to be evaluated at the mean of γ and of θ, respectively.

When the random errors in measurements of γ and θ are assumed to be independent, $\sigma_{\gamma\theta} = 0$ and equation (B.10) is reduced to the following form:

$$\sigma_{\hat{w}}^2 = \sigma_{\gamma}^2\left[\frac{\partial w}{\partial \gamma}\right]^2 + \sigma_{\bar{\theta}}^2\left[\frac{\partial w}{\partial \theta}\right]^2 \quad \textbf{(B.12)}$$

The value of σ_{γ}^2 can be obtained from literature. The value of $\sigma_{\bar{\theta}}{}^2$ is, however, unknown and it is estimated as (1/r)*variance of "r" replicate measurements of θ. That is:

$$\hat{\sigma}_{\bar{\theta}}{}^2 = \frac{1}{r}\hat{\sigma}_{\theta}{}^2 = \frac{1}{r}\frac{1}{(r-1)}\sum_{k=1}^{r}\left(\theta_k - \bar{\theta}\right)^2 \quad \textbf{(B.13)}$$

Also, note from equation (B.1) that

$$\frac{\partial w}{\partial \gamma} = 0.5(1+\cos\theta), \quad \textbf{(B.14)}$$

and

$$\frac{\partial w}{\partial \theta} = -0.5\gamma \sin\theta . \qquad \textbf{(B.15)}$$

Thus,

$$\left[\frac{\partial w}{\partial \gamma}\right] = 0.5\left(1+\cos\bar{\theta}\right) \qquad \textbf{(B.16)}$$

and

$$\left[\frac{\partial w}{\partial \theta}\right] = -0.5\sin\bar{\theta} . \qquad \textbf{(B.17)}$$

Using (B.12), (B.13), (B.16), and (B.17), the propagated variance of error in the work of adhesion can be calculated for each liquid as follows:

$$\hat{\sigma}^2_{\hat{w}} = \sigma^2_{\gamma}\left\{0.5\left(1+\cos\bar{\theta}\right)\right\}^2 + \frac{1}{r}\frac{1}{(r-1)}\sum_{k=1}^{r}\left(\theta_k - \bar{\theta}\right)^2\left\{-0.5\gamma\sin\theta\right\}^2 \qquad \textbf{(B.18)}$$

Singular Value Decomposition

As discussed earlier, in the case when more than three liquids are used the system of equations becomes over determinate and the matrix A is a mx3 rectangular matrix. The Singular Value Decomposition (SVD) technique can be used to solve such as system of equations. The SVD technique can also be used to calculate the condition number of the selected liquids (even without any contact angle measurements) to assess if the choice of liquids is appropriate for calculating the surface free energy components of the solid. The SVD is based on a linear algebra theorem that states that any mxn matrix **A** where m>n can be represented as follows:

$$\mathbf{A} = \mathbf{U}\,\mathbf{W}\,\mathbf{V}^{\mathrm{T}} \qquad \textbf{(B.19)}$$

where, **U** is a mxn orthogonal matrix, **W** is a nxn diagonal matrix, and $\mathbf{V}^T$ is a nxn orthogonal matrix. In the present case n = 3, since there are three unknown components of surface free energy and m = number of probe liquids being used. Further, the condition number of the matrix **A** is defined as the ratio of the largest to the smallest diagonal element in the **W** matrix. Typically a condition number above 10 can result in a solution where square roots of the surface free energy components are negative.

The inverse of the matrix **A** is obtained as follows:

$$\mathbf{A}^+ = \mathbf{V}\,[\text{diag}\,(1/w_j)]\,\mathbf{U}^T \qquad \textbf{(B.20)}$$

where, $\mathbf{A}^+$ is refered to as the Moore-Penrose inverse.

Now, equation (B.18) can be used easily with equation (B.7) to calculate **x** which is a vector comprising of the square roots of the three surface free energy components as follows:

$$\mathbf{x} = \mathbf{V}\,[\text{diag}\,(1/w_j)]\,\mathbf{U}^T\,\mathbf{B} \qquad \textbf{(B.21)}$$

However, take into account the different error variances in work of adhesion for different probe liquids, the matrices **A** and **B** are changed as follows:

$$A' = \begin{bmatrix} \frac{\sqrt{\gamma_{l1}^{LW}}}{\sigma_1} & \frac{\sqrt{\gamma_{l1}^{+}}}{\sigma_1} & \frac{\sqrt{\gamma_{l1}^{-}}}{\sigma_1} \\ ..... & ..... & ..... \\ \frac{\sqrt{\gamma_{lm}^{LW}}}{\sigma_m} & \frac{\sqrt{\gamma_{lm}^{+}}}{\sigma_m} & \frac{\sqrt{\gamma_{lm}^{-}}}{\sigma_m} \end{bmatrix}_{mx3}, \qquad \textbf{(B.22)}$$

$$B' = 0.5\begin{bmatrix} \dfrac{\gamma_{l1}(1+Cos\theta_1)}{\sigma_1} \\ ..... \\ \dfrac{\gamma_{lm}(1+Cos\theta_m)}{\sigma_m} \end{bmatrix}_{mx1} \qquad \textbf{(B.23)}$$

where, $\hat{\sigma}_1$ through $\hat{\sigma}_m$ are the estimates of the propagated error standard deviations in the work of adhesion of the *m* liquids calculated using equation (B.18).

The matrix **A'** is referred to as the design matrix. **x** can now be calculated using the design matrix **A'** and vector **B'** in place of **A** and **B** using the same procedure as described earlier. The SVD matrices must be generated for **A'** and not **A** for calculating **x** when the errors are to be included.

The variance in the estimate of the parameters of vector **x**, say x_1 through x_3, which actually represent the square roots of the surface free energy components, can be estimated from the following equation when SVD is used:

$$\hat{\sigma}^2_{x_i} = \sum_{j=1}^{n}\left(\frac{V_{ij}}{w_j}\right)^2 \text{ for } i = 1,\text{L } ,n \text{ (here, } n\text{=3).} \qquad \textbf{(B.24)}$$

This provides an estimate of the variance of errors of the components of X. Since the vector X contains the square roots of the surface free energy components the values obtained upon solving X must be squared to get the estimate of actual components and the variance estimate of the errors in the surface free energy components can be obtained by propagation of errors as follows:

$$\hat{\sigma}^2_{x_i^2} = \hat{\sigma}^2_{x_i}\left[\frac{\partial x_i^2}{\partial x_i}\right]^2 = \left[2x_i\right]^2 \hat{\sigma}^2_{x_i} = 4x_i^2\hat{\sigma}^2_{x_i} \qquad \textbf{(B.25)}$$

APPENDIX C

COMPUTING SURFACE ENERGIES FROM SPREADING PRESSURES

Equations for Work of Adhesion

The sequence of calculations for the USD is same as the WP method. The only difference is in the work of adhesion formula which in this case is:

$$w = W_{adhesion} / 2 = \gamma + 0.5\pi \qquad \textbf{(C.1)}$$

where, Γ is the total surface free energy of the probe liquid, and π is the spreading pressure of a probe vapor on the surface of the solid being investigated. The equation (B.3) remains the same where only the definition of **B** changes to accommodate spreading pressure instead of contact angle:

$$\mathbf{A\ x = B}, \qquad \textbf{(C.2)}$$

where,

$$A = \begin{bmatrix} \sqrt{\gamma_{l1}^{LW}} & \sqrt{\gamma_{l1}^{+}} & \sqrt{\gamma_{l1}^{-}} \\ ..... & ..... & ..... \\ \sqrt{\gamma_{lm}^{LW}} & \sqrt{\gamma_{lm}^{+}} & \sqrt{\gamma_{lm}^{-}} \end{bmatrix}_{mx3}, \qquad \textbf{(C.3)}$$

$$x = \begin{bmatrix} \sqrt{\gamma_{s}^{LW}} \\ \sqrt{\gamma_{s}^{-}} \\ \sqrt{\gamma_{s}^{+}} \end{bmatrix}_{3x1}, \qquad \textbf{(C.4)}$$

$$B = \begin{bmatrix} \gamma_{l1} + 0.5\pi_1 \\ ..... \\ \gamma_{lm} + 0.5\pi_m \end{bmatrix}_{mx1} \quad \textbf{(C.5)}$$

Further, the error propagation in "w" given by equations (B.12), (B.13), (B.16), and (B.17) is modified as follows:

$$\sigma_{\hat{w}}^2 = \sigma_\gamma^2 \left[\frac{\partial w}{\partial \gamma}\right]^2 + \sigma_\pi^2 \left[\frac{\partial w}{\partial \pi}\right]^2 \quad \textbf{(C.6)}$$

where γ is the total surface free energy value of the liquid available from literature, and $\bar{\pi}$ is the average spreading pressure from "r" replicate measurements, $\sigma_\Gamma{}^2$ is the variance of γ, and $\sigma_{\bar{\pi}}{}^2$ is the variance of $\bar{\pi}$. The value of σ_γ^2 is available from literature. The value of $\sigma_{\bar{\pi}}^2$ is, however, unknown and it is estimated as (1/r)*sample variance of "r" replicate measurements on π. Also, note from equation (B.23) that:

$$\left[\frac{\partial w}{\partial \gamma}\right] = 1, \quad \textbf{(C.7)}$$

and

$$\left[\frac{\partial w}{\partial \theta}\right] = 0.5 \quad \textbf{(C.8)}$$

The propagated variance of error in the work of adhesion can be calculated for each liquid as follows:

$$\hat{\sigma}_{\hat{w}}^2 = \sigma_\gamma^2 + (0.5)^2 \frac{1}{r} \frac{1}{(r-1)} \sum_{k=1}^{r} (\pi_k - \bar{\pi})^2 \quad \textbf{(C.9)}$$

All other steps to calculate **x** remain the same as in the case of the WP method.

VITA

Name: Amit Bhasin

Address: 601A CE/TTI Building, MS 3135
Texas A&M University
College Station, TX 77843-3135

Email Address: a-bhasin@ttimail.tamu.edu

Education: B.Tech. in Civil Engineering, Institute of Technology, India, 1997.
M.Eng. in Civil Engineering, Texas A&M University, 2003.
Ph.D. in Civil Engineering, Texas A&M University, 2006.

Work History: 2002-2006
Graduate Research Assistant, Texas Transportation Institute,
College Station, Texas.

2001-2002
Design Engineer, Samveshak, India.

2000-2001
Project Coordinator, Madhucon Projects Limited, India.

1997-2000
Civil Engineer, Engineers India Limited, India.